Decentralized Stablecoins and Collateral Risk*

Roman Kozhan† and Ganesh Viswanath-Natraj‡

First version: June 17, 2021 (posted SSRN)

This version: April 16, 2023 (posted SSRN)

Abstract

In this paper, we study the mechanisms that govern price stability of MakerDAO's DAI token, the first decentralized stablecoin. DAI works through a set of autonomous smart contracts, in which users deposit cryptocurrency collateral and borrow a fraction of their positions as DAI tokens. Using data on the universe of collateralized debt positions, we show that peg volatility is related to collateral risk. The DAI price covaries negatively with returns to risky collateral, even after controlling for safe-haven demand and the mechanical impact of collateral liquidations. The introduction of safe collateral types has led to an increase in peg stability.

Keywords: Cryptocurrency, fixed exchange rates, monetary policy, stablecoins, collateralized debt positions.

JEL Classifications: F31, G14, G15, G18, G23

*For help with obtaining data for this project, we would like to thank Mike McDonald, Lou Kerner, and members from the MakerDAO team, Greg Di Prisco and Kenton Prescott. The views expressed in this paper are independent to MakerDAO. For detailed comments, we thank discussants Yeguang Chi, Oliver Gloede, Simon Mayer, Gustavo Schwenkler, Faten Ben Slimane, Zhuo Zhong, and Adrien d'Avernas, Dirk Baur, Bruno Biais, Agostino Capponi, Jonathan Chiu, Darrell Duffie, Barry Eichengreen, Hermann Elendner, Jean Flemming, Pierre-Olivier Gourinchas, Jorge Herrada, Engin Iyidogan, Brett Lyons, Rich Lyons, Andreas Park, Ingolf Pernice, Bryan Routledge, David Skeie, Ruslan Sverchkov,Quentin Vandeweyer, Junxuan Wang, and seminar participants at the Australasian Banking and Finance Conference, Australian National University, Bayes Business School, CBER Blockchain conference, CEBRA annual meeting, the 17th Central Bank Conference on the Microstructure of Financial Markets, Federal Reserve Board, French Finance Association, New Zealand Finance Conference, NYU Tokenomics Conference, Office of Financial Research, San Francisco Fintech Conference, UCL Blockchain Conference, University of Southampton Cryptocurrency Conference, the University of Western Australia Blockchain Conference and Weizenbaum Institut. We thank Amit Chaudhary for valuable research assistance.

†Warwick Business School, The University of Warwick, Scarman Road, Coventry CV4 7AL, UK. E-mail: Roman.Kozhan@wbs.ac.uk

‡Warwick Business School, The University of Warwick, Scarman Road, Coventry CV4 7AL, UK. E-mail: ganesh.viswanath-natraj@wbs.ac.uk

1 Introduction

"I expect DAI (and newer alternatives eg. RAI) to have much higher survivability than Tether long term."[1] **Vitalik Buterin, the cofounder of Ethereum**

Stablecoins are a class of cryptocurrencies designed to maintain a stable peg to USD. While the majority of stablecoin designs rely on a centralized issuer, decentralized stablecoins led by MakerDAO's DAI have grown dramatically over the recent years with market capitalization exceeding 5 USD Billion. Their key characteristic is that issuance of new tokens is decentralized through using autonomous smart contracts on the Ethereum blockchain.[2] DAI tokens are generated when an investor deposits a set amount of collateral, typically Ethereum (ETH), into a collateralized debt position (CDP). Based on the value of ETH collateral, the investor can borrow a fraction of their collateral as DAI tokens. While DAI's decentralized method of issuance eliminates custodial risk, it is exposed to risks associated with fluctuations in the price of collateral coins.

In this paper we study the short-term fluctuations of the DAI peg. There are two main functions that market participants can achieve by means of trading DAI. First, speculators use DAI to take long leveraged positions in the collateral asset. Second, DAI can be used to hedge against movements of unstable coins and fulfil its "safe-haven" property. Fluctuations in either speculative or safe-haven demands coupled with limits to arbitrage can lead to DAI deviations from the peg. Changes in the relative demand for DAI, in turn, can be due to changes in the expectations of future ETH performance or liquidations of DAI by MakerDAO's protocol in response to a reduction of collateral value. Through both a model and empirical evidence, we quantify the importance of each of these channels for instability of the DAI peg.

We start by developing a simple model of equilibrium price formation. In the model there are three types of agents: speculators that deposit risky ETH collateral and borrow a fraction as DAI tokens, arbitrageurs that short DAI when the peg trades at a premium, and a demand shock for DAI from investors that seek DAI to earn savings and gain utility from its use in Decentralized Finance (DeFi) applications. Speculators' beliefs about future performance of collateral follow a two-state process. In equilibrium, DAI peg-prices are dependent on the state of the collateral. When ETH returns increase (good state), investors collateralize ETH, borrow DAI, and then sell DAI on an exchange to buy more ETH. This puts a downward pressure on the price of DAI and generate discounts in the DAI price. In contrast, in the bad state, the decline in ETH returns cause investors to reduce their DAI borrowings. Therefore, the relative decline in DAI

1. `https://twitter.com/VitalikButerin/status/1263191590543253504`
2. A smart contract is a set of instructions, written in computer code, that defines the conditions of the contract for each counterparty under different scenarios. Being managed by computer code and visible on the blockchain, it can be verified publicly by all nodes in the blockchain.

supply from speculators and an increase in DAI demand from the secondary market (safe-haven effect) generate peg premiums, leading to a negative correlation between DAI prices and returns to ETH collateral. The model implies that both channels – speculative beliefs and safe-haven effect – are important to generate both premia and discounts in DAI price.

The model also generates testable implications regarding the behavior of DAI prices during periods of low and high safe-haven demand, changes in ETH volatility and the interest rate on DAI borrowings, which is known as the stability rate. Peg-premiums in the bad state are higher in periods of high safe-haven demand, high ETH volatility and when the stability rate is higher. A comparative statics exercise shows that the peg volatility increases with volatility of ETH collateral.

We then extend the model by introducing an additional collateral type, the USDC stablecoin, that has lower volatility than ETH. Arbitrageurs have an opportunity to reduce their risk by issuing DAI with a lower volatility collateral type. To close a peg-price premium, arbitrageurs deposit collateral, borrow DAI tokens and sell it in the secondary market. We show that in equilibrium, arbitrageurs use the new collateral type to conduct arbitrage. The share of USDC collateral used by arbitrageurs increases as the USDC volatility declines. A comparative statics exercise shows that the addition of a stable collateral type causes a decline in the DAI premium in the bad state, and a decline in the volatility of the DAI peg. This is consistent with stable collateral leading to a decrease in the limits to arbitrage. Arbitrageurs now require a lower premium to borrow DAI and sell it in the secondary market.

We present empirical evidence to support model predictions. We use the entire history of data on individual Collateralized Debt Positions (CDP), which includes the amounts of ETH collateral deposited, DAI borrowed, and the timestamp of each transaction. Consistent with model predictions, we find DAI borrowings respond positively to an increase in ETH returns.

We then test the channels through which collateral risk can generate peg-price deviations and volatility. The first channel is fluctuations in speculative beliefs on the collateral. Through the lens of the model, an increase in collateral risk reduces the capacity of arbitrageurs to deposit ETH collateral, borrow DAI tokens and sell them in the secondary market at a premium. The limits to arbitrage cause peg-price deviations to persist, and an increase in peg volatility. Second, extreme declines in the price of collateral result in liquidation events. The corresponding decline in supply cause peg-prices to increase, all else equal. Third, premiums can occur in periods of elevated demand, and are triggered in the bad state due to safe-haven effects.

We empirically test the contemporaneous correlation between the DAI price and ETH returns, liquidations and demand shocks. Consistent with our hypothesis, we document a significant negative correlation between DAI prices and ETH returns. Our model chan-

nel of speculative beliefs can rationalize this result; a bad state of ETH collateral causes investors to deleverage, reducing DAI supply and generating a premium. Large drops in ETH prices can result in a substantial decline in DAI supply and significant peg premiums. For example, on 12 March 2020, known as *Black Thursday* to the cryptocurrency community, ETH crashed by up to 50% in a single day and resulted in a DAI peg-premium of 800 basis points, and 10 Million USD of liquidations of ETH collateral.

We quantify the relative importance of collateral risk, liquidations and secondary market demand through an analysis of variance (ANOVA) of our explanatory variables. For peg-prices, our decomposition reveals that speculative beliefs play an important role: ETH returns is the most robust predictor of peg-price deviations explaining up to 51.1%, followed by liquidations at 30.5% and the stability fee at 13.2%. For intra-day volatility, we find liquidations is the biggest contributor at 42.9%, followed by the changes in DAI trading volume at 42.7%, and ETH volatility at 13.7%. Taken together, our model channel of speculative beliefs is therefore quantitatively significant in explaining DAI premiums and the observed negative correlation between DAI prices and ETH returns. In contrast, elevated DAI volatility can be explained by periods of high secondary market demand and liquidations.

To mitigate the collateral risk, MakerDAO attempted to increase the share of DAI borrowing through stable collateral types since March 2020. The introduction of USDC collateral was in direct response to the *Black Thursday* event of March 2020, to reduce the exposure of the DAI peg to mass liquidations from a risk-off event in the crypto market. Empirically, we find an increase in the share of stable collateral by 1% reduces the DAI price and the volatility of the DAI peg by approximately 0.5 basis points. This is consistent with the model prediction of stable collateral increasing the capacity for arbitrageurs to step in and absorb differences between the primary and secondary market rates.

In addition to depositing USDC collateral, the MakerDAO protocol introduced a peg stability module (PSM) in December 2020. Investors can directly swap DAI for USDC at a 1:1 rate.[3] By eliminating liquidation risk for investors, the PSM incentivizes arbitrage participants to swap USDC for DAI when DAI prices trade at a premium. The increase in DAI supply by arbitrageurs pushes prices toward one. We document a decline in both the magnitude of peg-price deviations and intra-day volatility of approximately 70 basis points after the introduction of PSM on December 18th, 2020. To rule out the possibility of a tighter peg due to idiosyncratic developments in the USDC stablecoin, we test a difference-in-difference (DiD) design to determine how DAI/USD prices changed relative to a control group of USDC/USD prices. The results of the test confirm the findings

3. A technical difference between the PSM and having stable collateral type is liquidation risk. For example, if investors deposit USDC collateral into a vault, there is risk of a collapse of the USDC peg which can trigger a sufficient decline in the value of collateral and a liquidation event.

of an increase in peg efficiency. Relative to the USDC/USD price, we find a decline in absolute peg-price deviations of 101.8 basis points, and a 61.0 basis point decline in volatility following the PSM. Following the PSM, the increased ability of arbitrageurs to short sell DAI results in a compression of peg premiums.

The peg is naturally more resilient to extreme declines in the price of collateral, with smaller premiums and a shift toward safe collateral during an extreme ETH price decline in May 2021. However, the PSM means the peg is more exposed to run-risk in USDC. We show that DAI prices mirrored USDC's de-pegging event in March 2023. To diversify against USDC run-risk, the Maker protocol has voted to increase their holdings of U.S. Treasuries by tokenizing their reserves.

The remainder of the paper is structured as follows. In Section 2 we summarize the contributions of our paper to related literature. In Section 3 we summarize the properties of DAI and describe the data sources for our empirical work. In Section 4 we introduce the model of DAI prices. We produce testable implications on the determinants of the price and a discussion of stability tools. In Section 5 we conduct our empirical analysis. Section 6 concludes.

2 Related literature

The empirical research most closely related to our paper focuses on investigating properties of stablecoins (Berentsen and Schär 2019; Bullmann, Klemm, and Pinna 2019; BIS 2019; Eichengreen 2019; Dell'Erba 2019; Arner, Auer, and Frost 2020; Frost, Shin, and Wierts 2020; Force et al. 2020; Barthelemy, Gardin, and Nguyen 2021), arbitrage in stablecoin and cryptocurrency markets (Lyons and Viswanath-Natraj 2023; Makarov and Schoar 2019, 2020; Borri and Shakhnov 2018; Pernice 2021), governance and voting behavior of decentralized stablecoin protocols (Gu, Raghuvanshi, and Boneh 2020; Zhao et al. 2022; Sun, Stasinakis, and Sermpinis 2022) and intraday price changes to support the role of stablecoins as safe-havens (Baur and Hoang 2020; Baumöhl and Vyrost 2020; Wang, Ma, and Wu 2020; Bianchi, Rossini, and Iacopini 2020; Gloede and Moser 2021). An example is provided by Eichengreen (2019), who notes that stablecoins can be backed by national currencies or cryptocurrencies and that these systems can be vulnerable to speculative attacks if the peg is perceived to be under-collateralized. Empirical evidence supporting an arbitrage mechanism for dollar-backed stablecoins is found by Lyons and Viswanath-Natraj (2023). This mechanism involves private investors depositing (withdrawing) dollars when the stablecoin trades at a premium (discount), which drives prices toward one. Our thesis of collateral risk argues that stablecoins backed by risky collateral lack a functioning arbitrage mechanism to stabilize the peg, making collateral risk a limit to arbitrage. We show, both empirically and through our model, that the addi-

tion of stable collateral types increases the role of arbitrage in stabilizing the peg. The differences in volatility across stablecoin regimes are also empirically supported by Jarno and Kołodziejczyk (2021), who compare the volatility of dollar-backed, crypto-backed, and algorithmic (un-collateralized) stablecoins and find that the peg-price deviations of crypto-collateralized stablecoins are larger and more dispersed.

Our contribution to the existing literature on DeFi (Harvey, Ramachandran, and Santoro 2021; Schär 2021) focuses on the use of decentralized stablecoins and DeFi lending protocols, such as Compound, which use algorithms to set interest rates and allocate funds (Gudgeon et al. 2020; Perez et al. 2020; Qin et al. 2021; Lehar and Parlour 2022; Chiu et al. 2022). Decentralized exchanges, or automated market makers (AMMs), which use algorithms to trade without the need for a limit order book, are another popular DeFi application on the Ethereum blockchain. Research has been conducted on the design of AMMs, the role of arbitrage and liquidity provision, and the competition between DEXs and centralized exchanges, and governance risk(Angeris and Chitra 2020; Capponi and Jia 2021; Aoyagi and Ito 2021; Lehar and Parlour 2021; Barbon and Ranaldo 2021; Park 2022; Han, Huang, and Zhong 2021; Zhao et al. 2022). DAI is mainly used as a source of savings in lending protocols and in liquidity pools for trading on decentralized exchanges. While Perez et al. (2020) find that lending protocols are susceptible to liquidation risk, we complement their findings by examining how liquidation events for DAI affect the dynamics of the peg. Additionally, we are the first to use rich data on the universe of CDP positions to shed light on the determinants of individual CDP leverage and the probability of liquidation. Our analysis shows that the borrowing of DAI by individual investors decreases with respect to ETH returns, ETH volatility, and higher interest rates. Liquidations are more likely during periods of extreme negative returns and high volatility of ETH collateral.

Recent work has modeled the price dynamics of stablecoins (Routledge and Zetlin-Jones 2021; Klages-Mundt and Minca 2020; Li and Mayer 2020; d'Avernas, Bourany, and Vandeweyer 2022). Routledge and Zetlin-Jones 2021 adapt a model of fixed exchange rates with speculative attacks to stablecoins and point out that centralized stablecoin regimes can collapse due to expectations of insufficient backing of dollar reserves. Klages-Mundt and Minca 2020 model over-collateralized stablecoins and show that high liquidation costs can lead to CDPs optimally creating a reserve buffer by posting excess collateral to insure against extreme negative price movements. They also model the dynamics of liquidation events on DAI peg-price premiums. Li and Mayer 2020 examine a centralized issuer of dollar-backed stablecoins that has autonomous control of token supply and maximizes the dividend of shareholders that own a governance token. Through the lens of their model, the issuer conducts open market operations to stabilize the price around its peg. Under this centralized arrangement, they consider reserve management

and over-collateralization as potential solutions to avoid speculative attacks and peg discounts. d'Avernas, Bourany, and Vandeweyer 2022 determine the equilibrium conditions in which both dollar-backed and decentralized stablecoins backed by crypto collateral can maintain parity in response to a negative demand shock or a liquidation of collateral. With respect to decentralized stablecoins, they show that a buffer reserve maintained by the governance protocol can be used as a stabilizing mechanism to restore peg stability in response to peg-discounts, similar to reserve management of a central bank.

We contribute to a literature on arbitrage with financial constraints (Gromb and Vayanos 2002, 2018; Brunnermeier and Pedersen 2009; Nyborg and Rösler 2019) and draw insights from Brunnermeier and Pedersen (2009) and Gromb and Vayanos (2018). Brunnermeier and Pedersen (2009) investigate the relationship between funding margins, asset prices, and market liquidity. Although our model assumes an exogenous process for collateral, we test the possibility of feedback effects from DAI liquidations to ETH prices in Appendix D and find no statistically significant effect on ETH returns. Gromb and Vayanos (2018) show that shocks to arbitrage capital can increase spreads and risk-premia. In our paper, we contribute to this literature by introducing an alternative limit to arbitrage, namely, the riskiness of capital via stable and risky collateral types. We model the role of arbitrageurs and show that risky collateral generates a limit to arbitrage. We demonstrate that in equilibrium, arbitrageurs can use stable collateral to conduct arbitrage, increasing relative supply in response to peg-price premiums and driving prices back towards one. This is supported empirically by the introduction of the USDC collateral type in 2020, which led to a significant decline in the absolute size and intra-day volatility of peg-price deviations. Our paper's focus on the limit to arbitrage via the riskiness of collateral types adds to the existing literature on arbitrage with financial constraints.

3 Definitions and data

3.0.1 DAI creation process

An investor can initiate a collateralized debt position (CDP) by depositing a specific amount of collateral, such as ETH, into a vault. They are then able to borrow a fraction of their collateral as DAI tokens. The CDP's valuation of collateral and DAI borrowings is regulated by a set of autonomous contracts that adjust in real-time. There are three primary use cases for DAI tokens. Firstly, DAI can be deposited as savings in the DAI savings protocol, where the MakerDAO protocol sets the DAI savings rate as a potential stability tool.[4] Secondly, DAI is a popular currency for use in decentralized finance (DeFi)

4. Adjustments of the DAI savings rate is set by the MakerDAO protocol as a potential stability tool, which we discuss in more detail in a following section.

protocols such as Compound, which employ algorithms to automatically set interest rates and allocate funds. As of 10 May 2021, over 4 billion USD of DAI savings have been lent in the Compound protocol, with lending rates hovering around 3% per annum.[5] Thirdly, DAI can be used as a vehicle currency to purchase other cryptocurrencies, such as BTC and ETH. To close a CDP position, an investor must first redeem all DAI tokens by either selling the investment currency for DAI tokens in the secondary market or removing their DAI savings from the DSR or a DeFi lending protocol. Once all borrowed DAI tokens have been redeemed, the smart contract is adjusted to unlock the collateral, resulting in the closure of the CDP.[6]

3.0.2 Leverage Ratio and Liquidations

The CDP requires investors to over-collateralize their borrowings, which means that the leverage ratio is calculated as the ratio of generated DAI (with a smart contract price of 1 USD) to the collateral value in USD, as shown in Equation (1).

$$\text{Leverage Ratio} = \frac{\text{Generated DAI}}{\text{Collateral Price} \times \text{Collateral Amount}} \times 100 \tag{1}$$

If the ETH price falls, an investor can inject more ETH collateral or redeem DAI to maintain their collateral level. Each vault has a maximum leverage ratio, which we denote as Leverage Ratiomax. For ETH collateral, the maximum DAI that can be borrowed is two-thirds of the dollar value of the ETH collateral, hence Leverage Ratio$max = \frac{2}{3}$. The Maker Protocol calculates a real-time liquidation price using Equation (2), which is the price of collateral at which the Vault leverage is equal to the maximum leverage ratio. If the collateral price falls below the liquidation price, a liquidation event is triggered.

$$\text{Liquidation price} = \frac{\text{Generated DAI}}{\text{Collateral Amount}} \times \frac{1}{\text{Leverage Ratio}_{max}} \times 100 \tag{2}$$

In a liquidation event, the investor is required to repay the DAI debt using their remaining collateral and pay a liquidation penalty. For example, at an ETH price of 100 USD, DAI borrowings of 100 USD, and 2 ETH, the leverage ratio is 50%, and the liquidation price is 75 USD, as calculated in Equation (2). Suppose the ETH price falls below the liquidation price to 60 USD in the next period. As the new ETH price is lower than the liquidation price, DAI borrowings are liquidated to zero. To pay off the DAI loan, the investor needs to cover the total value of the loan through their ETH collateral, which is 120 USD at the new price. Subtracting the value of the DAI loan gives a post-

5. See `https://compound.finance/markets` for more details.
6. We outline the steps in creating DAI in a schematic in Appendix A.

liquidation amount of ETH collateral equal to 20 USD or $\frac{1}{3}$ ETH. To pay off the loan, the smart contract forces an auction of $\frac{5}{3}$ ETH.

The MakerDAO system enforces an auction mechanism through smart contracts that sell the system collateral and burn DAI tokens. When a vault becomes under-collateralized, a set of agents called keepers triggers a liquidation. The collateral is put up for auction to cover the outstanding DAI and a liquidation penalty. Once the bid reaches the amount of the DAI loan plus any liquidation fees, the auction reverses, and bidders compete by offering to accept less collateral for the DAI they bid in the previous phase. Once an auction settlement is reached, the bidder receives the sold collateral, and an amount of DAI equal to the loan and liquidation fees is burned from the system. The Vault owner receives leftover collateral, if any remains.

The vault owners in the MakerDAO system are incentivized to maintain low leverage to prevent liquidation events. To achieve this, they can set up price alerts for the collateral asset(s) being used or develop a rule to recapitalize when the collateral price falls below a certain level. Additional safeguards have been put in place by MakerDAO governance in the event liquidation auctions do not raise sufficient funds to cover the outstanding DAI and penalty fees, which are detailed in Appendix F.

In addition to paying off the loan, investors are required to post penalty fees that can be up to 15% of the borrowed DAI. These fees make liquidation costly and encourage investors to post sufficient collateral as a buffer against extreme price movements. Figure 1 shows the USD price response, the ETH price, and DAI liquidations on March 12th, 2020. Extreme price changes in the collateral caused a large liquidation, contraction in DAI borrowings, and significant peg-price premiums, as evidenced by DAI premiums of up to 800 basis points following a 50% daily decline in ETH prices. Due to congestion on the blockchain, Vault owners experienced delays in attempting to add more collateral and redeem DAI tokens within the Protocol's one-hour window. Gas prices, measured in GWEI, spiked to over 100 GWEI per transaction from the 10 GWEI average seen just one day prior. Gas prices, as well as daily amounts of Ether Gas used, are provided on `https://ethgasstation.info/`. For more information on gas prices, see `https://blockonomi.com/ETH-gas-prices-surged/`. The drop in collateral value triggered liquidation auctions for approximately 1,200 Vaults and led to a peak liquidation value of around 10 million USD on March 12th.

The failure of the auction mechanism created pressure on the DAI peg. Keepers, who sell DAI tokens for collateral from the auctions, did not have sufficient DAI liquidity to participate in the auctions. To burn DAI from liquidations, the governance body decided to auction MakerDAO tokens (MKR) as an effective open market operation, diluting MKR's value. Further details on the dynamics of the MKR price can be found in Appendix F. For more information on the MakerDAO liquidations in March 2020,

please refer to MakerDAO's public release on the event at https://blog.makerdao.com/the-market-collapse-of-march-12-2020-how-it-impacted-makerdao/.

3.0.3 DAI stability rate

The MakerDAO protocol employs various tools to address situations where the DAI coin is trading persistently above or below parity. One such tool is the stability fee on DAI, which can be thought of as similar to an interest rate on money set by a central bank. However, unlike central banks, DAI's stability fee is determined through a decentralized, continuous voting process for approving rate changes. Voters can select from a range of options for the future stability rate, and if the number of votes in favor exceeds those against the prior decision, the stability rate will change. [7] The stability rate is intended to maintain the peg by adjusting the level of DAI borrowings and, consequently, the system's leverage. Holding all else constant, a higher stability fee increases the cost of DAI borrowings and reduces the system's total leverage.

3.0.4 Multiple Collateral DAI and the peg stability module

On November 18th, 2019, the MakerDAO protocol underwent a significant change with the introduction of multiple collateral types. Instead of relying solely on risky collateral types, users can now lock in alternative types of collateral, such as WBTC, which is a token pegged to BTC prices trading on the Ethereum blockchain. The MakerDAO community further adopted the stablecoin USDC as collateral on March 12th, 2020, allowing for a much higher degree of leverage than with other collateral types due to the stablecoin's leverage ratio of one.

To incentivize the use of stable collateral types, the Maker Protocol introduced the peg stability module (PSM) in December 2020. Through the PSM, users can swap DAI with the USDC stablecoin, effectively anchoring the DAI/USD peg to the value of USDC. This process allows users to swap USDC with DAI at a 1:1 rate without having to create a vault and deposit collateral. Although there is no liquidation risk, users are required to pay a one-time fee to use the PSM, increasing the incentive for arbitrageurs to close peg-price deviations using this module.

The PSM differs from having stable collateral types in terms of liquidation risk. Depositing USDC collateral into a vault, for instance, entails the risk of a collapse in the USDC peg that can trigger a decline in the value of the collateral and a liquidation event. In contrast, the PSM transfers the liquidation risk to the Maker Protocol. The protocol will exchange DAI for USDC tokens at a 1:1 rate even when USDC prices are trading at

7. Votes are cast by staking the Maker Governance token MKR, with 1 MKR locked equal to 1 vote. For further details on the fundamental valuation of the MKR token, please refer to Appendix F.

a significant discount, making it a more secure option for users.[8] We discuss the effects of the March 2023 USDC de-pegging event on DAI governance in Section 5.3.5.

3.1 Data and summary statistics

We have utilized a data set that records every transaction made by an individual CDP to test the effects of collateral returns on the borrowing behavior of investors. The data set includes amounts of ETH collateral deposited, DAI borrowed, and the timestamp of each transaction. "Lock" and "free" are defined as the actions of depositing and closing the ETH CDP, respectively, while the action of the investor borrowing and redeeming DAI tokens is classified as a "draw" and "wipe," respectively. The sample starts on January 1st, 2017, and ends on November 17, 2019.[9]

For an individual CDP, we can trace the amounts of ETH collateral and the amounts of DAI borrowed and redeemed at any point in time. This allows us to calculate a real-time leverage ratio, defined as the ratio of total DAI borrowed to the value of ETH Collateral. Aggregate data on the amounts of DAI borrowed for each collateral type is obtained at `https://makerburn.com/#/`. The dataset also provides policy parameters, such as the stability rate on borrowings and the debt ceilings for each collateral type. For the total amounts of each type of collateral deposited in the system, we use data from DuneAnalytics, an open-source platform with statistics on decentralized finance applications `https://duneanalytics.com/hagaetc/maker-dao---mcd`. Consolidating DAI borrowings with total collateral, we can calculate the total system leverage, as well as the leverage of each collateral type. DAI liquidations and governance token MKR mints and burns are available at `https://www.mkranalytics.com/`.

To obtain price data on ETH, DAI, and other collateral types, we use `https://www.coinapi.io/`. Coinapi offers a monthly subscription with access to their data API, which gives historical cryptocurrency OHLCV data. Where multiple cryptocurrency exchanges offer the same data, we choose the exchange that (i) has the longest time series and (ii) is one of ten exchanges that has "trusted volume" according to a report filed by the SEC.[10] For the pairs of ETH/USD, DAI/USD we use price data from the Bitfinex exchange from 13 April 2018 to 31 March 2021, and for the USDC/USD pair we use price data from the Kraken exchange available from 8 January 2020 to 31 March 2021.

8. Further details on how the PSM works can be found at `https://community-development.makerdao.com/en/learn/governance/module-psm/`.

9. The dataset is obtained from Mike Mcdonald, who developed an online mkrtools application that recorded investor transactions for the single collateral version. The ending date of November 17, 2019, corresponds to the date at which users migrated from the single to multi collateral DAI system.

10. See `https://www.sec.gov/comments/sr-nysearca-2019-01/srnysearca201901-5164833-183434.pdf`. The report tests exchanges for fraudulent activities (e.g., suspicious variability in bid-ask spreads, systematic patterns in histograms of transaction size) and finds that the exchanges we use price data from do not have the telltale patterns in trading volume or spreads.

In Table 1, we provide summary statistics for DAI and ETH returns as well as system parameters for stability rate and leverage over the entire sample period from April 13, 2018, to March 31, 2021. In Figure 2, we show the time series of DAI and ETH prices, stability rate, and leverage. On average, DAI peg-price premiums are 100 basis points over the entire sample period. The average ETH return is 0.17%, with a standard deviation of 5.8%. The largest decline in ETH returns occurred on March 12, 2020, with a -58.2% decline. The stability rate for borrowing DAI in ETH vaults is typically 3% on average, with high interest rates of 20% set in 2019. The leverage ratio for ETH collateral is 0.3 over the entire sample period, which is much lower than the maximum leverage of two thirds. This low system leverage provides a capital buffer in case of a collapse in collateral value. With a leverage ratio of 30%, the ETH price can drop by 50% in one day, and the CDP is still sufficiently collateralized.

To understand the relationship between prices and system parameters, we provide a correlation matrix of all variables in Table 2. We find a negative correlation between DAI and ETH returns of -0.05, with peg-price premiums being associated with negative ETH returns. We also observe a negative correlation of -0.34 between DAI leverage and stability rate, indicating that high borrowing rates on DAI are associated with a decline in DAI borrowings and system leverage. Finally, the stability rate is negatively associated with DAI price (-0.19). This interest rate-setting for DAI borrowing responds to peg-price deviations, with stability rates being increased during periods of discounts and decreased during periods of premiums.

4 Model

To structure our testable hypotheses, we first introduce a model with three types of agents: ETH speculators, arbitrageurs, and safe-haven demand. Speculators deposit ETH collateral and borrow DAI tokens to invest in risky cryptocurrencies, while arbitrageurs take long or short positions in DAI based on mispricing of the peg. Safe-haven demand for DAI captures its role in algorithmic lending and other DeFi applications, allowing users to deposit DAI and accrue savings. The primary goal of the model is to provide testable implications on leverage and peg stability mechanisms.

We show that peg-premiums differ depending on the level of safe-haven demand, with high demand leading to significant premiums that arbitrageurs require to short DAI and clear the market. We also demonstrate that peg-premiums occur when collateral prices are in a bad state, resulting in a negative covariance between peg-prices and returns on ETH collateral. Furthermore, we reveal that an increase in collateral volatility leads to higher peg-price premiums, a decline in investor borrowings and leverage, and an increase in the volatility of peg-price deviations.

Finally, we discuss stability tools, including the interest rate on DAI borrowings and the introduction of stable collateral types. We demonstrate that a rise in the interest rate on DAI borrowings leads to price increases, while stable collateral reduces arbitrageurs' exposure to collateral risk and results in smaller premiums needed to absorb safe-haven demand and clear the market.

4.1 Timing

We present a two-period model where investors open a CDP by depositing non-stable collateral, ETH, into a MakerDAO vault before trading begins. The first period is a trading round where DAI tokens are borrowed and secondary market trading occurs for two cryptocurrencies - non-stable ETH and stable DAI. Cash is denominated in dollars and earns a constant rate of return r. We assume investors are small and price-takers in the markets for ETH and USD, and thus, the USD rate and ETH prices are exogenously given. ETH speculators and/or arbitrageurs borrow DAI tokens in response to a demand shock for DAI in the secondary market during period 1. In period 2, all investors close their CDPs and redeem all DAI tokens without secondary market trading. DAI prices are determined by market clearing conditions in period 1, and we assume zero net supply of DAI. The timing of the model is shown below.

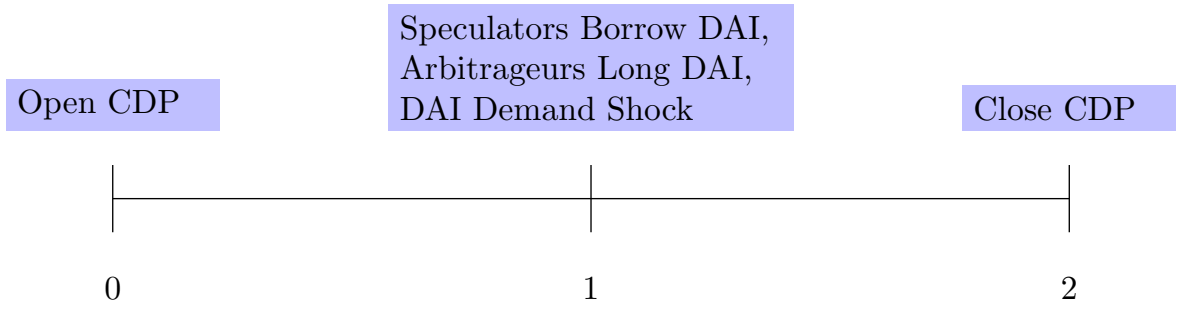

The price of DAI in period t is denoted as p_t, and in period 2, DAI is liquidated at the risky price p_2 with mean 1 and variance σ^2, as MakerDAO does not guarantee 1:1 parity of DAI to USD during a liquidation event. Additionally, it is possible that the governance body can vote to change the target rate of 1 in a case of instability episodes. The DAI stability rate and saving rate are denoted as i^B and i^L, respectively, with $i^L < i^B$. The return on ETH in period 2 is a random variable R^E with mean μ^E and variance σ_E^2.

4.2 Agents

The model comprises three investor types: ETH speculators, arbitrageurs, and safe-haven DAI demand. In the first period, ETH speculators invest their wealth W_1^s in ETH and determine the optimal amount of leverage to issue DAI, maximizing their expected utility function. Speculators' beliefs about ETH's expected return are influenced by

their sentiments, which are based on the state of nature $s = G$ or B, occurring with probabilities π and $1-\pi$, respectively. They believe that the expected return on ETH is higher in state G than in state B, and these beliefs can be affected by recent performance.

Arbitrageurs observe the DAI price and finance their positions by borrowing any amount in USD at the Dollar rate r. If DAI is trading at a discount, they buy it in the secondary market and earn i^L on their DAI holdings. If DAI is trading at a premium, they issue DAI tokens and deposit ETH collateral into the vault at the highest possible leverage ratio $\bar{\theta}$. Arbitrageurs do not have any sentiment towards ETH and believe that its returns are serially uncorrelated, with the expected return being $\mu^A = \mu^E$. Both speculators and arbitrageurs have the same mean-variance risk preferences, with a risk aversion coefficient γ.

Safe-haven demand is modeled as an aggregate demand D from customers seeking safety during periods of unstable coin collapse or having intrinsic needs to purchase a stablecoin currency. It captures DAI's use in decentralized finance protocols, such as Compound, that set interest rates and allocate funds through algorithms. To model the safe-haven effect of DAI, we assume that demand changes depending on the state of ETH collateral: $D(B) > D(G)$. In the baseline calibration, demand is set to zero in the good state and positive in the bad state, capturing the safe-haven component of stablecoins that typically appreciate during downturns in risky crypto asset prices (Baur and Hoang 2020).

We describe the structure of the model and speculators' demand backward starting from period 2, where there is no trading. Each investor type converts their ETH positions into USD based on the realization of the return distribution. Additionally, DAI is liquidated at the final liquidation price p_2. In period 1, speculators' demand is formed by leveraging their ETH positions with DAI and converting it into ETH, with their leverage ratio θ being optimally calculated by maximizing their expected utility function given their beliefs in period 1. Their wealth W_2^s evolves as shown in Equation (3):

$$W_2^s = W_1^s \left(R^E(1+\theta p_1) - \theta p_2 - \theta i^B \right). \tag{3}$$

The first term of this expression is the return earned on the leveraged position of ETH, the second term is the USD amount of DAI the speculators buy back to release their collateral, and the third term is the DAI borrowing fee paid by the speculators.

The arbitrageurs' wealth changes according to the following dynamics:

$$W_2^a = \begin{cases} W_1^a \left(\omega(1+i^L)p_2/p_1 + (1-\omega)(1+r) \right), & \omega \geq 0, \\ W_1^a \left(-\frac{\omega}{\theta} R^E + \omega(p_2 - p_1(1+r) + i^B) + \left(1+\frac{\omega}{\theta}\right)(1+r) \right), & \omega < 0, \end{cases} \tag{4}$$

where ω denotes the fraction of arbitrageurs' wealth invested in DAI.

The first equation represents the scenario where arbitrageurs buy DAI in the secondary market. They allocate a fraction $(1-\omega)$ of their dollar wealth to risk-free dollar investments, while the remaining fraction is used to buy DAI at the price p_1 and earn the DAI savings rate i^L. In period 2, they convert DAI back to dollars at the price p_2. The dollar profit they earn by going long on DAI is $(1+i^L)p_2/p_1$. Typically, they take a long position to exploit the mispricing when DAI trades at a discount. In theory, they may also purchase DAI at a premium if the profit from the savings rate i^L exceeds the losses from buying DAI at a premium and the risk of holding it.

The second equation pertains to the scenario where arbitrageurs find it more profitable to short-sell DAI. They allocate a fraction $1+\frac{\omega}{\bar{\theta}}$ of their wealth to risk-free dollar investments at the rate r, and use the remaining fraction to purchase ETH collateral. They post $\frac{|\omega|W_1^a}{\bar{\theta}}$ of ETH collateral, borrow $|\omega|W_1^a$ worth of DAI, and sell it for dollars in the secondary market. They then invest the proceeds in risk-free dollar investments at the rate r, and convert back to DAI in the next period. The dollar profit they make by short-selling 1 unit of DAI is given by the term $p_1(1+r)-p_2-i^B$. The DAI savings and borrowing rates i^L and i^B are dollar reference rates, as the investor's wealth is in dollars.

Both types of investors maximize their mean-variance utility functions subject to the evolution of wealth in Equations (3) and (4), and constraints on the share of DAI borrowing, which must lie between 0 and $\bar{\theta}$, the maximum level of leverage an investor can take.

$$U(W_2^j) = \mathbb{E}_1[W_2^j] - \frac{1}{2}\gamma Var_1[W_2^j],\ 0 \le \theta \le \bar{\theta},\ j = s, a. \tag{5}$$

Speculators' optimal leverage ratio for period 1 is given by

$$\theta \ = \ \max\left\{0, \min\left\{\frac{\frac{p_1\mu^E(s_1)-1-i^B}{\gamma W_1^s} - p_1\sigma_E^2}{p_1^2\sigma_E^2+\sigma^2}, \bar{\theta}\right\}\right\}. \tag{6}$$

Arbitrageurs' optimal DAI portfolio weight ω is:

$$\omega \ = \ \begin{cases} \max\left\{0, \frac{\left((1+i^L)/p_1-(1+r)\right)p_1^2}{\gamma W_1^a(1+i^L)^2\sigma^2}\right\}, & U^+(W_2^a) \ge U^-(W_2^a), \\ -\max\left\{0, \frac{\bar{\theta}\left(\mu^A-\bar{\theta}(1-p_1(1+r))+\bar{\theta}i^B\right)}{\gamma W_1^a(\sigma_E^2+\bar{\theta}^2\sigma^2)}\right\}, & U^+(W_2^a) < U^-(W_2^a), \end{cases} \tag{7}$$

where

$$U^+(W_2^a) \ = \ \max_{\omega_1 \ge 0} U(W_2^a) \tag{8}$$

$$U^{-}(W_2^a) \quad = \quad \max_{\omega_1<0} U(W_2^a). \tag{9}$$

Proof: See Appendix B.

Arbitrageurs determine the optimal portfolio weights by assuming $E_1[p_2] = 1$. While they recognize that the objective ETH returns are independent of the state s, there is still a non-zero covariance that arises endogenously. This is due to the beliefs and actions of speculators, as well as the market clearing condition and its impact on the equilibrium price in period 1.

4.3 Equilibrium

Speculators borrow θW_1^s DAI to sell and obtain ETH. Arbitrageurs buy $\omega_1 W_1^a$ DAI (or short sell if $\omega < 0$). Safe-haven demand $D(s)$ is also present. The borrowing of DAI by speculators and the positions of arbitrageurs depend on the price in each state, where $\theta = \theta(p_1, s_1)$ and $\omega = \omega(p_1, s_1)$. Since there is no trading in periods 0 and 2, we focus on the market clearing condition for period 1 given by:

$$0 \quad = \quad -\theta W_1^s + \omega W_1^a + D(s_1) \tag{10}$$

We solve the model numerically to generate testable predictions about equilibrium prices and quantities in the model. We set the following parameter values: $\gamma = 0.5$, $\pi = 0.5$, $W_1^s = \$350$, $\bar{\theta} = 0.66$. The rest of the primitive parameters of the model are calibrated to the sample. Specifically, we set daily rates of returns to: $i^B = 0.0324/252$, $i^L = 0.0139/252$, $r = 0.015/252$, $\sigma = 0.0188$, $\sigma_E = 0.0459$, $\mu_A = 1.0033$, $\mu(G) = 1.0668$, $\mu(B) = 1.0033$. We set μ_A equal to the full sample average of daily ETH return, and $\mu(G)$ to the 90th percentile of ETH return distribution. σ_E is set to the sample standard deviation of ETH daily returns. Finally, we set $D(G) = 0$ and $D(B) = \$50$. These values are chosen to emphasize the safe-haven demand effect. Setting higher values of $D(G)$ will reduce DAI peg discounts in the good state.

The choice of parameters π, γ, and W_1^s is arbitrary, and we present a sensitivity analysis with respect to these parameters in Appendix C. We demonstrate that the model's predictions are largely unaffected by this choice.

4.4 Baseline specification

Figure 3 plots the equilibrium DAI prices for both good and bad states of nature, which refer to high and low ETH returns respectively. Panel A displays the DAI prices for a scenario where there is no safe-haven demand and only speculators and arbitrageurs are trading in period 1. In the bad state, DAI prices trade at par because speculators do not deposit ETH collateral due to their pessimistic beliefs and there is no supply of DAI in

the secondary market. In the good state, speculators deposit ETH collateral and borrow DAI in period 1, which requires arbitrageurs to take a long position in DAI to balance the supply of DAI by speculators. This leads to arbitrageurs buying DAI at a discount to induce a long position.

Panel B plots DAI prices for a specification with safe-haven demand and arbitrageurs but no speculators trading in period 1. Safe-haven demand is endogenous to the state of ETH collateral, and it is zero in the good state and positive in the bad state. In the good state, safe-haven demand is zero and arbitrageurs do not need to supply DAI in the secondary market, leading to DAI prices trading at par. However, in the bad state, DAI prices trade at a premium as arbitrageurs have to absorb the positive safe-haven demand shock from public investors and short sell DAI. This is risky due to valuation effects of collateral, so arbitrageurs charge a premium and are only willing to short sell at high prices.

To create a two-sided distribution of stablecoin prices, the full specification includes speculators, arbitrageurs, and safe-haven demand, and is plotted in Panel C. DAI prices in period 1 correlate negatively with the states of nature of ETH collateral. During the bad state, speculators do not leverage ETH aggressively due to their pessimistic beliefs, and arbitrageurs have to absorb the positive safe-haven demand shock and short sell DAI. Given that shorting DAI is risky due to valuation effects of collateral, arbitrageurs charge a premium and are only willing to short sell at high prices. In contrast, DAI trades at a discount during the good state due to excessive price pressure coming from speculators leveraging ETH and selling DAI. In summary, the model generates a large premium during the bad state and discount during the good state of nature. The following section explores the effects of ETH volatility, the stability rate, and safe-haven demand on the properties of the DAI peg.

4.5 Comparative statics

4.5.1 Volatility of collateral

Figure 4 illustrates the results of comparative statics analysis for period 1 DAI prices, expected DAI price, DAI price volatility, and leverage ratios, with respect to ETH volatility. When ETH volatility is low, speculators borrow more DAI, leading to an excess supply of DAI in the market. This excess supply results in arbitrageurs purchasing DAI at a discount to induce a long position to clear the market. In contrast, when ETH volatility is high, speculators deleverage, and arbitrageurs are required to short sell DAI to clear the market in the bad state of the world. As a result of the short-selling pressure on arbitrageurs, DAI prices in period 1 are higher in the bad state as ETH volatility increases, increasing the volatility of the peg. The channel through which DAI prices are affected is through deleveraging by speculators. Panel D documents a decline in the leverage

ratio of speculators in response to increased ETH volatility. Overall, the stability of DAI deteriorates as the volatility of ETH returns increases.

4.5.2 Stability rate

The stability rate is set by the MakerDAO governance body to target DAI prices, Figure 5 presents comparative statics analysis for period 1 DAI prices, expected DAI price, DAI price volatility, and leverage ratios. As the stability rate increases, the reduction in DAI borrowings by speculators requires arbitrageurs to short sell DAI to clear the market in the bad state of the world. Arbitrageurs charge a premium and are therefore willing to short sell only at high prices, increasing the peg's volatility. Although the stability rate can be used as a policy instrument to control leverage and target DAI prices, quantitatively, it has little effect in stabilizing the peg. Holding all else constant, increasing the stability rate from 0% to 20% increases the expected DAI price by approximately 5 basis points based on numerical calibration.

4.5.3 Safe-haven demand shock

Figure 6 presents comparative statics analysis for period 1 DAI prices, expected DAI price, DAI price volatility, and leverage ratios in periods of low and high safe-haven public demand. This exercise captures, in a stylized way, the demand for DAI due to its use in decentralized finance protocols and its role as a safe-haven. Arbitrageurs have to absorb this demand during the bad state through a peg-price premium. When public demand is low, arbitrageurs do not have to short sell very aggressively. Therefore, peg-premiums and volatility are higher in states of high demand.

Finally, the comparative statics results are robust to changes in system parameters, as shown in Appendix C. The probability of the good state π amplifies the slope of comparative static figures, but does not change the sign. The probability of the good state π amplifies the slope of comparative static figures, but does not change the sign (see Figures A3 - A5). An increase in γ and W_1^s amplify premia and discounts of DAI price deviations, and a decrease in $\bar{\theta}$ amplify premia of DAI price deviations (see Figure A6). The parameter values in the baseline specification are chosen to approximately match the magnitude of DAI price deviations in the data.

4.6 Model extension: multiple collateral types

We introduce the stablecoin USDC as an additional collateral type to be used by arbitrageurs in stabilizing the peg. The expected value of USDC returns is assumed to be$E[R^U] = 1 + r$ and the variance of returns is given by $Var[R^U] = \sigma_U^2$. We also assume

USDC returns are uncorrelated with ETH and DAI returns.[11] Speculators do not invest in USDC and instead put all their wealth into ETH, choosing their optimal leverage ratio θ_1. This is evident from the portfolio choice shown in (6). However, arbitrageurs have the opportunity to reduce their risk by borrowing DAI with USDC collateral and investing in both ETH and DAI. Therefore, the dynamics of the arbitrageurs' wealth in this case can be expressed as follows:

$$W_2^a = \begin{cases} W_1^a \left(\omega(1+i^L)p_2/p_1 + (1-\omega)(1+r)\right), & \omega \geq 0, \\ W_1^a \left(-\frac{\omega^E}{\theta} R^E - \omega^U R^U + (\omega^E + \omega^U)(p_2 - p_1(1+r) + i^B) \right. & \\ \qquad \left. + \left(1 + \frac{\omega^E}{\theta} + \omega^U\right)(1+r)\right), & \omega^U, \omega^E < 0. \end{cases} \tag{11}$$

In the first equation, $\omega \geq 0$ represents the fraction of arbitrageurs' wealth used to purchase DAI, while in the second equation, arbitrageurs short sell $-\omega$ fraction of their wealth. Here, $\omega = \omega^E + \omega^U < 0$, where $\omega^E < 0$ is the fraction of DAI issued by arbitrageurs through ETH collateral and $\omega^U < 0$ is the fraction of DAI issued through USDC collateral. A negative value for ω indicates that arbitrageurs sell DAI after issuing it. It should be noted that the maximum leverage ratio for USDC collateral is limited to 1. The optimal fractions of DAI borrowed through ETH and USDC collateral in the arbitrageurs' portfolio are determined as follows:

$$\omega = \begin{cases} \max\left\{0, \frac{\left((1+i^L)/p_1 - (1+r)\right)p_1^2}{\gamma W_1^a (1+i^L)^2 \sigma^2}\right\}, & U^+(W_2^a) \geq U^-(W_2^a), \\ \omega^U + \omega^E, & U^+(W_2^a) < U^-(W_2^a), \end{cases} \tag{12}$$

where the precise values of ω^E and ω^U are provided in Appendix B.

Figure 7 illustrates the prices of DAI over two periods, representing good and bad states of nature. It is noteworthy that peg premiums are comparatively smaller in the bad state than the baseline specification. When the market is in the bad state, speculators refrain from issuing DAI, and arbitrageurs have to meet the positive public demand to stabilize the market. They can achieve this by shorting DAI and depositing USDC collateral. Arbitrageurs can reduce their risk profile by using two uncorrelated collateral types and by taking advantage of the smaller volatility of USDC. Consequently, they are willing to issue DAI at lower premiums than the baseline equilibrium with only ETH collateral. In contrast, in the good state, the supply of DAI by speculators exceeds public

11. The assumption of zero correlation between the USDC and DAI returns can be justified by the fact that the speculators do not have sentiments about USDC as such; moreover, we show below that speculators do not use USDC as collateral which reduces the dependency of DAI on USDC fluctuations. We provide a proof that speculators only use ETH collateral instead of USDC in Appendix B.

demand, leading arbitrageurs to take a long position in DAI. They purchase DAI at a discount to induce a long position, similar to an equilibrium with only ETH collateral. In summary, the model with USDC collateral generates smaller premiums and peg-price deviations compared to the baseline with only ETH collateral.

Figure 8 presents comparative statics results for period 1 DAI prices (Panel A), the expected DAI price (Panel B), DAI price volatility (Panel C), leverage ratio of speculators (Panel D), and the share of USDC collateral (Panel E).[12] The capacity of arbitrageurs to borrow DAI through USDC collateral can help stabilize the peg and reduce price deviations. In panel E, the share of USDC collateral is decreasing in USDC volatility. Using USDC as collateral reduces the risk profile of arbitrageurs due to smaller volatility of USDC as well as through diversification benefits of using two uncorrelated collateral types.

4.7 Model simulations

To evaluate the model's ability to produce long-lasting deviations from the pegged price, we conduct simulations using data on DAI prices and ETH returns. We estimate the expected returns of ETH in the good and bad states, $\mu_E(G)$ and $\mu_E(B)$, respectively, as the 80th percentile and the sample average based on a rolling window. The rolling window sample standard deviations of daily ETH and USDC returns, σ_E and σ_U, respectively, are used to estimate ETH and USDC volatility. We use a 90-day rolling window for these estimates. The parameters used in the simulations are identical to those in Section 4.3.

Panel A of Figure 9 illustrates DAI prices for both good and bad states based on simulated data from the model. Panel B shows a histogram of the deviations of the DAI/USD price from parity for sub-samples corresponding to pre- and post-PSM periods, where arbitrageurs are able to use USDC as a collateral type in the post-PSM period. [13] Our simulations demonstrate that the model can generate persistent premiums in the bad state and persistent discounts in the good state. Importantly, the histogram of deviations reveals a compression of peg-price deviations in the post-PSM period. Specifically, the increased ability of arbitrageurs to supply DAI using USDC collateral leads to much smaller premiums in the bad state, indicating that the improvement in peg efficiency is asymmetric.

12. We calculate the equilibrium DAI price assuming the expected return on USDC is equal to $\mu^U = 1 + r = 1.015$ and the standard deviation of USD returns $\sigma^U = 0.0013$.

13. The histogram aggregates all DAI prices in the good and bad states in panel A. Therefore it is equivalent to a distribution of DAI prices under the assumption that good and bad states occur with probability 0.5. The sample dates for the pre- and post-PSM are from 18 November 2019 to 17 December 2020 and from 18 December 2020 to 31 March 2021, respectively.

4.8 Model testable predictions

The model generates a number of testable predictions that we can take to the data.

4.8.1 Investor behavior: DAI borrowing

P1.1: *DAI borrowing is positively related to ETH returns*
P1.2: *DAI borrowing is negatively related to ETH volatility*
P1.3: *DAI borrowing is negatively related to DAI stability rate*

These predictions are derived from Equation (6), which shows that the amount of DAI borrowed by speculators is a function of θW_s, where speculators deposit ETH collateral and borrow DAI tokens in the good state to take a leveraged position in ETH. Conversely, in the bad state, they will deleverage and reduce their borrowings of DAI. Thus, we expect DAI borrowings to be positively related to ETH returns and negatively correlated with ETH volatility and the DAI stability rate at an individual investor level.

4.8.2 DAI peg fundamentals

P2.1: *DAI prices are negatively related to ETH returns*
P2.2: *DAI prices are positively related to stability rate on DAI borrowing*
P2.3: *DAI prices are positively related to safe haven demand*
P2.4: *DAI volatility is positively related to ETH volatility*

In our baseline specification in Figure 3, we document a negative co-movement between DAI prices and ETH collateral. In the bad state, speculators deleverage, and arbitrageurs must supply DAI at a premium to absorb public demand. Conversely, in the good state, speculators supply excess DAI, and arbitrageurs take a long position and buy DAI at a discount to clear the market. Our comparative statics exercises in Section 4.5 demonstrate how DAI prices vary with the stability rate on DAI borrowing and safe haven demand.

4.8.3 Introduction of USDC collateral

P3.1: *Arbitrageurs can diversify risk using USDC as collateral type, reducing limits to arbitrage and increasing efficiency of the peg.*
P3.2: *Efficiency of the peg is asymmetric: arbitrageurs have an increased ability to close peg premiums by depositing stable collateral and issuing DAI.*
P3.3: *Attenuation of correlations of the DAI price with risky ETH collateral.*
P3.4: *Share of USDC collateral used by arbitrageurs is increasing in the volatility of ETH and decreasing in the volatility of USDC.*

Figure 7 provides support for the increase in peg efficiency following the introduction of a stable collateral type. Arbitrageurs can use USDC collateral to diversify risk, resulting in smaller premiums in DAI relative to the baseline model with only ETH collateral. Based on our analysis in Figures 7 and 9, we find that the increase in peg efficiency is asymmetric. This is because the addition of USDC collateral provides additional arbitrage capital when arbitrageurs are required to short sell DAI, but not when they take a long position. A compression of peg premiums in the bad state in Figure 7 suggests an attenuation in the correlation between DAI prices and ETH collateral. As the volatility of USDC declines in Panel E of Figure 8, the proportion of USDC collateral utilized by arbitrageurs increases. This allows arbitrageurs to diversify their collateral risk and issue DAI with lower premiums, thereby improving the stability of the peg.

5 Empirical evidence

5.1 Investor behavior: DAI borrowing

In Section 4.8.1, we present testable predictions regarding the determinants of DAI borrowing. We begin our analysis by examining the behavior of individual investors in response to changes in ETH returns, volatility, and policy rates. To achieve this, we utilize the entire transaction history of single collateral DAI CDPs, which includes records of all transactions carried out by individual CDPs, such as amounts of ETH collateral deposited, DAI borrowed, and the timestamps of each transaction. There are eight types of actions that investors can execute, including actions using ETH collateral, such as opening and closing the vault, depositing and withdrawing collateral, and an action to transfer ownership of the ETH vault across digital wallet addresses. Actions using DAI involve borrowing and redeeming DAI tokens, and when the vault is under-collateralized, it triggers a "bite" action, in which the collateral is liquidated to pay off the DAI loan.

We take the total stock of collateral $ETH_{i,t}$ locked in a CDP i at time t and the amount of borrowings $DAI_{i,t}$ locked in the CDP at time t. We then calculate the dollar prices of DAI borrowings and ETH collateral, $P_{DAI,t}$ and $P_{ETH,t}$ respectively, to obtain the dollar value of each component. To prevent investors from over-leveraging, the system has a "bite" action, which is a liquidation event. A bite occurs when the leverage ratio is above the threshold of $\frac{2}{3} \times 100$ percent, at which positions are liquidated.[14] Table 3 summarizes the statistics of DAI borrowing, ETH collateral, the leverage ratio, and liquidations. The sample contains a total of 11,718 CDPs, with an average leverage of 30.55%, well below the threshold leverage of 66.67%. Of the total CDPs, 7,097 have

14. For more details on the nomenclature of each CDP action, please see MakerDAO documentation at `https://docs.makerdao.com/DAI.js/single-collateral-DAI/collateralized-debt-position`.

liquidated at least once during their lifetime, with a maximum number of liquidations of 14 for a single CDP.

We illustrate the time series of the leverage ratio, DAI borrowings, and ETH collateral for two individual CDPs in Figure 10. In the top panel (CDP id 5199), we plot the time series for the CDP with the maximum DAI borrowings and ETH collateral over the full sample. This CDP is an example of an investor who maintains a leverage ratio averaging 30 to 40%. This is well below the threshold level of 66%. In the bottom panel of Figure 10, we show an investor (CDP id 1272) that has the maximum number of liquidation events (14) in our sample. For this CDP, we observe that the leverage ratio calculated based on end-of-day ETH and DAI prices rises above the threshold. In each case, this triggers a liquidation event, when DAI borrowings are reset to zero, and the investor's ETH collateral value declines to pay off the debt. The value of ETH collateral declines by more due to liquidation fees, which amount up to 15% of the value of DAI borrowings.

Figure 11 shows the leverage ratio density for CDPs across the entire sample period from January 2017 to November 2019. The top panel stratifies the sample based on periods of extreme positive returns (greater than +2 std) and extreme negative returns (less than -2 std). The density shifts to the right during periods of negative extreme events, indicating a higher leverage ratio, all else equal. The increase in system leverage during negative events is mechanical, resulting from a decline in ETH collateral. In the bottom panel, the sample is stratified based on high and low interest rates, where high interest rates are above 18%, and low interest rates are below 1%. A bimodal distribution is observed with high interest rates, indicating a higher density towards small loans when interest rates are excessively high.

To formalize the determinants of CDP positions, a panel regression specification is used in Equation (13), where the dependent variable is the amount of DAI borrowing ($DAI_{i,t}$), the amount of ETH collateral ($ETH_{i,t}$), or a dummy variable indicating a "bite" liquidation event ($Bite_{i,t}$) for CDP i at time t. The independent variables include the daily contemporaneous ETH return ($R_{ETH,t}$), intra-day volatility of collateral ($\sigma_{ETH,t}$), and the stability rate on DAI borrowing ($sfee_t$).[15] Individual CDP fixed effects are captured by α_i, controlling for idiosyncratic risk preferences. CDPs with transactions over 30 days in the sample are filtered to create a panel with sufficient observations for all CDPs.[16] This gives us a total of 456 individual CDPs with at least 30 daily observations each.

15. In our model, we rely on $R_{ETH,t}$ as an indicator of speculators' views on future ETH returns, rather than using lagged returns as a predictor of expected returns. This approach is due to our assumption that speculators in our model are not necessarily rational and thus the rational expectations hypothesis cannot be relied upon. Instead, we view speculators as short-term momentum or positive feedback traders who respond to current changes in ETH to establish their speculative positions. Consequently, positive contemporaneous returns are viewed as a sign of a favorable state while negative returns are considered an unfavorable state signal.

16. Statistical bias can occur due to an unbalanced panel with individual CDPs having too few observations.

$$Y_{i,t} = \alpha_i + \beta_1 R_{ETH,t} + \beta_2 \sigma_{ETH,t} + \beta_3 sfee_t + u_{i,t}, \tag{13}$$

Table 4 summarizes the results. An increase in ETH returns by 1% increases DAI borrowing and ETH collateral by 460 USD and 3,434 USD respectively (see columns (1) and (2)). A 1% increase in the stability fee reduces DAI borrowing and ETH collateral by 632 USD and 1684 USD respectively. To estimate the effect of a change in the explanatory variable on the probability of liquidation, a panel probit specification is used in column (3). A 1% increase in ETH returns reduces the probability of liquidation by 7.5%, while a 1% increase in ETH volatility and stability rate increases the probability of liquidation by 12.6% and 1.90% respectively.

5.2 DAI peg fundamentals

In Section 4.8.2, we provide testable predictions on the factors that can generate peg-price deviations and volatility. Using our model, we observe that when there is access to only the risky collateral type, arbitrageurs are less able to deposit ETH collateral, borrow DAI tokens, and sell them at a premium in the secondary market. This limitation on arbitrage leads to the persistence of peg-price deviations and an increase in peg volatility. DAI peg-price premiums typically occur during periods of negative ETH returns and can also occur during periods of high demand, which are triggered by safe-haven effects in the bad state. Other factors that can influence DAI prices include the interest rate on DAI borrowing and decreases in the price of collateral, which can lead to liquidation events.

To empirically test the relationship between DAI prices and ETH returns, liquidations, and demand shocks, we use Equation (14):

$$Y_t = \beta_0 + \beta_1 R_{ETH,t} + \beta_2 \sigma_{ETH,t} + \beta_3 sfee_t + \beta_4 L_t + \beta_5 D_t + u_t. \tag{14}$$

Here, Y_t is the DAI peg-price deviation $\Delta_{DAI,t}$ and the intra-day volatility $\sigma_{DAI,t}$. Intra-day volatility is calculated by taking the square root of the average sum of squared hourly returns over the trading day. The explanatory variables are $R_{ETH,t}$ and $\sigma_{ETH,t}$, which measure contemporaneous returns and intra-day volatility of ETH. We use contemporaneous return to capture the model assumption of extrapolative beliefs of speculators and to proxy signals about the good and bad states of future ETH returns, similar to the specification in Equation (13). [17] $sfee_t$ is the stability rate on DAI borrowings (annualized). L_t measures aggregate liquidations of ETH collateral in USD Million, and D_t measures the percentage change in aggregate secondary market trading volume of

17. To control for the effect of lagged returns, we test for feedback effects in Appendix D and we find negative ETH returns cause persistent peg-premiums.

DAI, which reflects growth in aggregate trading volume in exchanges. All variables are measured in basis points.

The results for peg-price deviations are presented in Table 5. Columns (3) to (5) examine the impact of ETH returns, ETH volatility, and stability fee. In column (3), it is shown that a 1% increase in ETH returns corresponds to a 3.7 basis point decrease in DAI prices, which supports the first model channel of speculative beliefs on collateral. The negative correlation between DAI prices and ETH returns is due to speculators' extrapolative beliefs. In the bad state, investors decrease ETH collateral and DAI borrowings, reducing the supply of DAI and pushing its prices up. In the good state, investors increase ETH collateral and DAI borrowings, increasing the supply of DAI and reducing its price. Columns (4) and (5) reveal that a 1% increase in intra-day volatility of ETH is associated with a 1.3 basis point increase in DAI prices, and a 1% increase in the stability rate is associated with a 3.5 basis point decrease in DAI prices. DAI liquidations and safe-haven demand are also controlled for, as shown in column (1) where liquidations are more likely to occur in periods of negative ETH returns and increased ETH volatility. Column (6) shows that a 1 USD million increase in liquidations leads to a 17.7 basis point increase in DAI price deviations. However, liquidations alone cannot account for the large premiums on *Black Thursday*. The third channel is that DAI premiums exhibit safe-haven properties, as indicated in specification (2) where trading volume growth increases during negative ETH returns and high ETH volatility. Column (7) shows that a 1% increase in secondary market trading volume is associated with a 0.3 basis point increase in DAI price deviations, confirming our hypothesis. Specification (8), which includes all explanatory variables, reveals that ETH returns and safe-haven demand remain statistically significant.

In addition to peg-prices, the model also predicts a positive relationship between peg volatility and collateral risk, as documented in Figure 12. The results for intra-day volatility are summarized in Table 6. In contrast to the analysis on peg-prices, ETH volatility is a stronger predictor of DAI volatility, as shown in column (2) where a 1% increase in ETH volatility leads to a 2.3 basis point increase in DAI volatility. Column (4) shows that a 1 million USD increase in liquidations corresponds to a 10.5 basis point increase in DAI volatility. Column (5) tests the effect of change in DAI secondary market trading volume on DAI volatility and show that a 1% increase in DAI trading volume leads to a 0.2 basis point increase in DAI peg volatility. Finally, column (6), which includes all variables, indicates that trading volume is the only statistically significant variable corresponding to periods of elevated DAI volatility.

5.2.1 Decomposition of Channels

We have demonstrated that various factors, such as speculative beliefs regarding collateral, liquidations, and secondary market trading volume, can account for peg-prices and intra-day volatility. To determine the relative importance of each factor, we conducted an analysis of variance (ANOVA) on our explanatory variables. Figure 13 displays the decomposition of peg-price deviations and intra-day volatility into five explanatory variables, indicating the percentage contribution of each variable to the explanatory sum of squares.

Regarding peg-prices, speculative beliefs are a significant factor, with ETH returns being the most reliable predictor of peg-price deviations, accounting for up to 51.1%. Liquidations come in second at 30.5%, while the stability fee explains 13.2%. For intra-day volatility, liquidations are the most significant contributor, accounting for 42.9%, followed by trading volume at 42.7% and ETH volatility at 13.7%.

Our results suggest that speculative beliefs play a crucial role in explaining DAI premiums and the negative correlation between DAI prices and ETH returns. In contrast, elevated DAI volatility can be attributed to periods of high secondary market trading volume and liquidations.

5.2.2 Robustness: dynamic effects of ETH returns

In Appendix D, we employ a method of local projections, as described in Jordà (2005), to examine the dynamic effects of ETH returns, changes in secondary market demand, liquidations, and the stability rate. This approach controls for feedback effects through lags of the DAI price and other controls.

Our findings are consistent with our earlier analysis, demonstrating that a negative shock to ETH returns, an increase in liquidations, and changes in secondary market demand have persistent effects on peg-premiums and result in reduced aggregate DAI borrowings. Additionally, we show that a shock to the stability rate has a positive, long-term impact on the DAI price. However, this effect is limited by the voting procedure of the MakerDAO protocol, which introduces delays in updating the rates, as well as the existence of a lower bound on the stability rate.

5.3 Introduction of USDC collateral

The MakerDAO protocol introduced USDC collateral to improve stability and during the ETH price collapse on March 12, 2020. A peg stability module (PSM) was also introduced on December 18, 2020, enforcing a 1:1 peg between USDC and DAI. This allowed users to exchange USDC for DAI at a 1:1 rate without creating a vault and depositing collateral, albeit with a one-time fee. We hypothesize that the addition of USDC collateral and the

swap arrangement contributed to the stability of the peg by reducing limits to arbitrage.

In Section 4.8.3, we examine our model predictions. First, we demonstrate that the PSM has led to dynamically more stable peg prices. Second, we show that most of the increase in peg efficiency resulted from compressing peg premiums. Third, we observe that the introduction of USDC collateral has increased peg-sustaining arbitrage and the share of stable collateral. Fourth, we find that stable collateral has reduced correlations between risky ETH collateral and DAI prices, while increasing the sensitivity of DAI to USDC volatility. Finally, we discuss how the PSM can improve resilience to extreme ETH returns and liquidation events, but also expose the peg to USDC run-risk.

5.3.1 PSM and peg efficiency

We proceed to examine the impact of the PSM introduction on the efficiency of the peg. Figure 15 plots the USD denominated prices and intra-day volatility of USDC and DAI stablecoins. A visual analysis of the figure reveals that DAI peg-price deviations and intra-day volatility are higher than those of USDC. Although the volatility decreased immediately after the PSM launch, we observe that the decline in absolute peg-deviations began 2 to 3 months before the launch, which coincides with an increase in the share of USDC collateral in September 2020. To evaluate the increase in peg efficiency, we conduct a difference-in-difference (DiD) analysis presented in Equation (15). The outcome variable $Y_{j,t}$ is either the absolute level of peg deviations $|\Delta_{j,t}|$, or the intra-day volatility of peg deviations $\sigma_{j,t}$ for $j = DAI, U$, both measured in basis points. We estimate:

$$Y_{j,t} = \alpha_0 + \beta\ T_j + \gamma\ post_t + \delta\ post_t \times T_j + u_{j,t}, \tag{15}$$

where the treatment indicator T_j takes a value of 1 for DAI and 0 for USDC, and $post_t$ takes a value of 0 for t prior to 18 December 2020 (the PSM launch date) and 1 afterward. The coefficient δ measures the net impact of peg stabilization relative to any trends in USDC.

Table 7 presents the results of our analysis. We observe an average decline of 53.7 basis points in the absolute level of peg deviations and a 39.9 basis point reduction in intra-day volatility. The differences-in-differences analysis is presented in columns (3) and (4), indicating a net convergence in peg prices of DAI toward USDC prices during the post-PSM period. The DiD coefficients estimated report a decline of 101.5 basis points in the absolute size of peg-price deviations and a 61.2 basis point reduction in intra-day volatility relative to USDC prices. The results suggest that the increase in peg efficiency is attributed to a reduction in limits to arbitrage. The swap arrangement enables arbitrageurs to short sell DAI when it trades at a premium by exchanging USDC for DAI.

An empirical issue we address in Appendix E is whether the difference-in-difference

tests are sensitive to the choice of $post_t$. While we justify our structural change as the PSM launch on 18 December 2020, MakerDAO added USDC as a collateral type on March 12, 2020, and there was a significant use of USDC collateral since September 2020. Therefore, we show that our DiD coefficients are robust to alternative specifications with an earlier treatment date. Using a dynamic DiD, we show that most efficiency gains occurred in Q4 2020, which is consistent with a gradual transition to USDC collateral just before the PSM introduction.

5.3.2 Asymmetric increase in peg efficiency

We found that the efficiency of the peg has increased after the implementation of the peg stability mechanism (PSM), and our model indicates that the increase is asymmetric. The compression of peg premiums is due to arbitrageurs being able to diversify risk when short-selling DAI. In Figure 16, we plot histograms of the distribution of peg-price deviations, which demonstrate that the distribution is skewed towards peg premiums in the pre-PSM period but becomes more symmetric in the post-PSM period. Table 8 displays summary statistics of peg-price deviations, which show that the distribution is much more compact in the post-PSM period with a lower range of peg-price deviations, ranging from -20 to 50 basis points compared to a range of -84.8 to 800 basis points in the pre-PSM period. Moreover, the half-life of peg-price deviations has reduced from 5.95 days to 1.76 days.[18]

To evaluate the stabilizing properties of the pre- and post-PSM periods, we perform a self-exciting threshold auto-regressive (SETAR) analysis. We characterize the peg-price deviation $\Delta_{DAI,t}$ in Equation (16) using three auto-regressive processes based on a low, middle, and high regime, where the middle regime represents a band of inaction.[19]

$$\Delta_{DAI,t} = \begin{cases} \rho_L \Delta_{DAI,t-1} + \epsilon_t, & \Delta_{DAI,t-1} < \Delta_L \\ \rho_M \Delta_{DAI,t-1} + \epsilon_t, & \Delta_L \leq \Delta_{DAI,t-1} \leq \Delta_U \\ \rho_U \Delta_{DAI,t-1} + \epsilon_t, & \Delta_{DAI,t-1} > \Delta_U \end{cases} \tag{16}$$

We estimate the SETAR for the sub-samples pre- and post-PSM, and our results are presented in Table 9. The band of inaction for peg premiums ranges from 24 to 290 basis points in the pre-PSM period, indicating a significant risk in short-selling DAI. Once premiums exceed 290 basis points, the model estimates a half-life of 2.51 days. In

18. To measure the half-life, we run an auto-regressive process of order 1 on the deviations, $\Delta_{DAI,t} = \rho \Delta_{DAI,t-1} + u_t$. The half-life, or the time it takes for a shock to dissipate by 50%, is $T = \frac{log(0.5)}{log(\rho)}$.

19. The low regime is given by the threshold of deviations ranging from $[-\infty, \Delta_L]$, the middle regime is $[\Delta_L, \Delta_U]$ and the high regime is $[\Delta_U, \infty]$.

the post-PSM period, the band of inaction is much smaller, ranging from 1 to 27 basis points, due to the addition of a swap arrangement with USDC that facilitates a risk-free arbitrage opportunity by swapping USDC for DAI when DAI trades at a premium. For deviations in excess of 27 basis points, the half-life is only 0.78 days. Overall, our findings suggest that arbitrageurs have a greater ability to short sell DAI in the post-PSM period, leading to a compression of peg premiums and increased peg stability.

5.3.3 ETH-DAI correlations Pre and Post USDC

We will now assess the model's ability to predict the attenuation of correlations between the DAI price and risky ETH collateral. To test this, we split our sample into two periods: pre- and post-USDC collateral, which is based on the introduction of USDC collateral by MakerDAO governance on March 12, 2020. We utilize the following baseline specifications:

$$\Delta_{DAI,t} = \beta_0 + \beta_1 \Delta_{DAI,t-1} + \beta_2 R_{ETH,t} + \beta_3 \sigma_{ETH,t} + \beta_4 \Delta_{U,t} + \beta_5 \sigma_{U,t} + \beta_6 sfee_t + u_t,$$
$$\sigma_{DAI,t} = \beta_0 + \beta_1 \sigma_{DAI,t-1} + \beta_2 R_{ETH,t} + \beta_3 \sigma_{ETH,t} + \beta_4 \Delta_{U,t} + \beta_5 \sigma_{U,t} + \beta_6 sfee_t + u_t,$$

where $\Delta_{U,t}$ represents the daily peg-price deviations of USDC prices (in basis points).

Table 10 presents the estimation results. Columns (1) and (3) display the pre-USDC collateral period estimates, while columns (2) and (4) exhibit the post-USDC collateral period estimates. As expected, we observe a reduction in the correlation between ETH returns and DAI prices from -0.054 to -0.012 in the post-USDC collateral period. This confirms our hypothesis that the correlation between the good and bad states of ETH returns is weakened following the introduction of stable collateral.[20] In the post-period, we find that USDC is a more substantial predictor of DAI peg prices and volatility than ETH. A 1 basis point increase in USDC volatility raises DAI peg-prices and volatility by 0.8 and 2.2 basis points, respectively.

5.3.4 Determinants of share of stable collateral

We now test the model prediction that the share of stable collateral increases in response to a relative increase in ETH volatility. Figure 14 plots the decomposition of DAI borrowing by collateral type. To construct the share of stablecoin collateral, we combine both stablecoin collateral and stablecoin borrowing via the PSM. This accounts for up to 30% of DAI borrowing over the sample of 12 March 2020 to 31 March 2021. We define the variable $share_t$ to be equal to DAI borrowings from stable collateral types as a fraction of

20. Figure 7 illustrates the model peg-prices before and after the introduction of stable collateral. The introduction of stable collateral weakens the link between the bad ETH state and DAI peg-premiums. The use of stable collateral makes it easier for arbitrageurs to short sell DAI at smaller premiums.

aggregate DAI borrowings. Stable collateral types include stablecoins USDC, TrueUSD and Tether.

In order to determine the fundamentals driving the share of stablecoin collateral, we estimate the following regression model:

$$share_t = \alpha + \beta_1 R_{ETH,t} + \beta_2 \sigma_{ETH,t} + \beta_3 \sigma_{U,t} + u_t. \tag{17}$$

Table 11 presents the main findings of our estimation. In column (3), we observe that a 1 basis point rise in the volatility of USDC leads to a reduction of 1.73% in the share of stable collateral. Although the intra-day volatility of ETH is not statistically significant in column (2), it becomes significant in column (4) after we control for the intra-day volatility of USDC. Specifically, we find a positive association between the share of stable collateral and the intra-day volatility of ETH. In column (4), we observe that a 1 basis point increase in the intra-day volatility of USDC causes a decline of 1.77% in the share of stable collateral, whereas a 1 basis point increase in the intra-day volatility of ETH increases the share of stable collateral by 0.005%. These results confirm our theoretical prediction that arbitrageurs tend to increase the share of USDC collateral in response to an upsurge in ETH volatility (see Panel E of Figure 8).

5.3.5 Peg resilience post PSM: liquidations and USDC run-risk

In this section, two case studies are presented to illustrate the resilience and risks associated with the peg during the post PSM period. The first case study analyzes the May 19, 2021 crypto crash and compares it to the "Black Thursday" crash on March 12, 2020. Figure 17 plots the USD price response, the ETH price, and DAI liquidations in May 2021. In contrast to the "Black Thursday" crash, DAI exhibited much smaller premiums in May 2021, with a peak of 40-50 basis points. Liquidations of ETH were correspondingly smaller at 0.4 USD million compared to 10 USD million. Panel C of Figure 17 shows that DAI borrowing via ETH collateral fell from a peak of 2.75 to 1.75 USD billion over the month of May 2021, while borrowing via the PSM increased from 1 to 2 USD billion, consistent with the PSM reducing limits to arbitrage and increasing the stability of the peg during periods of extreme ETH returns.

The second case study examines the USDC de-pegging event in March 2023, where Silicon Valley Bank, which held cash reserves of USDC, went bankrupt. USDC had reported cash reserves of 3.3 USD billion with SVB. This led to investor concerns and speculation on whether the coin was fully backed. USDC and DAI both fell to approximately 87 cents on March 11th before prices stabilized on March 13th when USDC transferred their cash reserves at SVB to other banking partners (Figure 18).[21] DAI prices mirrored

21. For a full account of USDC's reserve composition and the de-pegging event, readers can refer to `https://www.circle.com/blog/an-update-on-usdc-and-silicon-valley-bank`.

USDC, as the PSM exposed it to USDC run-risk. The resulting increase in supply of DAI put downward pressure on DAI in the secondary market. Furthermore, the PSM increased governance risk, as the protocol held reserves in USDC. A decline in the value of USDC reserves caused investors to speculate on the peg, reducing the demand for DAI in the secondary market. To diversify against USDC run-risk, the Maker protocol voted to increase their holdings of U.S. Treasuries by tokenizing their reserves. Specifically, the protocol increased its holdings of US Treasuries by 500 USD million to 1.25 billion USD, using 750 USDC million worth of reserves from the PSM to make the purchase.[22]

6 Conclusion

This paper investigates the role of collateral risk in maintaining the stability of the DAI stablecoin peg. To understand the dynamics of the peg-price relationship, we introduce a model with three agents: investors who deposit risky collateral and borrow DAI tokens, arbitrageurs who short DAI when the peg trades at a premium, and a demand shock for DAI in period 1 from investors who seek DAI for savings and DeFi applications. In equilibrium, DAI peg-prices depend on investors' beliefs about the collateral's state. The model generates peg premiums (discounts) in the bad (good) state and a positive correlation between the peg's volatility and the collateral's volatility. To dampen peg deviations, stable collateral types are introduced for arbitrageurs to borrow against. The model emphasizes the importance of both state-dependent speculative behavior and safe-haven demand to generate realistic DAI price discounts and premiums.

We provide empirical evidence to support the model's predictions. Using the universe of collateralized debt positions, we find that DAI borrowings and ETH collateral deposited by speculators are lower in periods of extreme negative returns and high collateral volatility. We then turn to fundamental determinants of DAI prices, highlighting that DAI peg-prices are determined through three channels: speculative beliefs about the collateral's state, liquidations, and safe-haven demand. Consistent with the channel of speculative beliefs, they observe a negative correlation between DAI prices and ETH returns. A decomposition analysis reveals that the state of ETH collateral, via ETH returns, is the most important determinant for DAI prices, whereas liquidations and demand contribute more to the peg's volatility. We also document a trend toward peg-price stability since the introduction of the peg stability module in December 2020. Stable collateral increases the capacity for arbitrageurs to step in and absorb differences between the primary and secondary market rates.

Looking to future research, our findings suggest implications for the regulation of stablecoins backed by cryptocurrency collateral. Both our model and empirical evidence

22. For details on the MakerDAO proposal, see `https://twitter.com/MakerDAO/status/1636423561941327873?s=20`.

suggest that stable collateral is a necessary condition for maintaining a stable peg. Although alternative tools like borrowing rates for the stablecoin may have the ability to influence the effective supply, using risky collateral leads to increased volatility in the peg. The relationship between collateral risk and peg volatility can also guide the optimal design of stablecoins. While the Peg Stability Module (PSM) increases the peg's resilience against extreme returns of ETH collateral, the DAI peg remains exposed to the risk of a run on USDC. A key consideration in design is balancing the trade-off between using risky cryptocurrency collateral and the custodial and run risks associated with stablecoin collateral dependent on off-chain reserves. A digital tokenized version of the US dollar, such as a central bank digital currency issued by the Federal Reserve, can provide a dominant solution for stable collateral that minimizes custodial risk. Our conclusion is that stablecoins must be backed by liquid, risk-free reserves to maintain price stability.

References

Angeris, Guillermo, and Tarun Chitra. 2020. "Improved price oracles: Constant function market makers." In *Proceedings of the 2nd ACM Conference on Advances in Financial Technologies,* 80–91.

Aoyagi, Jun, and Yuki Ito. 2021. "Liquidity Implication of Constant Product Market Makers." *Available at SSRN 3808755.*

Arner, Douglas W, Raphael Auer, and Jon Frost. 2020. "Stablecoins: risks, potential and regulation." *Financial Stability Review. Nº 39 (Autumm 2020), p. 95-123.*

Barbon, Andrea, and Angelo Ranaldo. 2021. "On The Quality Of Cryptocurrency Markets: Centralized Versus Decentralized Exchanges." *arXiv preprint arXiv:2112.07386.*

Barthelemy, Jean, Paul Gardin, and Benoıt Nguyen. 2021. "Stablecoins and the real economy." *Available at SSRN 3973538.*

Baumöhl, Eduard, and Tomas Vyrost. 2020. "Stablecoins as a crypto safe haven? Not all of them!"

Baur, Dirk G, and Lai T Hoang. 2020. "A Crypto Safe Haven against Bitcoin." *Finance Research Letters.*

Berentsen, Aleksander, and Fabian Schär. 2019. "Stablecoins: The quest for a low-volatility cryptocurrency."

Bianchi, Daniele, Luca Rossini, and Matteo Iacopini. 2020. "Stablecoins and cryptocurrency returns: Evidence from large bayesian vars." *Available at SSRN 3605451.*

BIS. 2019. "Investigating the impact of global stablecoins."

Borri, Nicola, and Kirill Shakhnov. 2018. "Cryptomarket discounts." *Available at SSRN 3124394.*

Brunnermeier, Markus K, and Lasse Heje Pedersen. 2009. "Market liquidity and funding liquidity." *The review of financial studies* 22 (6): 2201–2238.

Bullmann, Dirk, Jonas Klemm, and Andrea Pinna. 2019. "In search for stability in crypto-assets: Are stablecoins the solution?" *ECB Occasional Paper,* no. 230.

Capponi, Agostino, and Ruizhe Jia. 2021. "The Adoption of Blockchain-based Decentralized Exchanges: A Market Microstructure Analysis of the Automated Market Maker." *Available at SSRN 3805095.*

Chiu, Jonathan, Emre Ozdenoren, Kathy Yuan, and Shengxing Zhang. 2022. "The Fragility of DeFi Lending."

d'Avernas, Adrien, Thomas Bourany, and Quentin Vandeweyer. 2022. "Can Stablecoins be Stable?" *Working Paper.*

Dell'Erba, Marco. 2019. "Stable Cryptocurrencies? Assessing the Case for Stablecoins." *New York University Journal of Legislation and Public Policy, Forthcoming.*

Eichengreen, Barry. 2019. *From Commodity to Fiat and Now to Crypto: What Does History Tell Us?* Technical report. National Bureau of Economic Research.

Force, ECB, et al. 2020. *Stablecoins: Implications for monetary policy, financial stability, market infrastructure and payments, and banking supervision in the euro area.* Technical report. European Central Bank.

Frost, Jon, Hyung Song Shin, and Peter Wierts. 2020. "An early stablecoin? The Bank of Amsterdam and the governance of money."

Gloede, Oliver, and Thomas Moser. 2021. "Crypto Havens: Are Stablecoins Safe Havens?" *Swiss National Bank Working Paper, presented at SNB-CIF Conference on Cryptoassets and Financial Innovation, 20-21 May 2021, Virtual conference, Swiss National Bank, Zurich, University of Basel, Center for Innovative Finance, Basel.*

Gromb, Denis, and Dimitri Vayanos. 2002. "Equilibrium and welfare in markets with financially constrained arbitrageurs." *Journal of financial Economics* 66 (2-3): 361–407.

———. 2018. "The dynamics of financially constrained arbitrage." *The Journal of Finance* 73 (4): 1713–1750.

Gu, Wanyun Catherine, Anika Raghuvanshi, and Dan Boneh. 2020. "Empirical measurements on pricing oracles and decentralized governance for stablecoins." *Available at SSRN 3611231.*

Gudgeon, Lewis, Sam Werner, Daniel Perez, and William J Knottenbelt. 2020. "DeFi protocols for loanable funds: Interest rates, liquidity and market efficiency." In *Proceedings of the 2nd ACM Conference on Advances in Financial Technologies,* 92–112.

Han, Jianlei, Shiyang Huang, and Zhuo Zhong. 2021. "Trust in defi: an empirical study of the decentralized exchange." *Available at SSRN 3896461.*

Harvey, Campbell R, Ashwin Ramachandran, and Joey Santoro. 2021. *DeFi and the Future of Finance.* John Wiley & Sons.

Jarno, Klaudia, and Hanna Kołodziejczyk. 2021. "Does the Design of Stablecoins Impact Their Volatility?" *Journal of Risk and Financial Management* 14 (2): 42.

Jordà, Òscar. 2005. "Estimation and inference of impulse responses by local projections." *American economic review* 95 (1): 161–182.

Klages-Mundt, Ariah, and Andreea Minca. 2020. "While stability lasts: A stochastic model of stablecoins." *arXiv preprint arXiv:2004.01304.*

Kozhan, Roman, and Ganesh Viswanath-Natraj. 2022. "Fundamentals of the MakerDAO Governance Token." In *3rd International Conference on Blockchain Economics, Security and Protocols (Tokenomics 2021).* Schloss Dagstuhl-Leibniz-Zentrum für Informatik.

Lehar, Alfred, and Christine Parlour. 2021. "Decentralized Exchanges." *Working Paper.*

Lehar, Alfred, and Christine A Parlour. 2022. "Systemic Fragility in Decentralized Markets."

Li, Ye, and Simon Mayer. 2020. "Managing Stablecoins: Optimal Strategies, Regulation, and Transaction Data as Productive Capital." *Fisher College of Business Working Paper,* nos. 2020-03: 030.

Lyons, Richard K, and Ganesh Viswanath-Natraj. 2023. "What keeps stablecoins stable?" *Journal of International Money and Finance* 131:102777.

Makarov, Igor, and Antoinette Schoar. 2019. "Price discovery in cryptocurrency markets." In *AEA Papers and Proceedings,* 109:97–99.

———. 2020. "Trading and arbitrage in cryptocurrency markets." *Journal of Financial Economics* 135 (2): 293–319.

Nyborg, Kjell G, and Cornelia Rösler. 2019. "Repo rates and the collateral spread: Evidence."

Park, Andreas. 2022. "Conceptual Flaws of Decentralized Automated Market Making."

Perez, Daniel, Sam M Werner, Jiahua Xu, and Benjamin Livshits. 2020. "Liquidations: DeFi on a Knife-edge." *arXiv preprint arXiv:2009.13235.*

Pernice, Ingolf Gunnar Anton. 2021. "On Stablecoin Price Processes and Arbitrage." In *Financial Cryptography.*

Qin, Kaihua, Liyi Zhou, Pablo Gamito, Philipp Jovanovic, and Arthur Gervais. 2021. "An empirical study of defi liquidations: Incentives, risks, and instabilities." In *Proceedings of the 21st ACM Internet Measurement Conference,* 336–350.

Routledge, Bryan, and Ariel Zetlin-Jones. 2021. "Currency stability using blockchain technology." *Journal of Economic Dynamics and Control:* 104155.

Schär, Fabian. 2021. "Decentralized finance: On blockchain-and smart contract-based financial markets." *FRB of St. Louis Review.*

Sun, Xiaotong, Charalampos Stasinakis, and Georigios Sermpinis. 2022. "Decentralization illusion in DeFi: Evidence from MakerDAO." *arXiv preprint arXiv:2203.16612.*

Wang, Gang-Jin, Xin-yu Ma, and Hao-yu Wu. 2020. "Are stablecoins truly diversifiers, hedges, or safe havens against traditional cryptocurrencies as their name suggests?" *Research in International Business and Finance:* 101225.

Zhao, Xi, Peilin Ai, Fujun Lai, Xin Luo, and Jose Benitez. 2022. "Task management in decentralized autonomous organization." *Journal of Operations Management.*

Figures

Figure 1: DAI price and liquidations response to negative price shock of ETH in March 2020

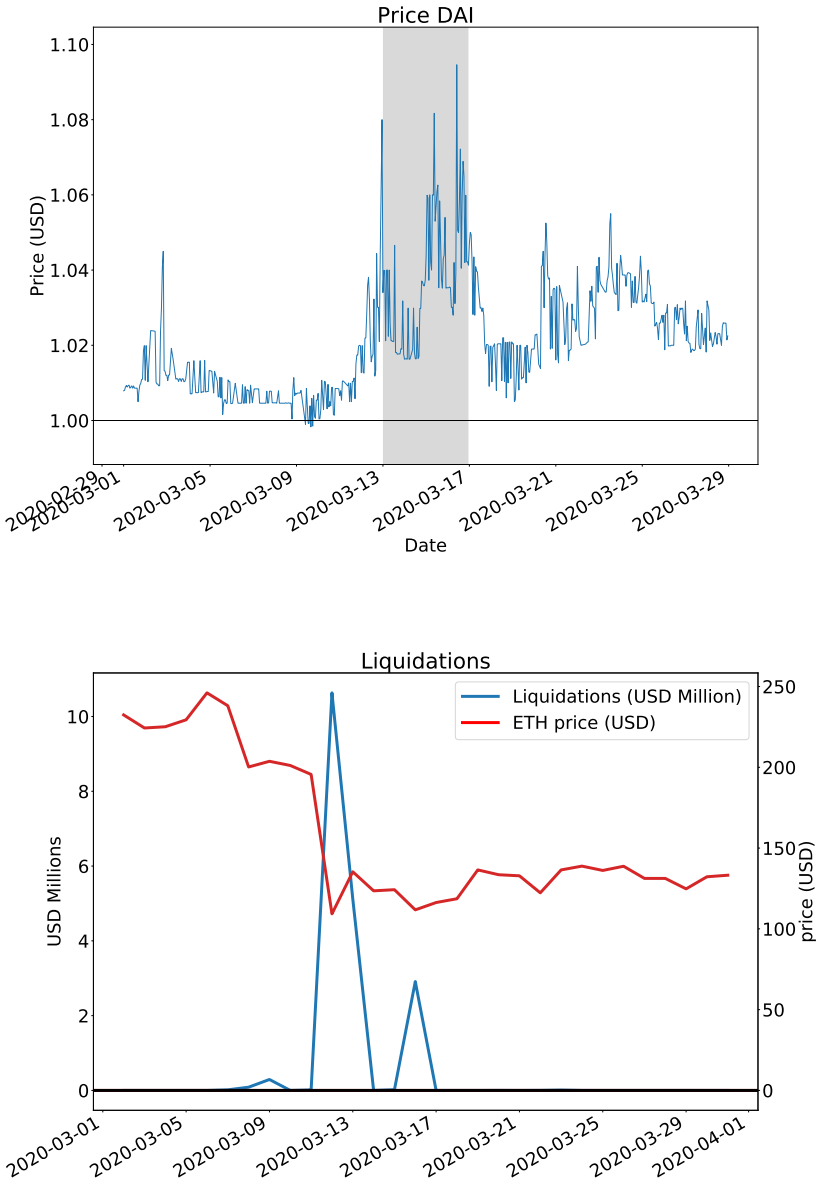

DAI price in USD, ETH price in USD and DAI liquidations during the month of March 2020. Shaded areas indicate the period when the price of ETH fell approximately 50% from 12 March 2020 to 13 March 2020.

Figure 2: DAI price, ETH price, Leverage, Stability rate

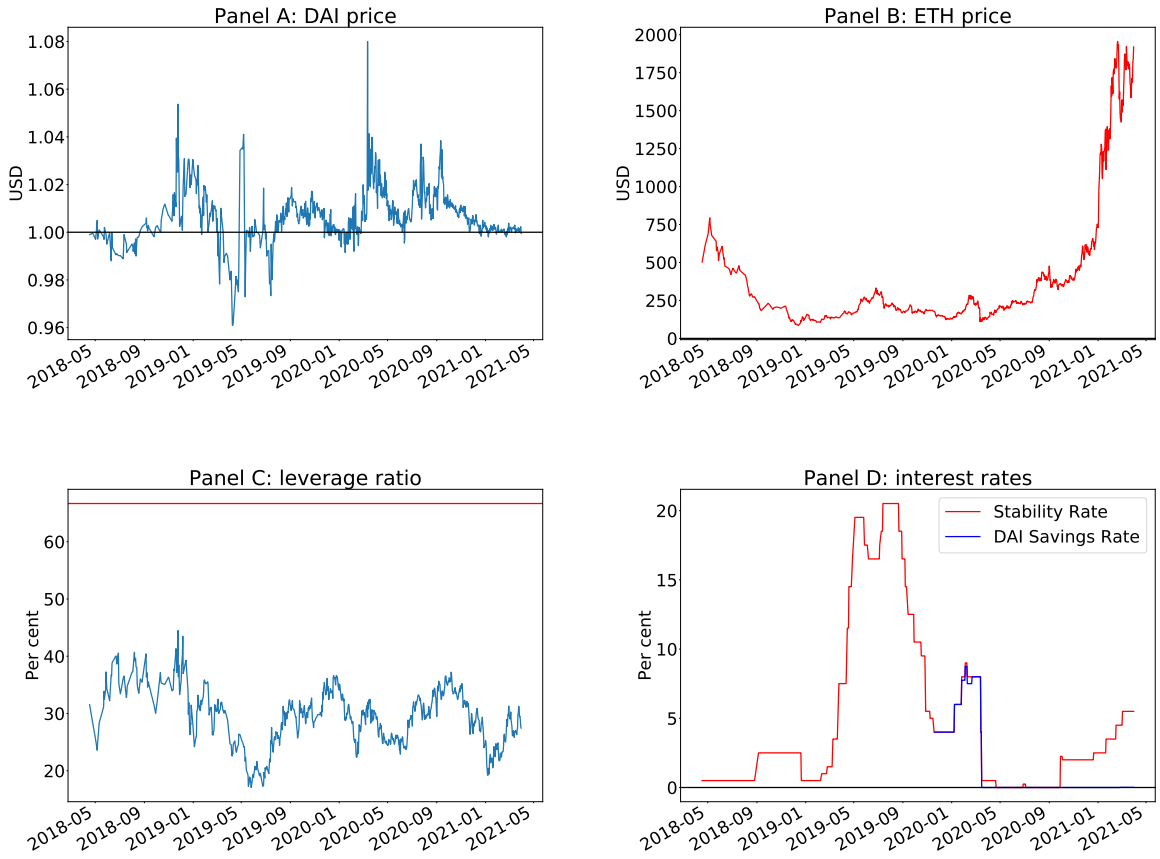

This figure plots Panel A: DAI price, Panel B: ETH price Panel C: leverage in ETH vaults, and Panel D: the interest rate on DAI borrowings. Sample period is from 13 April 2018 to 31 March 2021.

Figure 3: DAI prices across good and bad states of ETH collateral

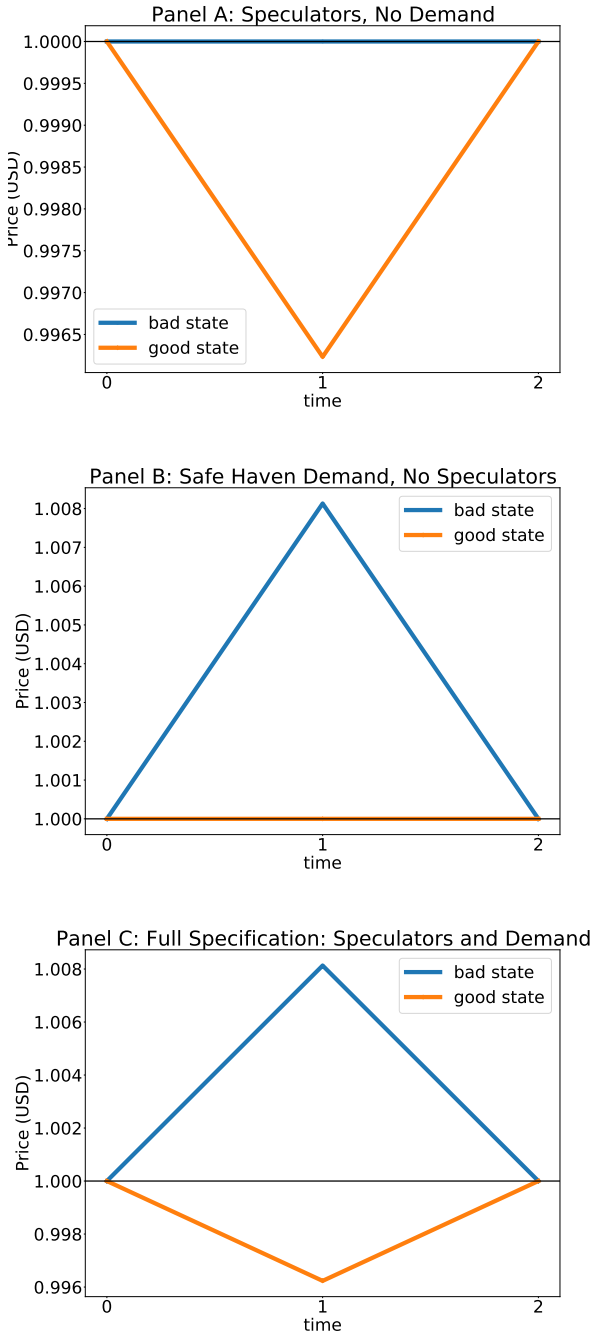

This figure plots DAI prices for both good and bad states of nature. Panel A plots DAI prices for a specification with no safe-haven demand ($D(G) = D(B) = 0$) and only speculators and arbitrageurs trading in period 1. Panel B plots DAI prices for a specification with safe-haven demand ($D(B) = \$50$, $D(G) = \$0$) and arbitrageurs but no speculative trading in period 1 ($\mu_E(G) = \mu_E(B) = \mu_A$). Panel C plots DAI prices for the full specification with safe-haven demand, speculative beliefs and arbitrageurs present. The rest of the primitive parameters are as follows: $\gamma = 0.5$, $\pi = 0.5$, $W_1^s = \$350$, $\bar{\theta} = 0.66$, $\sigma = 0.0188$, $i^B = 0.0324/252$, $i^L = 0.0139/252$, $r = 0.015/252$, $\sigma_E = 0.0459$, $\mu_A = 1.0033$, $\mu_E(G) = 1.0668$, $\mu_E(B) = 1.0033$. The rest of the parameters in the model are computed numerically by optimizing the expected utilities (5).

Figure 4: DAI prices, volatility and leverage across different values of ETH volatility

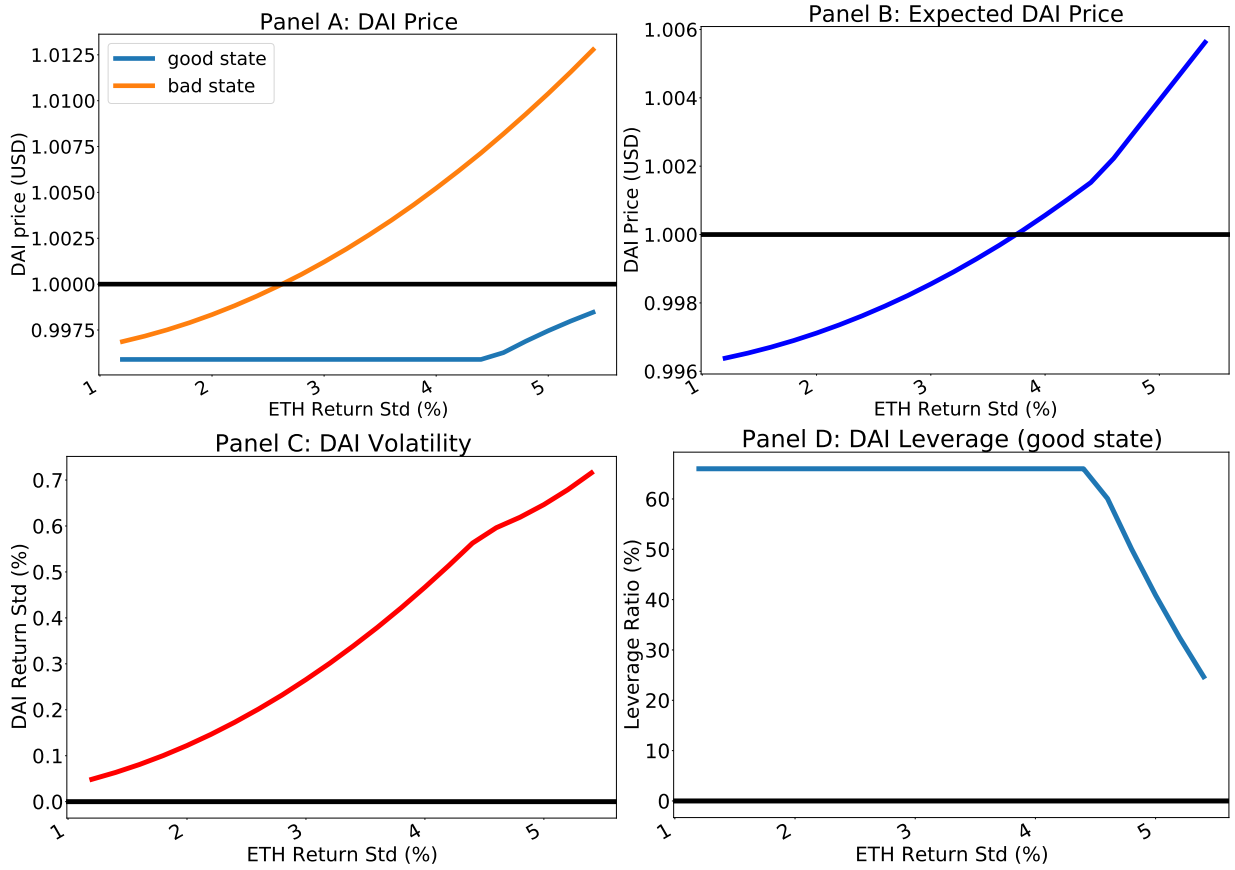

This figure plots DAI prices, volatility and leverage as a function of ETH volatility, holding all other parameters constant. Panel A corresponds to DAI prices in the good and bad states respectively. Panel B corresponds to the expected DAI price, with the good and bad states occurring with probability 0.5. Panel C corresponds to peg-price volatility, calculated as the standard deviation of peg-prices across the two states of collateral. Panel D corresponds to DAI leverage, calculated in percent. The primitive parameters are as follows: $\gamma = 0.5$, $\pi = 0.5$, $W_1^s = \$350$, $D(B) = \$50$, $D(G) = \$0$, $\bar{\theta} = 0.66$, $\sigma = 0.0188$, $i^B = 0.0324/252$, $i^L = 0.0139/252$, $r = 0.015/252$, $\mu_A = 1.0033$, $\mu_E(G) = 1.0668$, $\mu_E(B) = 1.0033$. The rest of the parameters in the model are computed numerically by optimizing the expected utilities (5).

Figure 5: DAI prices, volatility and leverage across different values of stability rate

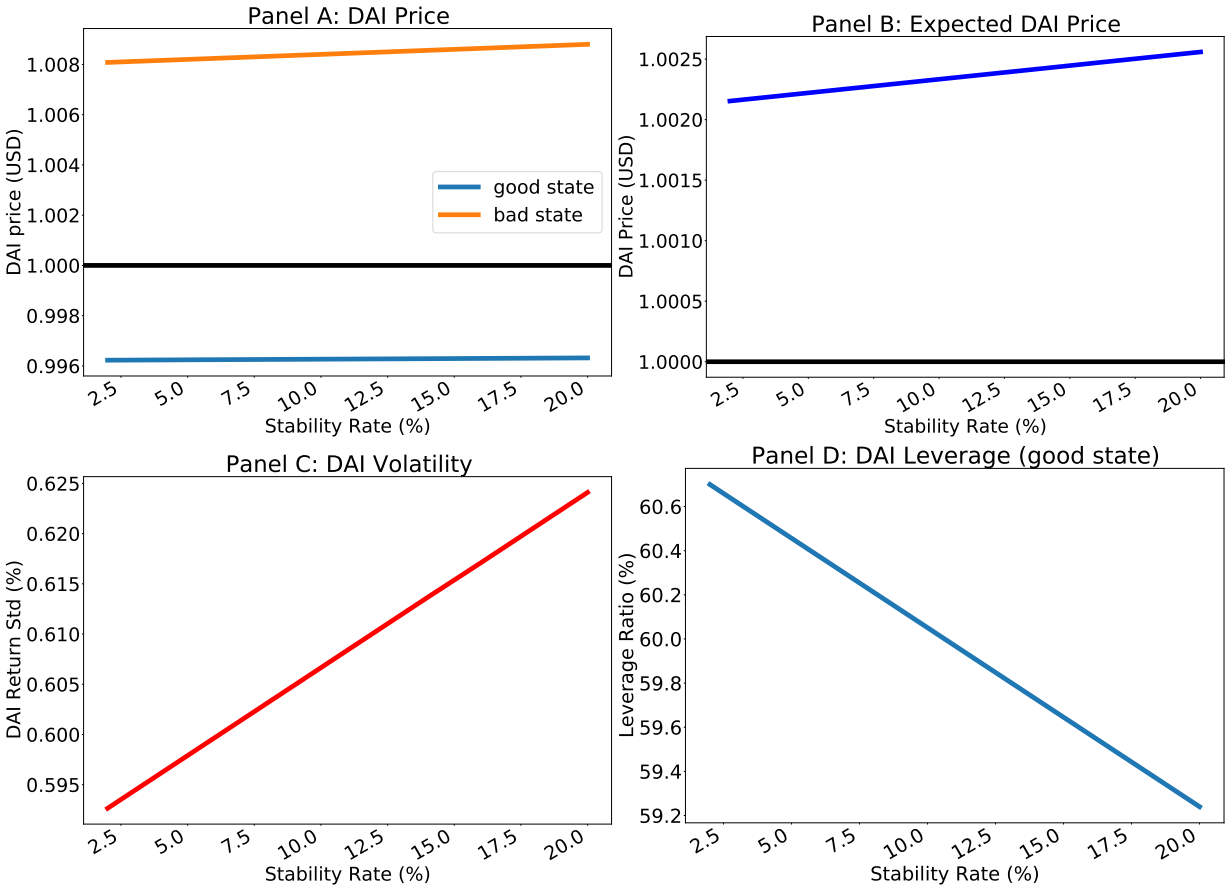

This figure plots DAI prices, volatility and leverage as a function of the interest rate on DAI borrowings, holding all other parameters constant. Panel A corresponds to DAI prices in the good and bad states respectively. Panel B corresponds to the expected DAI price, with the good and bad states occurring with probability 0.5. Panel C corresponds to peg-price volatility, calculated as the standard deviation of peg-prices across the two states of collateral. Panel D corresponds to DAI leverage, calculated in percent. The primitive parameters are f follows: $\gamma = 0.5$, $\pi = 0.5$, $W_1^s = \$350$, $D(B) = \$50$, $D(G) = \$0$, $\bar{\theta} = 0.66$, $\sigma = 0.0188$, $\sigma_E = 0.0459$, $i^L = 0.0139/252$, $r = 0.015/252$, $\mu_A = 1.0033$, $\mu_E(G) = 1.0668$, $\mu_E(B) = 1.0033$. The rest of the parameters in the model are computed numerically by optimizing the expected utilities (5).

Figure 6: DAI prices, volatility and leverage across different values of safe-haven demand

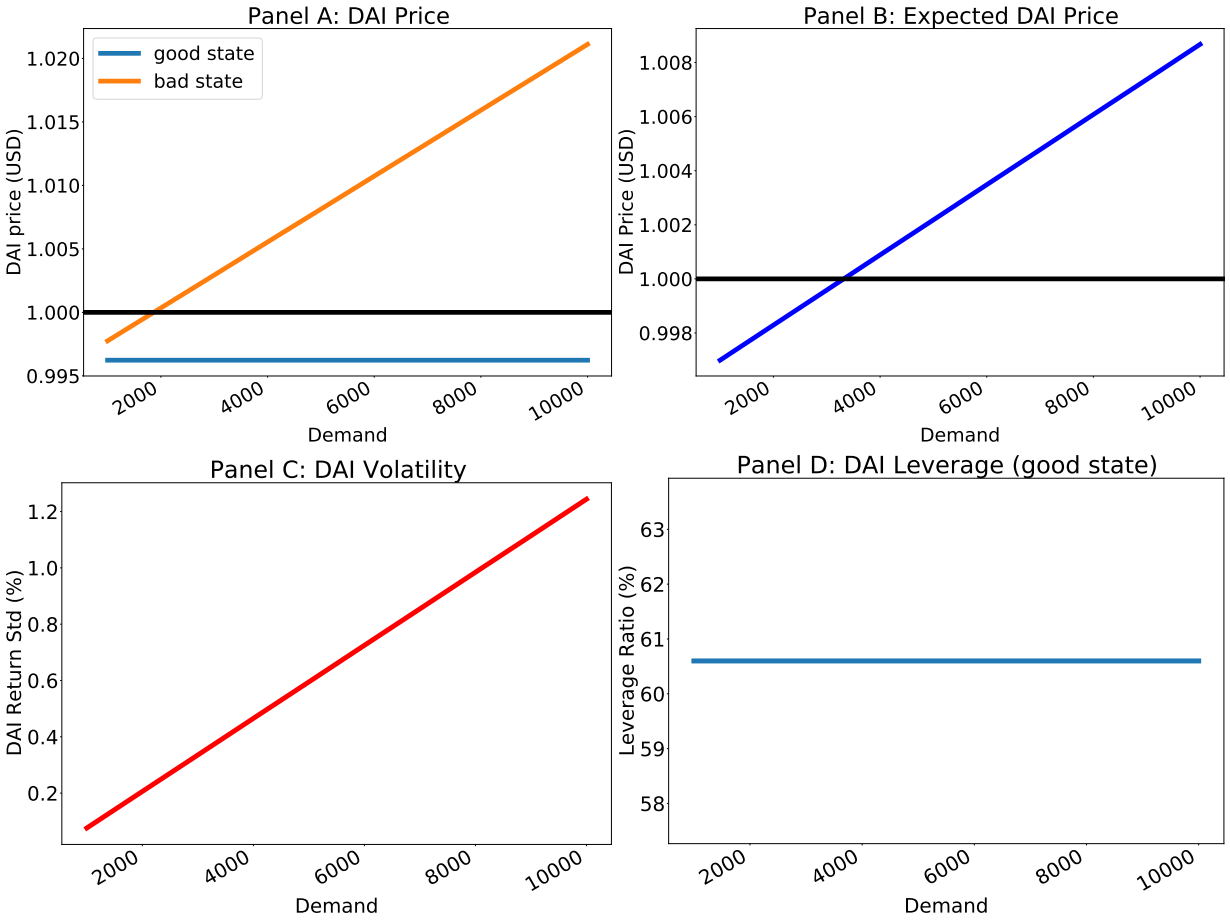

This figure plots DAI prices, volatility and leverage as a function of safe-haven demand, holding all other parameters constant. Panel A corresponds to DAI prices in the good and bad states respectively. Panel B corresponds to peg-price volatility, calculated as the standard deviation of peg-prices across the two states of collateral. Panel C corresponds to DAI leverage, calculated in percent. The primitive parameters are as follows: $\gamma = 0.5$, $\pi = 0.5$, $W_1^s = \$350$, $D(G) = \$0$, $\bar{\theta} = 0.66$, $\sigma = 0.0188$, $\sigma_E = 0.0459$, $i^B = 0.0324/252$, $i^L = 0.0139/252$, $r = 0.015/252$, $\mu_A = 1.0033$, $\mu_E(G) = 1.0668$, $\mu_E(B) = 1.0033$. The rest of the parameters in the model are computed numerically by optimizing the expected utilities (5).

Figure 7: DAI price for single and multiple collateral system

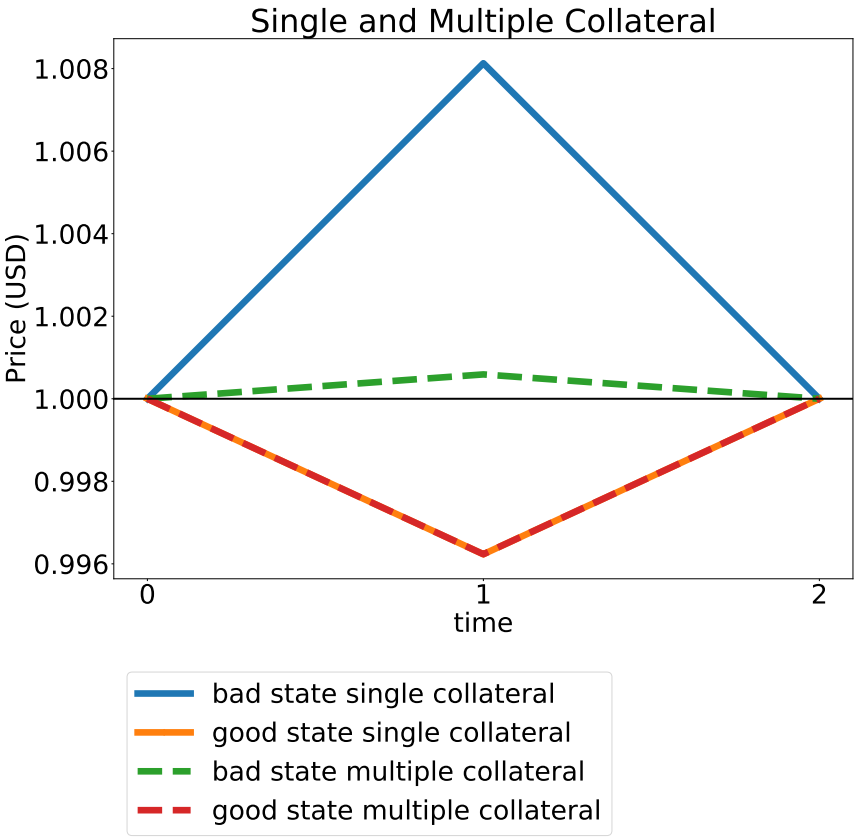

This figure plots DAI prices for both good and bad states of nature. Solid lines is for the specification with only unstable (ETH) collateral, and is a full specification with safe-haven demand and when speculators and arbitrageurs are both present. Dotted line indicates a specification with multiple collateral. In this case, while speculators have access to ETH collateral, arbitrageurs have access to USDC collateral with volatility $\sigma_U = 0.0013$. The primitive parameters are as follows: $\gamma = 0.5$, $\pi = 0.5$, $W_1^s = \$350$, $D(B) = \$50$, $D(G) = \$0$, $\bar{\theta} = 0.66$, $\sigma = 0.0188$, $i^B = 0.0324/252$, $i^L = 0.0139/252$, $r = 0.015/252$, $\sigma_E = 0.0459$, $\mu_A = 1.0033$, $\mu_E(G) = 1.0668$, $\mu_E(B) = 1.0033$. The rest of the parameters in the model are computed numerically by optimizing the expected utilities (5).

Figure 8: DAI prices, volatility, leverage and share of USDC collateral versus USDC volatility

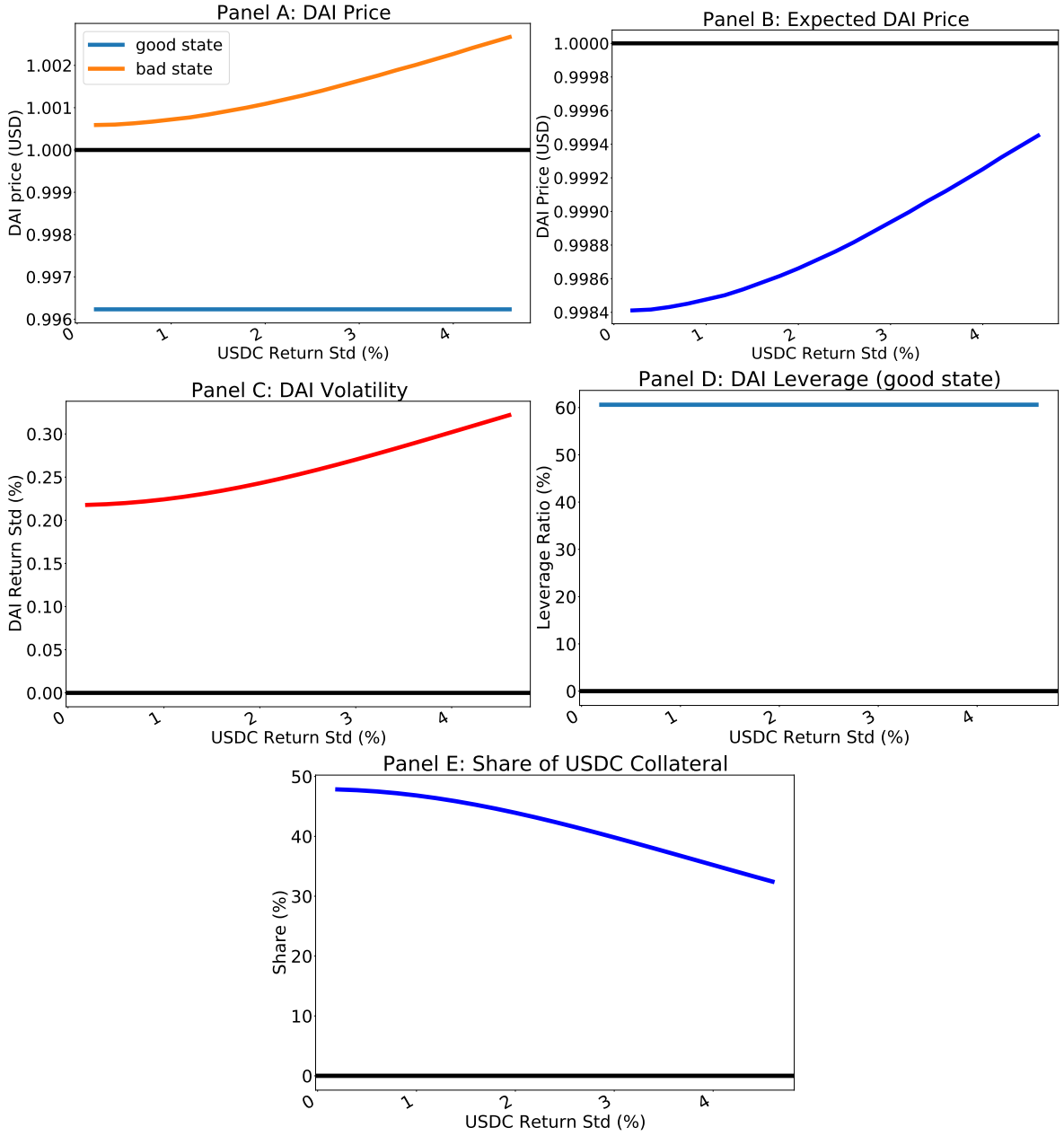

This figure plots DAI prices, volatility, leverage and the share of USDC collateral as a function of USDC volatility, holding all other parameters constant. Panel A corresponds to DAI prices in the good and bad states respectively. Panel B corresponds to the expected DAI price, with the good and bad states occurring with probability 0.5. Panel C corresponds to peg-price volatility, calculated as the standard deviation of peg-prices across the two states of collateral. Panel D corresponds to DAI leverage, calculated in percent. Panel E corresponds to the share of stable collateral as a ratio to total collateral deposited by both speculators and arbitrageurs. The primitive parameters are as follows: $\gamma = 0.5$, $\pi = 0.5$, $W_1^s = \$350$, $D(B) = \$50$, $D(G) = \$0$, $\bar{\theta} = 0.66$, $\sigma = 0.0188$, $\sigma_E = 0.0459$, $i^B = 0.0324/252$, $i^L = 0.0139/252$, $r = 0.015/252$, $\mu_A = 1.0033$, $\mu_E(G) = 1.0668$, $\mu_E(B) = 1.0033$. The rest of the parameters in the model are computed numerically by optimizing the expected utilities (5).

Figure 9: Model Simulated DAI prices

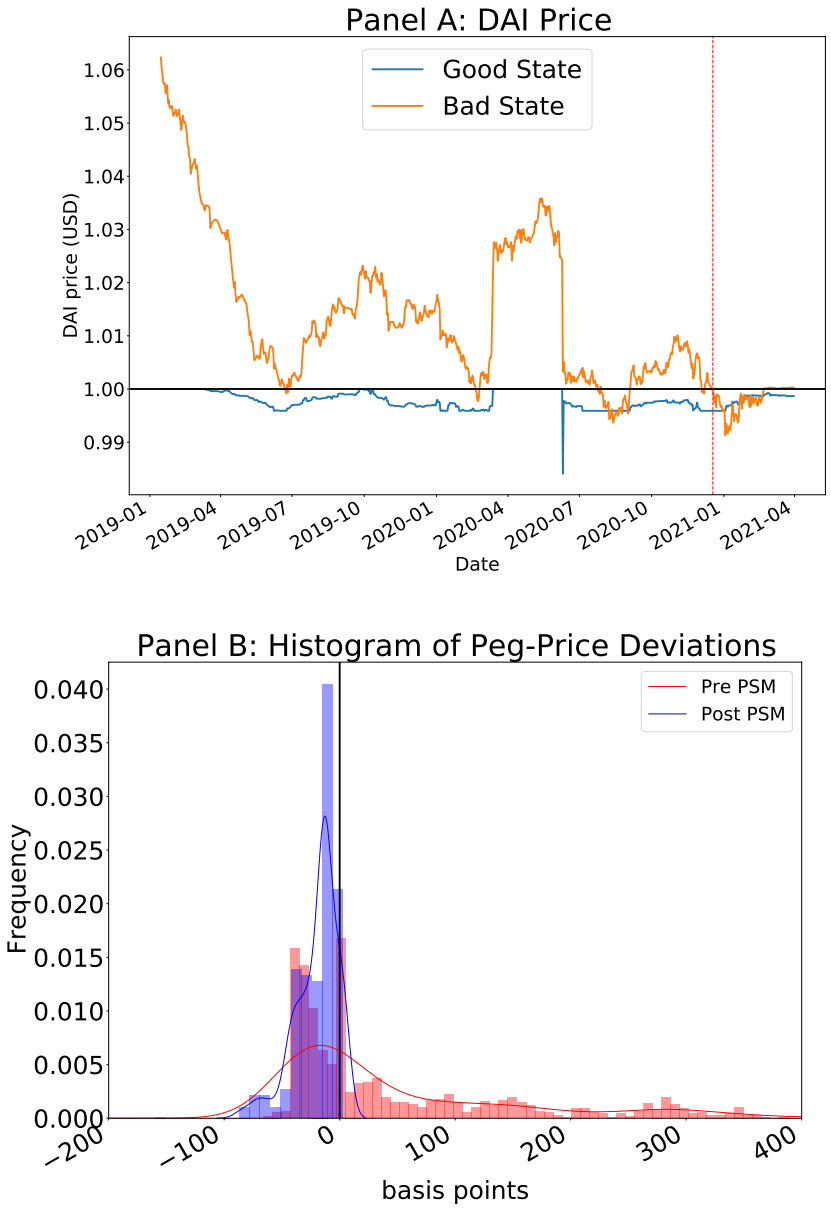

This figure plots DAI prices for both good and bad states of nature based on simulated data from the model. Panel A corresponds to DAI prices in the good and bad states, respectively. Panel B plots a histogram of deviations of the DAI/USD price from parity for sub-samples corresponding to pre and post PSM. A positive deviation indicates DAI/USD trades at a premium. The pre PSM sample is from 18 November 2019 to 17 December 2020. The post PSM sample is from 18 December 2020 to 31 March 2021. Dotted line in Panel A indicates date of introduction of PSM on 18 December 2020. The primitive parameters are as follows: $\gamma = 0.5$, $\pi = 0.5$, $W_1^s = \$350$, $D(G) = \$0$, $\bar{\theta} = 0.66$, $\sigma = 0.0188$, $\sigma_E = 0.0459$, $i^B = 0.0324/252$, $i^L = 0.0139/252$, $r = 0.015/252$, $\mu_A = 1.0033$. The expected returns of ETH in the good and bad states, $\mu_E(G), \mu_E(B)$ are estimated respectively as a sample 80%-percentile and average ETH returns based on 90 day rolling window. The standard deviations of ETH and USDC volatility σ_E, σ_{USDC} are 90 day rolling window sample standard deviations of ETH and USDC returns respectively. The rest of the parameters in the model are computed numerically by optimizing the expected utilities (5).

Figure 10: Time Series of Leverage Ratio, DAI borrowings and ETH collateral for two CDPs

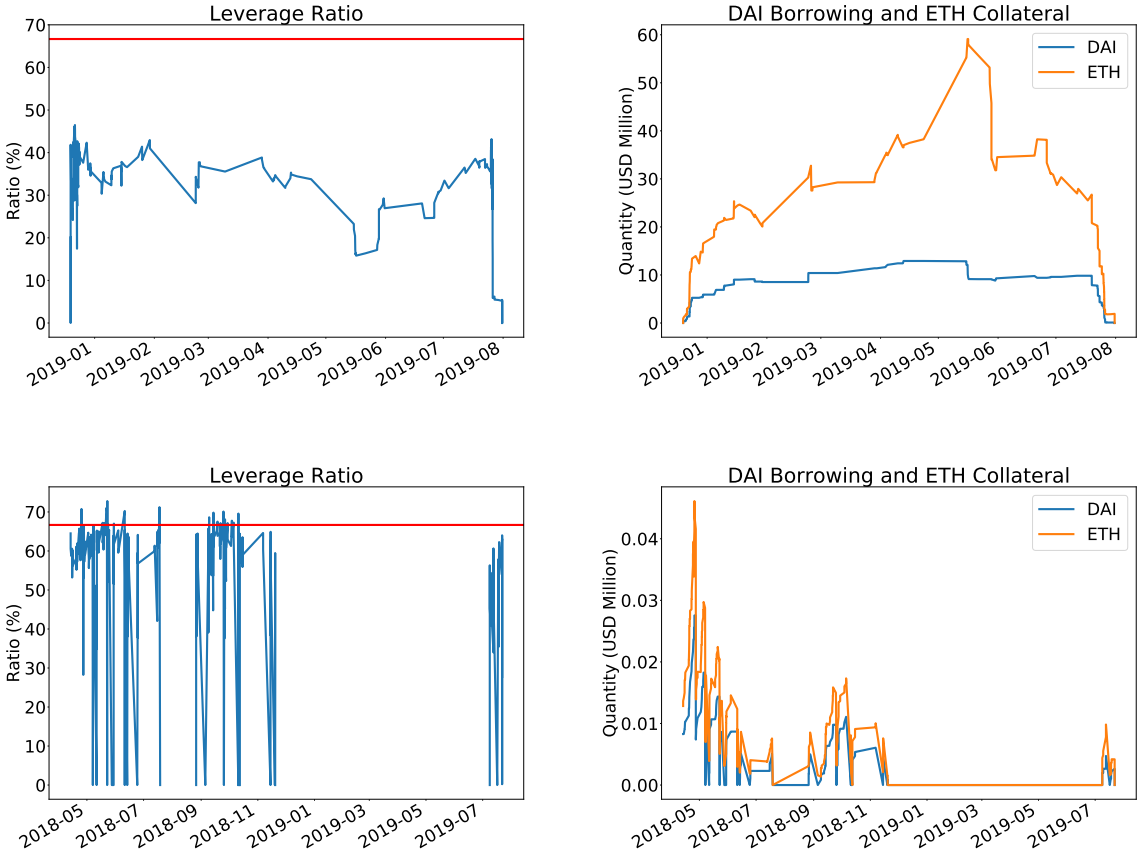

Top panel: Time series of leverage ratio (left) and DAI borrowings and ETH collateral for CDP #5199. Bottom panel: Time series of leverage ratio (left) and DAI borrowings and ETH collateral for CDP #1272. CDP transactions are aggregated to a daily frequency, with sample period from 13 April 2018 to 18 November 2019.

Figure 11: Distribution Conditional on ETH Returns

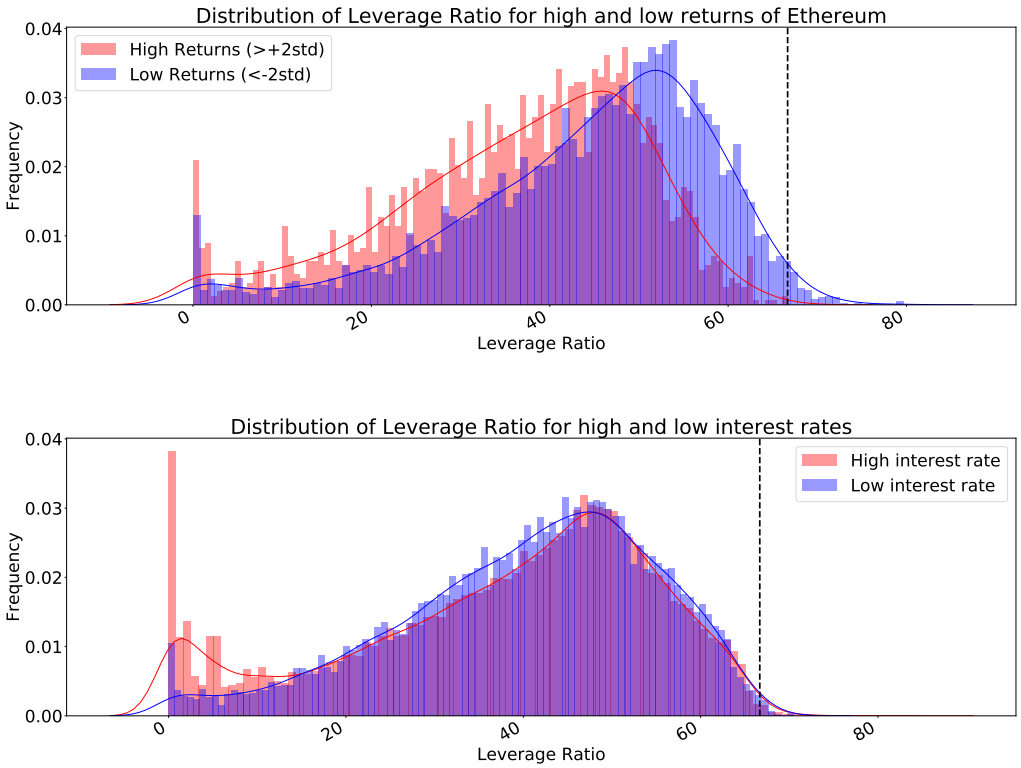

This figure plots the kernel density of the leverage ratio for all CDPs. Top panel: Distributions are conditioned on periods of high and low returns of ETH, where high returns corresponds to returns that exceed +2std of ETH returns, and low returns corresponds to returns that are less than -2 std of ETH returns. Bottom panel: Distributions are conditioned on periods of high and low interest rates. High interest rates correspond to the distribution of CDP leverage when the DAI stability rate reached its peak of 19.0%. Low interest rates correspond to the distribution of CDP leverage when the DAI stability rate is at the floor of 0%. CDP liquidations, when the action is "bite" and DAI borrowings are zero, are excluded from the sample. CDP transactions are aggregated to a daily frequency, with sample period from 13 April 2018 to 18 November 2019.

Figure 12: DAI and ETH intra-day volatility

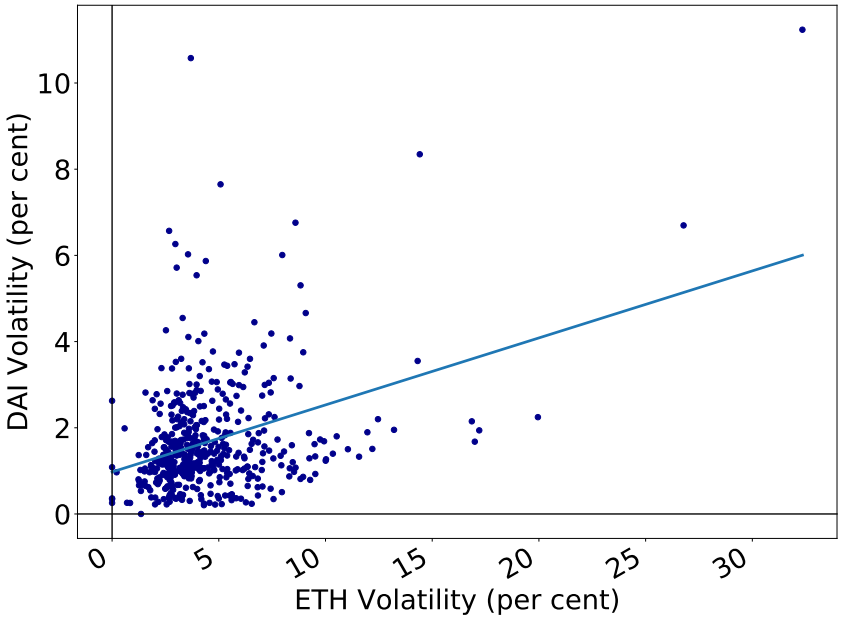

This figure plots a scatter plot of intra-day volatility of DAI and ETH. Intra-day volatility is measured in basis points. Price data for currencies obtained from coinapi and use intra-day prices from the Bitfinex exchange. Sample period is from 18 November 2019 to 31 March 2021, corresponding to the period of Multi Collateral DAI.

Figure 13: Contribution of fundamentals to peg-rice and volatility

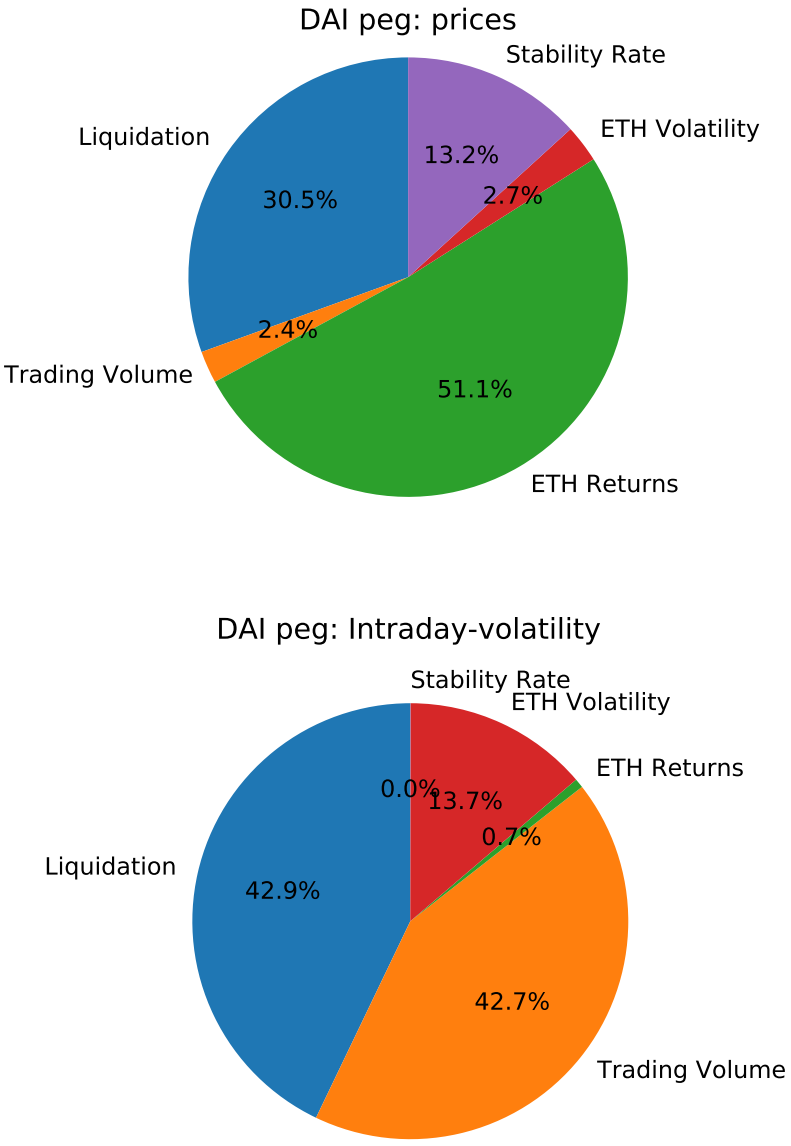

This figure plots a pie chart showing the contribution of fundamentals to peg-price and volatility. Variables include ETH returns and volatility, the stability rate, liquidations of ETH collateral and demand (measured by the percent change in secondary market trading volume of DAI). The decomposition is based on an ANOVA, which reports the sum of squares explained by each variable. In calculations, the percentage contribution is the sum of squares contribution of each variable.

Figure 14: DAI/USD prices

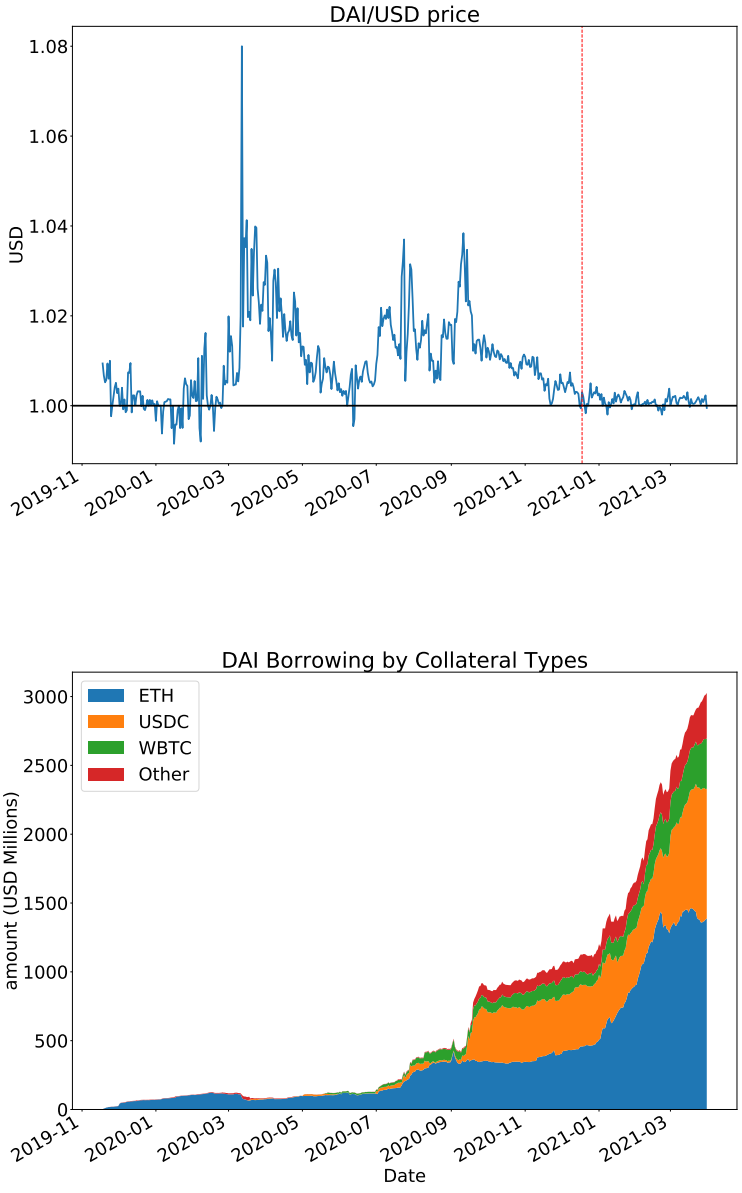

Left panel: This figure plots the deviations of the DAI/USD peg from parity. A positive deviation indicates DAI/USD trades at a premium. Sample period is from 18 November 2019 to 31 March 2021. Right panel: This figure plots the breakdown of total DAI borrowing by Vault. DAI borrowing is denominated in USD Million. Vault types include ETH, USDC, WBTC (synthetic BTC) and other. Sample period is from 18 November 2019 to 31 March 2021.

Figure 15: DAI vs. USDC: Absolute peg-price deviations and volatility

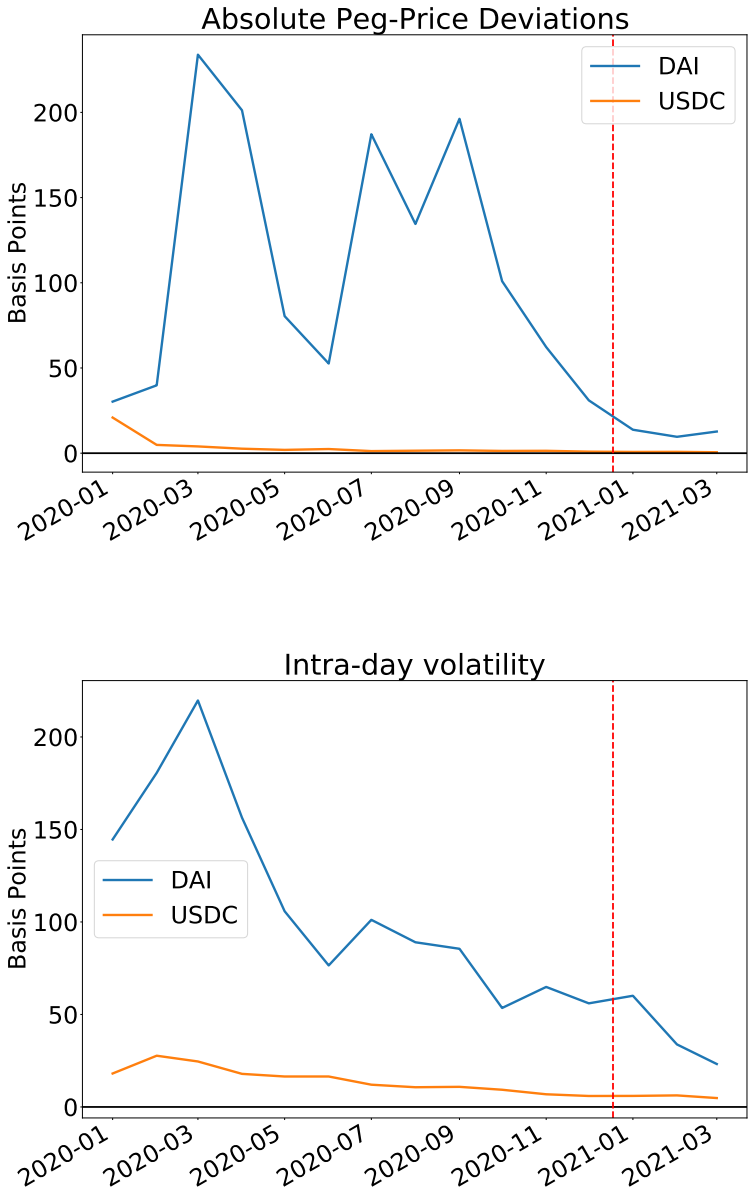

This figure plots average monthly stablecoin prices and intra-day volatility for the treatment (DAI) and the control group stablecoins. The treatment stablecoin is DAI. The control stablecoin is USDC. The red dotted line indicates the date of structural change of 18 December 2020 used in the baseline specification. Sample is 13 April 2018 through to 31 March 2021.

Figure 16: Distribution of peg-price deviations, pre- and post-PSM

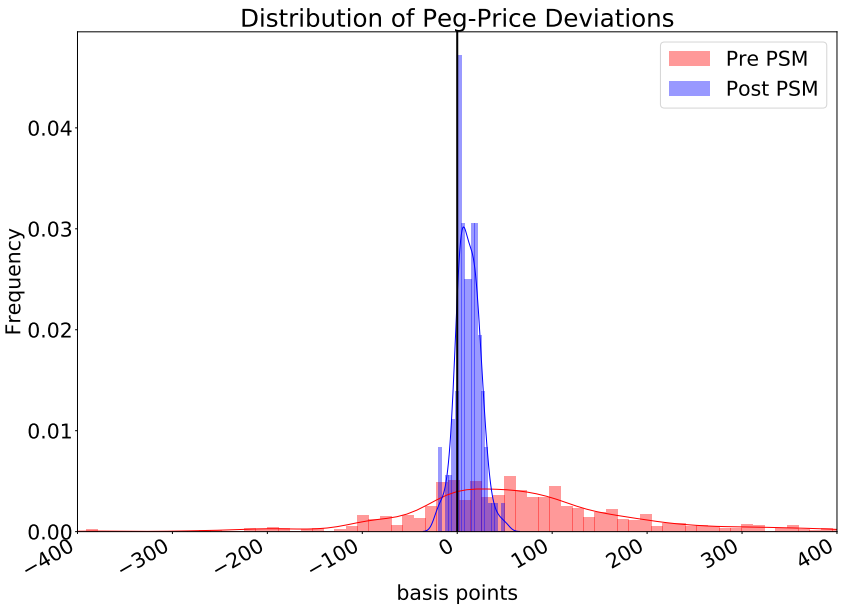

Figure plots a histogram of deviations of the DAI/USD price from parity for sub-samples corresponding to pre and post PSM. A positive deviation indicates DAI/USD trades at a premium. The pre PSM sample is from 18 November 2019 to 17 December 2020. The post PSM sample is from 18 December 2020 to 31 March 2021.

Figure 17: DAI price, liquidations and source of collateral in response to negative price shock of ETH in May 2021

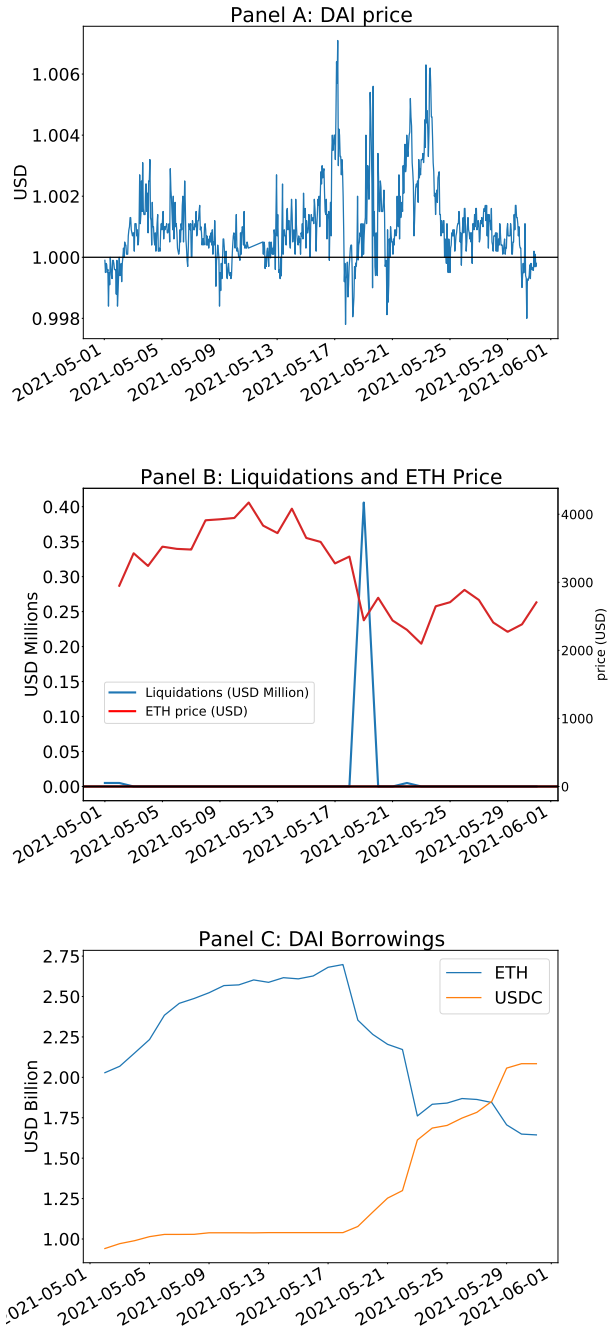

DAI price in USD, ETH price in USD and DAI liquidations and DAI borrowing by collateral type during the month of May 2021.

Figure 18: DAI and USDC prices during the USDC de-pegging event on March 11th, 2023

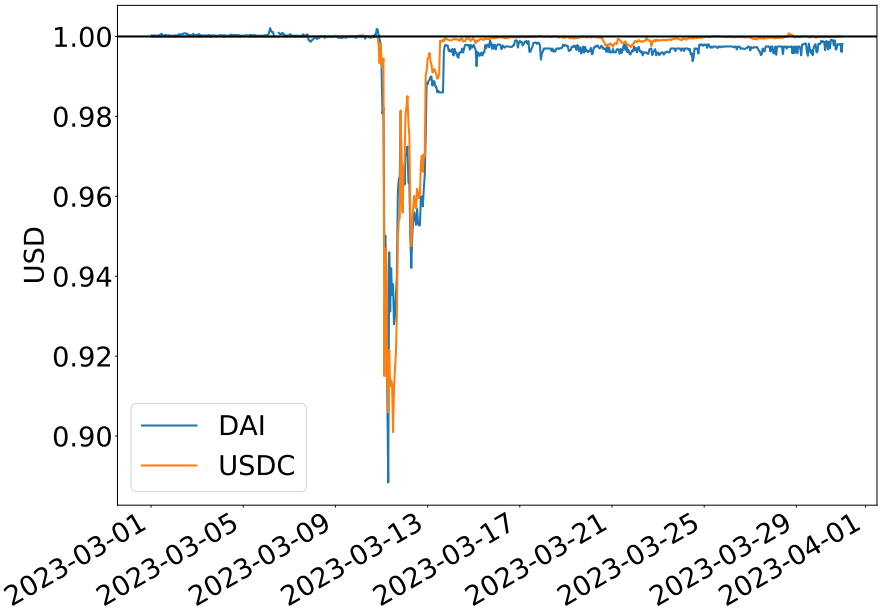

DAI and USDC prices in March 2023.

Tables

Table 1: Summary statistics

	count	mean	std	min	25%	50%	75%	max
R_{ETH} (%)	798.0	0.17	5.80	-58.22	-2.34	0.11	3.02	23.31
Δ_{DAI} (USD)	798.0	0.01	0.01	-0.04	0.00	0.01	0.01	0.08
Stability Rate (%)	798.0	3.24	6.34	0.00	0.02	0.04	2.50	20.52
Leverage Ratio (%)	798.0	29	5	17	26	30	33	44

This table presents summary statistics of key variables in empirical analysis. R_{ETH} measures daily returns in ETH in percent. Δ_{DAI} measures deviations from the peg and are expressed in USD (1 USD=100 basis points). The stability rate is an interest rate on DAI borrowing and is expressed in percent (annualized). The leverage ratio is the ratio of total DAI borrowings to total ETH collateral. Sample period is from 13 April 2018 to 31 March 2021.

Table 2: Correlation matrix

	R_{ETH}	Δ_{DAI}	Stability Rate	Leverage Ratio
R_{ETH}	1.000	-0.044	-0.015	-0.209
Δ_{DAI}	-0.044	1.000	-0.190	0.250
Stability Rate	-0.015	-0.190	1.000	-0.340
Leverage Ratio	-0.209	0.250	-0.340	1.000

This table presents pairwise correlation of key variables in empirical analysis. R_{ETH} measures daily returns in ETH in percent. Δ_{DAI} measures deviations from the peg and are expressed in USD (1 USD=100 basis points). The stability rate is an interest rate on DAI borrowing and is expressed in percent (annualized). The leverage ratio is the ratio of total DAI borrowings to total ETH collateral. Sample period is from 13 April 2018 to 31 March 2021.

Table 3: CDP summary statistics

	count	mean	std	min	25%	50%	75%	max
DAI (USD Million)	11,718	0.015	0.16	0.00	0.00	0.00	0.002	7.87
ETH (USD Million)	11,718	0.04	0.50	0.00	0.00	0.00	0.005	24.96
Leverage Ratio (%)	11,718	30.55	19.01	0.00	13.43	33.02	44.79	84.49
Liquidations	7,097	1.06	0.40	1	1	1	1	14

This table presents summary statistics of key variables of individual CDP data. DAI and ETH measure the total DAI borrowings and ETH collateral of each individual CDP, measured in USD million. The leverage ratio is the ratio of total DAI borrowings to total ETH collateral. Liquidations measures the number of times a CDP leverage ratio is above the threshold governed by the liquidation price. Only CDPs with at least 30 days of observations are included in the sample. Sample period is from 13 April 2018 to 17 November 2019, which corresponds to the period of single collateral DAI.

Table 4: Determinants of CDP DAI borrowing, ETH collateral, leverage and liquidation event

	$DAI_{i,t}$	$ETH_{i,t}$	$Bite_{i,t}$
$DAI_{i,t-1}$	0.993***		
	(0.005)		
$ETH_{i,t-1}$		0.976***	
		(0.004)	
$R_{ETH,t}$	0.460**	3.434**	-0.075***
	(0.221)	(1.441)	(0.006)
$\sigma_{ETH,t}$	-0.254	0.260	0.126***
	(0.347)	(1.952)	(0.011)
$sfee_t$	-0.632*	-1.684**	0.019***
	(0.332)	(0.735)	(0.005)
Intercept	9.178***	24.311**	-4.09***
	(2.633)	(11.248)	(0.129)
Nr. obs.	11,197	11,197	25,125
Nr. ids.	456	456	456
id FE	Yes	Yes	Yes

This table presents the estimation results of the following panel regression:

$$Y_{i,t} = \alpha_i + \beta_1 R_{ETH,t} + \beta_2 \sigma_{ETH,t} + \beta_3 sfee_t + u_{i,t},$$

where the dependent variable $Y_{i,t}$ is one of the following variables: $DAI_{i,t}$ (the individual DAI borrowing at time t of CDP i in thousands of USD), $ETH_{i,t}$ (the individual ETH collateral of CDP i in thousands of USD), and $Bite_{i,t}$ (a dummy variable indicating a "bite", which is a liquidation event at time t of CDP i). Explanatory variables include daily ETH returns $R_{ETH,t}$ (in percent), daily intra-day volatility of ETH returns $\sigma_{ETH,t}$ (in percent), the interest rate on DAI borrowings $sfee_t$ (in percent per annum). The sample runs from 13 April 2018 to 17 November 2019, which corresponds to the period of single collateral DAI. For $Bite_{i,t}$ dependent variable we use a panel probit specification. White heteroscedasticity-robust standard errors are reported in parentheses, and are clustered at the individual CDP level. All specifications include CDP fixed effects. *** denotes significance at the 1% level, ** at the 5% level, and * at the 10% level.

Table 5: DAI peg-price fundamentals

	(1)	(2)	(3)	(4)	(5)	(6)	(7)	(8)
	L_t	D_t	$\Delta_{DAI,t}$					
$\Delta_{DAI,t-1}$			0.818***	0.796***	0.758***	0.786***	0.808***	0.765***
			(0.074)	(0.077)	(0.114)	(0.090)	(0.086)	(0.075)
$R_{ETH,t}$	-0.000*	-0.943	-0.037**					-0.029**
	(0.000)	(0.636)	(0.018)					(0.012)
$\sigma_{ETH,t}$	0.001***	3.641***		0.013				-0.015
	(0.000)	(1.147)		(0.051)				(0.023)
$sfee_t$	0.000	-0.243			-0.035			-0.038**
	(0.000)	(0.836)			(0.032)			(0.017)
L_t						17.682		14.093
						(22.337)		(17.065)
D_t							0.003**	0.002***
							(0.001)	(0.001)
Intercept	-0.538***	-659.487	19.029***	12.394	30.130*	17.405**	14.884**	35.810*
	(0.163)	(557.736)	(5.987)	(25.243)	(15.954)	(7.613)	(6.405)	(18.478)
R-sq.	40.93%	6.78%	68.59%	64.50%	65.09%	66.14%	65.99%	71.00%
Nr. obs.	454	454	454	454	454	454	454	454

This table presents the estimation results of the following regression models:

$$L_t = a_0 + a_1 R_{ETH,t} + a_2 \sigma_{ETH,t} + a_3 sfee_t + u_t, \quad \text{Column (1)},$$
$$D_t = b_0 + b_1 R_{ETH,t} + b_2 \sigma_{ETH,t} + b_3 sfee_t + u_t, \quad \text{Column (2)},$$
$$\Delta_{DAI,t} = \beta_0 + \beta_1 \Delta_{DAI,t-1} + \beta_2 R_{ETH,t} + \beta_3 \sigma_{ETH,t} + \beta_4 sfee_t + \beta_5 L_t + \beta_6 D_t + u_t, \quad \text{Columns (3)-(8)},$$

where the dependent variables in columns (1) and (2) are L_t (value of liquidations in thousands of USD) and D_t (the aggregate growth in DAI trading volume across major exchanges in basis points) respectively. The dependent variable in columns (3) to (8) is $\Delta_{DAI,t}$ (the DAI peg-price deviation $p_{DAI,t} - 1$, in basis points). Explanatory variables include daily ETH returns $R_{ETH,t}$ (in basis points), daily intra-day volatility of ETH returns $\sigma_{ETH,t}$ (in basis points), the interest rate on DAI borrowings $sfee_t$ (in percent per annum), the value of liquidations L_t (in millions of USD) and aggregate growth in DAI secondary market trading volume D_t (in basis points). The sample runs from 18 November 2019 to 31 March 2021, corresponding to the period of Multi Collateral DAI. White heteroscedasticity-robust standard errors are reported in parentheses. *** denotes significance at the 1% level, ** at the 5% level, and * at the 10% level.

Table 6: DAI volatility fundamentals

	(1)	(2)	(3)	(4)	(5)	(6)
			$\sigma_{DAI,t}$			
$\sigma_{DAI,t-1}$	0.642***	0.624***	0.633***	0.634***	0.646***	0.635***
	(0.036)	(0.037)	(0.036)	(0.036)	(0.036)	(0.037)
$R_{ETH,t}$	-0.007					-0.002
	(0.005)					(0.005)
$\sigma_{ETH,t}$		0.023**				0.004
		(0.009)				(0.012)
$sfee_t$			0.013			0.009
			(0.010)			(0.010)
L_t				10.486***		7.017
				(3.524)		(4.554)
D_t					0.002***	0.002***
					(0.001)	(0.001)
					(0.001)	(0.001)
Intercept	34.742***	25.725***	31.774***	34.029***	32.243***	29.068***
	(4.365)	(5.583)	(4.786)	(4.329)	(4.362)	(6.206)
R-sq.	41.15%	41.67%	41.11%	42.01%	42.36%	43.26%
Nr. obs.	454	454	454	454	454	454

This table presents the estimation results of the following regression models:

$$\sigma_{DAI,t} = \beta_0 + \beta_1 \sigma_{DAI,t-1} + \beta_2 R_{ETH,t} + \beta_3 \sigma_{ETH,t} + \beta_4 sfee_t + \beta_5 L_t + \beta_6 D_t + u_t,$$

where the dependent variable $\sigma_{DAI,t}$ measures the daily intra-day volatility of DAI prices (in basis points). Explanatory variables include daily ETH returns $R_{ETH,t}$ (in basis points), daily intra-day volatility of ETH returns $\sigma_{ETH,t}$ (in basis points), the interest rate on DAI borrowings $sfee_t$ (in percent per annum), the value of liquidations L_t (in millions of USD) and aggregate growth in DAI secondary market trading volume D_t (in basis points). The sample runs from 18 November 2019 to 31 March 2021, corresponding to the period of Multi Collateral DAI. Standard errors are reported in parantheses *** denotes significance at the 1% level, ** at the 5% level, and * at the 10% level.

Table 7: Tests of a structural break in DAI peg deviations

	(1)	(2)	(3)	(4)
	$\|\Delta\|$	σ	$\|\Delta\|$	σ
$post_t$	-53.63***	-39.92***	-2.73***	-9.21***
	(3.44)	(3.25)	(0.60)	(0.54)
T_i			114.51***	97.44***
			(5.13)	(4.17)
$post_t \times T_i$			-101.47***	-61.16***
			(5.23)	(4.70)
Intercept	60.85***	63.74***	3.42***	14.88***
	(3.37)	(2.80)	(0.59)	(0.48)
R-sq.	7.85%	6.26%	46.55%	48.07%
Nr. obs.	896	896	896	896

Table presents estimation results of the following difference-in-difference regression:

$$Y_{j,t} = \alpha_0 + \beta T_j + \gamma\ post_t + \delta\ post_t \times T_j + u_{j,t},$$

where the outcome variable $Y_{j,t}$ is either the absolute level of peg deviation $|\Delta_{j,t}|$ (columns (1) and (3)), or the intra-day volatility of peg deviations $\sigma_{j,t}$ (columns (2) and (4)) for $j = DAI, U$, both measured in basis points. The post dummy $post_t$ takes a value of 1 from 18 December 2020, which is the launch date of the PSM (swap arrangement in which USDC is swapped with DAI at a 1:1 rate) and 0 otherwise. The Treatment dummy T_j takes a value of 1 for DAI/USD, and 0 for USDC/USD (control-group currency). The sample is based on the balanced panel from 8 January 2020 to 31 March 2021. White heteroscedasticity-robust standard errors are used in estimation. *** denotes significance at the 1% level, ** at the 5% level, and * at the 10% level.

Table 8: Summary statistics of peg deviations pre- and post-PSM periods

period	count	mean	std	min	25%	50%	75%	max	half-life (days)
Pre-PSM	396.0	101.95	98.83	-84.8	33.75	85.5	153.5	800.0	5.95
Post-PSM	103.0	11.27	12.38	-20.0	3.0	11.0	20.0	50.0	1.76

Table presents summary statistics of peg deviations in basis points. A positive deviation indicates DAI/USD trades at a premium. The pre PSM sample is from 18 November 2019 to 17 December 2020. The post PSM sample is from 18 December 2020 to 31 March 2021.

Table 9: SETAR of peg deviations pre- and post-PSM periods

period	ρ_L	ρ_M	ρ_U	Δ_L	Δ_U
Pre-PSM	0.84	1.011	0.759	24bps	290bps
Post-PSM	-0.228	0.913	0.412	1bps	27bps

Table presents results of SETAR analysis:

$$\Delta_{DAI,t} = \begin{cases} \rho_L \Delta_{DAI,t-1} + \epsilon_t, & \Delta_{DAI,t-1} < \Delta_L \\ \rho_M \Delta_{DAI,t-1} + \epsilon_t, & \Delta_L \leq \Delta_{DAI,t-1} \leq \Delta_U \\ \rho_U \Delta_{DAI,t-1} + \epsilon_t, & \Delta_{DAI,t-1} > \Delta_U \end{cases}$$

where Δ is peg-price deviations (measured in basis points), the auto-regressive parameter is ρ and the low regime is given by the threshold of deviations ranging from $[-\infty, \Delta_L]$, the middle regime is $[\Delta_L,\Delta_U]$ and the high regime is $[\Delta_U,\infty]$. The pre PSM sample is from 18 November 2019 to 17 December 2020. The post PSM sample is from 18 December 2020 to 31 March 2021.

Table 10: DAI-ETH return correlations in the pre- and post-USDC collateral periods

	(1) $\Delta_{DAI,t}$	(2) $\Delta_{DAI,t}$	(3) $\sigma_{DAI,t}$	(4) $\sigma_{DAI,t}$
$\Delta_{DAI,t-1}$	0.605***	0.706***		
	(0.110)	(0.077)		
$\sigma_{DAI,t-1}$			0.221***	0.473***
			(0.079)	(0.083)
$R_{ETH,t}$	-0.054***	-0.012*	0.045***	-0.003
	(0.012)	(0.007)	(0.014)	(0.004)
$\sigma_{ETH,t}$	0.130***	-0.021	0.177***	0.016*
	(0.033)	(0.020)	(0.029)	(0.008)
$\sigma_{U,t}$		0.812		2.208***
		(0.909)		(0.650)
$sfee_t$	0.785	-7.740**	9.862**	-5.411***
	(3.037)	(3.515)	(4.295)	(1.949)
Intercept	-39.246***	40.854*	-21.850	20.549*
	(14.970)	(23.174)	(18.506)	(11.598)
R-sq.	71.71%	75.04%	43.14%	58.35%
Nr.obs.	115	383	115	383
Pre USDC	Yes	No	Yes	No
Post USDC	No	Yes	No	Yes

This table presents the estimation results of the following regression models:

$$\Delta_{DAI,t} = \beta_0 + \beta_1 \Delta_{DAI,t-1} + \beta_2 R_{ETH,t} + \beta_3 \sigma_{ETH,t} + \beta_4 \Delta_{U,t} + \beta_5 \sigma_{U,t} + \beta_6 sfee_t + u_t, \quad \text{Columns (1) and (2)},$$
$$\sigma_{DAI,t} = \beta_0 + \beta_1 \sigma_{DAI,t-1} + \beta_2 R_{ETH,t} + \beta_3 \sigma_{ETH,t} + \beta_4 \Delta_{U,t} + \beta_5 \sigma_{U,t} + \beta_6 sfee_t + u_t, \quad \text{Columns (3) and (4)},$$

where the dependent variables in columns (1) and (2) is $\Delta_{DAI,t}$ (the DAI peg-price deviation $p_{DAI,t} - 1$, in basis points) and in columns (3) and (4) is the daily intra-day volatility of DAI prices $\sigma_{DAI,t}$ (in basis points). Explanatory variables include daily ETH returns $R_{ETH,t}$ (in basis points), daily intra-day volatility of ETH returns $\sigma_{ETH,t}$ (in basis points), daily peg-price deviations of USDC prices $\Delta_{U,t}$ (in basis points), the daily intra-day volatility of USDC per-price deviations $\sigma_{U,t}$ (in basis points), the interest rate on DAI borrowings $sfee_t$ (in percent per annum). The sample is divided into the Pre-USDC Collateral (columns (1) and (3)) and Post-USDC Collateral period (columns (2) and (4)). The Pre-USDC Collateral sample runs from 18 November 2019 to 11 March 2020. The Post-USDC Collateral sample runs from 12 March 2020 to 31 March 2021. White heteroscedasticity-robust standard errors are reported in parentheses. *** denotes significance at the 1% level, ** at the 5% level, and * at the 10% level.

Table 11: Determinants of the share of stable collateral share

	(1)	(2)	(3)	(4)
		$share_t$		
$R_{ETH,t}$	0.002			0.001
	(0.002)			(0.001)
$\sigma_{ETH,t}$		-0.002		0.005***
		(0.003)		(0.002)
$\sigma_{U,t}$			-1.727***	-1.766***
			(0.118)	(0.106)
Intercept	23.409***	24.470***	42.859***	40.819***
	(0.960)	(1.766)	(1.482)	(1.778)
R-sq.	0.28%	0.11%	39.13%	39.92%
Nr. obs.	385	385	385	385

Table presents the estimation results of the regression of the share of stable collateral on ETH returns and ETH and USDC intra-day volatility:

$$share_t = \alpha + \beta_1 R_{ETH,t} + \beta_2 \sigma_{ETH,t} + \beta_3 \sigma_{U,t} + u_t.$$

where the dependent variable $share_t$ measures the share of total stable collateral deposited in vaults: this includes stablecoins USDC, Tether and TrueUSD (in percent). The explanatory variables include daily ETH returns $R_{ETH,t}$ (in basis points), daily intra-day volatility of USDC ($\sigma_{U,t}$) and ETH ($\sigma_{ETH,t}$) returns (in basis points). The sample runs from 12 March 2020 to 31 March 2021. White heteroscedasticity-robust standard errors are reported in parentheses. *** denotes significance at the 1% level, ** at the 5% level, and * at the 10% level.

Online Appendix to

"Decentralized Stablecoins and Collateral Risk"

(Not for publication)

We provide a roadmap of each section of our appendix.

1. Appendix A provides supplementary Figures on DAI creation and liquidation dynamics.

2. Appendix B provides model proofs.

3. Appendix C presents sensitivity analysis with respect to model parameters.

4. Appendix D provides analysis on the dynamic effect of ETH returns, liquidations, stability rate on the DAI price.

5. Appendix E provides robustness tests of the DiD specification for peg efficiency.

6. Appendix F provides details on the MKR governance token supply and price dynamics.

A Definitions: CDP and liquidation process

Figure A1: Process of DAI creation

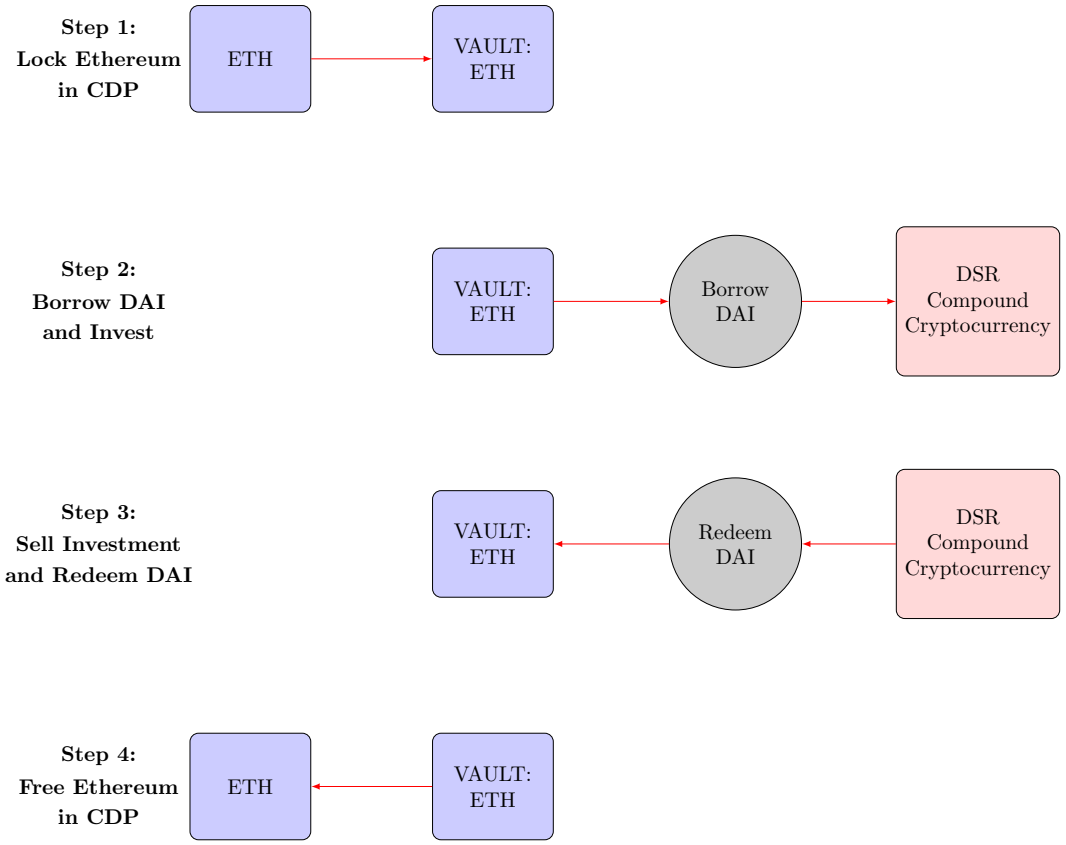

This figure illustrates the steps of depositing dollar wealth into a collateralized debt position (CDP) to create DAI tokens. In borrowing a fraction of ETH collateral as DAI to invest in an alternative currency. At the conclusion of the investment horizon, the investor sells investment for DAI tokens, redeems their DAI tokens and frees their ETH collateral.

Figure A2: DAI Liquidation Mechanism

Initial State
P_{ETH}:100 USD
P_{DAI}: 1 USD
Leverage:0.5
Liquidation Price: 75 USD

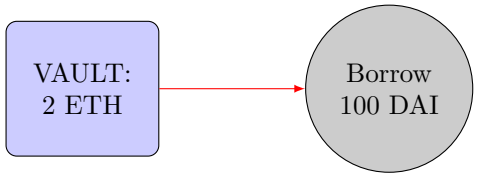

Liquidation
$P_{ETH} = 60USD$
$P_{DAI} = 1USD$
Leverage:0

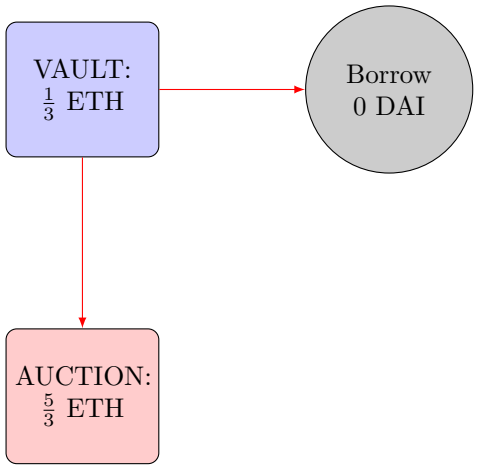

This figure illustrates the steps of liquidation for a hypothetical CDP. In the initial state, the investor deposits 2 ETH in a vault, and borrows 100 DAI tokens. At prices of $P_{ETH} = 100$ USD and $P_{DAI} = 1$ USD, the leverage of the CDP is 0.50. In the liquidation period, the price of ETH declines to 60 USD. This triggers liquidation as the price is less than the liquidation price of 75 USD. DAI borrowings are forced to zero. Keepers auction off 100 USD worth of collateral to pay off the DAI loan, this is equal to $\frac{5}{3}$ ETH at the new price of 60 USD. The new amount of ETH in the vault is $\frac{1}{3}$ ETH. This example is a simplified setting as it ignores additional liquidation costs, such as a liquidation penalty or the potential for fire sale auction prices of ETH.

B Model

Derivation of speculators' demand

To solve the speculators' optimization problem in Equation (5), we specify the following Lagrangian function:

$$\begin{aligned} L(\theta) &= \mathbb{E}_1[W_2^s] - \frac{1}{2}\gamma Var_1[W_2^s] + \lambda_1\theta + \lambda_2(\bar{\theta} - \theta) \qquad (18) \\ &= W_1^s\left[\mu^S(s)(1+\theta p_1) - \theta - \theta i^B\right] - \frac{\gamma W_1^{s2}}{2}\left[\sigma_E^2(1+\theta p_1)^2 + \theta^2\sigma^2\right] + \lambda_1\theta + \lambda_2(\bar{\theta} - \theta), \end{aligned}$$

for $\lambda_1, \lambda_2 \geq 0$. The first order conditions are:

$$\begin{aligned} 0 &= W_1^s\left[\mu^S(s)p_1 - 1\right] - i^B\Big] - \gamma W_1^{s2}\left[\sigma_E^2(1+\theta p_1)p_1 + \theta\sigma^2\right] + \lambda_1 - \lambda_2, \qquad (19) \\ 0 &= \lambda_1\theta, \qquad (20) \\ 0 &= \lambda_2(\bar{\theta} - \theta). \qquad (21) \end{aligned}$$

We consider the following cases of variable and Lagrange multipliers values:

1. $\theta = 0$.

   Condition $\theta = 0$ implies that $\lambda_1 \geq 0$ and $\lambda_2 = 0$. The first-order condition (19) becomes $\lambda_1 = -W_1^s\left[\mu^S(s)p_1 - 1 - i^B\right] + \gamma W_1^{s2}\sigma_E^2$. Hence, $\lambda_1 \geq 0$ is equivalent to

   $$\mu^S(s)p_1 - 1 - i^B \leq \gamma W_1^s\sigma_E^2 p_1.$$

2. $0 < \theta < \bar{\theta}$

   In this case, $\lambda_1 = \lambda_2 = 0$ and the first-order condition (19) becomes

   $$\theta = \frac{\frac{p_1\mu^S(s) - 1 - i^B}{\gamma W_1^s} - p_1\sigma_E^2}{p_1^2\sigma_E^2 + \sigma^2}. \qquad (22)$$

   In order to satisfy the initial restriction $0 < \theta < \bar{\theta}$, it should hold:

   $$p_1\sigma_E^2 < \frac{\mu^S(s)p_1 - 1 - i^B}{\gamma W_1^s} < p_1\sigma_E^2 + \bar{\theta}\left(p_1^2\sigma_E^2 + \sigma^2\right).$$

3. $\theta = \bar{\theta}$.

   In this case $\lambda_1 = 0$ and the first-order equation (19) implies

   $$\lambda_2 = W_1^s\left[\mu^S(s)p_1 - 1 - i^B\right] - \gamma W_1^{s2}\left[\sigma_E^2(1+\bar{\theta}p_1)p_1 + \bar{\theta}\sigma^2\right] \geq 0$$

which holds whenever

$$\frac{\mu^S(s)p_1 - 1 - i^B}{\gamma W_1^s} \geq p_1\sigma_E^2 + \bar{\theta}\left(p_1^2\sigma_E^2 + \sigma^2\right).$$

Combining the three cases, we get Equation (6).
Q.E.D.

Derivation of arbitrageurs' demand: single collateral

To solve the arbitrageurs' optimization problem in Equation (5), we optimize the expected utility function in each region $\omega \geq 0$ and $\omega \leq 0$ separately.

1. $\omega \geq 0$.

   For this case we specify the following Lagrangian function:

$$\begin{aligned} L(\omega) &= \mathbb{E}_1[W_2^a] - \frac{1}{2}\gamma Var_1[W_2^a] + \lambda_1\omega \\ &= W_1^a\left[\frac{\omega(1+i^L)}{p_1} + (1-\omega)(1+r)\right] - \frac{\gamma W_1^{a2}\omega^2(1+i^L)^2\sigma^2}{2p_1^2} + \lambda_1\omega, \end{aligned} \tag{23}$$

   for $\lambda_1 \geq 0$. The first order conditions are:

$$0 = W_1^a\left[\frac{1+i^L}{p_1} - (1+r)\right] - \frac{\gamma W_1^{a2}\omega(1+i^L)^2\sigma^2}{p_1^2} + \lambda_1, \tag{24}$$

$$0 = \lambda_1\omega. \tag{25}$$

   We consider the following cases of values of ω:

   a). $\omega = 0$.

   Condition $\omega = 0$ implies that $\lambda_1 \geq 0$. The first-order condition (24) becomes

$$\lambda_1 = -W_1^a\left[\frac{1+i^L}{p_1} - (1+r)\right].$$

   Hence, $\lambda_1 \geq 0$ is equivalent to

$$1 + i^L \leq (1+r)p_1.$$

   b). $\omega > 0$

   In this case, $\lambda_1 = 0$ and the first-order condition (24) becomes

$$\omega = \frac{\left((1+i^L)/p_1 - (1+r)\right)p_1^2}{\gamma W_1^a(1+i^L)^2\sigma^2}. \tag{26}$$

In order to satisfy the initial restriction $\omega > 0$, it should hold:

$$1 + i^L > (1 + r)p_1.$$

Now we consider the maximum of the expected utility function of the short-selling region.

2. $\omega \leq 0$.

For this case we specify the following Lagrangian function:

$$\begin{aligned} L(\omega) &= \mathbb{E}_1[W_2^a] - \frac{1}{2}\gamma Var_1[W_2^a] - \lambda_1\omega \\ &= W_1^a\left(-\frac{\omega}{\bar{\theta}}\mu^A + \omega(1 - p_1(1+r) + i^B) + \left(1 + \frac{\omega}{\bar{\theta}}\right)(1+r)\right) \\ &- \frac{\gamma W_1^{a2}\omega^2}{2}\left[\frac{\sigma_E^2}{\bar{\theta}^2} + \sigma^2\right] - \lambda_1\omega, \end{aligned} \tag{27}$$

for $\lambda_1 \geq 0$. The first order conditions are:

$$0 = W_1^a\left[-\frac{\mu^A}{\bar{\theta}} + (1 - p_1(1+r) + i^B) + \frac{1+r}{\bar{\theta}}\right] - \gamma W_1^{a2}\omega\left[\frac{\sigma_E^2}{\bar{\theta}^2} + \sigma^2\right] - \lambda_1, \tag{28}$$

$$0 = -\lambda_1\omega. \tag{29}$$

We consider the following cases of values of ω:

a). $\omega = 0$.

Condition $\omega = 0$ implies that $\lambda_1 \geq 0$. The first-order condition (28) implies

$$\lambda_1 = W_1^a\left[-\frac{\mu^A}{\bar{\theta}} + (1 - p_1(1+r) + i^B) + \frac{1+r}{\bar{\theta}}\right].$$

Hence, $\lambda_1 \geq 0$ is equivalent to

$$\mu^A \leq \bar{\theta}(1 - p_1(1+r) + i^B) + 1 + r.$$

b). $\omega < 0$

In this case, $\lambda_1 = 0$ and the first-order condition (28) implies

$$\omega = -\bar{\theta}\frac{\left[\mu^A - (1+r) - \bar{\theta}(1 - p_1(1+r) + i^B)\right]}{\gamma W_1^a(\sigma_E^2 + \bar{\theta}^2\sigma^2)}. \tag{30}$$

In order to satisfy the initial restriction $\omega < 0$, it should hold:

$$\mu^A > \bar{\theta}(1 - p_1(1+r) + i^B) + 1 + r.$$

Combining the cases and comparing the maxima values of the expected utility function in each region, we get Equation (7).

Q.E.D.

Derivation of arbitrageurs' demand: two types of collateral

To solve the arbitrageurs' optimization problem in the case of two collateral, we optimize the expected utility function in $\omega \leq 0$ region and compare it with the maximum of the expected utility in $\omega \geq 0$ region (the latter case is the same as in the single collateral case). Denote by $N = 1 - p_1(1+r) + i^B$ and $M = \frac{\mu^A - (1+r)}{\bar{\theta}}$. In order to simplify the calculations we make the following assumptions about the parameter values that are justified by the sample estimations in the main body of the paper and are verified in the equilibrium above: $\sigma_E^2 > \sigma^2$.

For this case we specify the following Lagrangian function:

$$\begin{aligned} L(\omega^E, \omega^U) &= \mathbb{E}_1[W_2^a] - \frac{1}{2}\gamma Var_1[W_2^a] - \lambda_1\omega^E - \lambda_2\omega^U \\ &= W_1^a\left[-\frac{\omega^E}{\bar{\theta}}\mu^A - \omega^U(1+r) + (\omega^E + \omega^U)N + \left(1 + \frac{\omega^E}{\bar{\theta}} + \omega^U\right)(1+r)\right] \\ &- \frac{\gamma W_1^{a2}}{2}\left[\frac{\omega^{E2}}{\bar{\theta}^2}\sigma_E^2 + \omega^{U2}\sigma_U^2 + (\omega^E + \omega^U)^2\sigma^2\right] - \lambda_1\omega^E - \lambda_2\omega^U, \end{aligned} \tag{31}$$

for $\lambda_1, \lambda_2 \geq 0$. The first order conditions are:

$$0 = W_1^a[N - M] - \gamma W_1^{a2}\left[\frac{\omega^E}{\bar{\theta}^2}\sigma_E^2 + (\omega^E + \omega^U)\sigma^2\right] - \lambda_1, \tag{32}$$

$$0 = W_1^a N - \gamma W_1^{a2}\left[\omega^U\sigma_U^2 + (\omega^E + \omega^U)\sigma^2\right] - \lambda_2, \tag{33}$$

$$0 = -\lambda_1\omega^E \tag{34}$$

$$0 = -\lambda_2\omega^U. \tag{35}$$

We consider the following cases of values of ω^E and ω^U:

a). $\omega^E = \omega^U = 0$.

Conditions $\omega^E = 0$ and $\omega^U = 0$ imply that $\lambda_1 \geq 0$ and $\lambda_2 \geq 0$. The first-order conditions (32) and (33) become

$$\lambda_1 = W_1^a[N - M],$$

$$\lambda_2 = W_1^a N.$$

Hence, $\lambda_1 \geq 0$ and $\lambda_2 \geq 0$ are equivalent to $N \geq M$ and $N \geq 0$.

b). $\omega^E = 0$ and $\omega^U < 0$

Conditions $\omega^E = 0$ and $\omega^U < 0$ imply that $\lambda_1 \geq 0$ and $\lambda_2 = 0$. The first-order conditions (32) and (33) become

$$\lambda_1 = W_1^a [N - M] - \gamma W_1^{a2} \omega^U \sigma^2,$$

$$\omega^U = \frac{N}{\gamma W_1^a (\sigma_U^2 + \sigma^2)}.$$

Inequality $\lambda_1 \geq 0$ is equivalent to

$$\frac{N}{\sigma_U^2 + \sigma^2} \geq \frac{M}{\sigma_U^2}$$

and $\omega^U < 0$ is equivalent to $N < 0$.

c). $\omega^E < 0$ and $\omega^U = 0$

Conditions $\omega^E < 0$ and $\omega^U = 0$ imply that $\lambda_1 = 0$ and $\lambda_2 \geq 0$. The first-order conditions (32) and (33) become

$$\omega^E = \frac{N - M}{\gamma W_1^a \left[\frac{\sigma_E^2}{\theta^2} + \sigma^2\right]},$$

$$\lambda_2 = W_1^a N - \gamma W_1^{a2} \omega^E \sigma^2.$$

Inequality $\lambda_2 \geq 0$ is equivalent to

$$\frac{N}{\sigma^2} \geq \frac{M}{\frac{\sigma_E^2}{\theta^2}}$$

and $\omega^E < 0$ is equivalent to $N < M$.

d). $\omega^E < 0$ and $\omega^U < 0$

In this case, $\lambda_1 = \lambda_2 = 0$ and the first-order conditions (32) and (33) become

$$\omega^E = \frac{\frac{N}{\sigma^2 + \sigma_U^2} - \frac{M}{\sigma_U^2}}{\gamma W_1^a \left(\frac{\frac{\sigma_E^2}{\theta^2} + \sigma_U^2}{\sigma_U^2} - \frac{\sigma_U^2}{\sigma^2 + \sigma_U^2} \right)}.$$

$$\omega^U = \frac{\frac{N\sigma_E^2}{\theta^2} - M\sigma^2}{\gamma W_1^a \left(\sigma^2 \sigma_U^2 + \frac{\sigma_E^2}{\theta^2} (\sigma^2 + \sigma_U^2) \right)}.$$

In order to satisfy the initial restrictions $\omega^U < 0$ and $\omega^E < 0$, it should hold:

$$\frac{N}{\sigma^2 + \sigma_U^2} < \frac{M}{\sigma_U^2} \qquad \text{and} \qquad \frac{N\sigma_E^2}{\bar{\theta}^2} < M\sigma^2.$$

Simple calculations verifies the following summary of the results:

- If $N \geq 0$ and $N \geq M$ then

$$\omega^E = 0, \tag{36}$$
$$\omega^U = 0. \tag{37}$$

- If $N < 0$ and $M \leq \delta N$ then

$$\omega^E = 0, \tag{38}$$
$$\omega^U = \frac{N}{\gamma W_1^a(\sigma_U^2 + \sigma^2)}, \tag{39}$$

  where

$$\delta = \frac{\sigma_U^2}{\sigma_U^2 + \sigma^2}.$$

- If $N \geq 0$ and $N < M \leq \Delta N$ then

$$\omega^E = \frac{N - M}{\gamma W_1^a \left[\frac{\sigma_E^2}{\bar{\theta}^2} + \sigma^2\right]}, \tag{40}$$
$$\omega^U = 0, \tag{41}$$

  where

$$\Delta = \frac{\sigma_E^2}{\bar{\theta}^2\sigma^2}.$$

- If $N \geq 0$ and $M > \Delta N$ or $N < 0$ and $M > \delta N$ then

$$\omega^E = \frac{\frac{N}{\sigma^2+\sigma_U^2} - \frac{M}{\sigma_U^2}}{\gamma W_1^a \left(\frac{\frac{\sigma_E^2}{\bar{\theta}^2}+\sigma_U^2}{\sigma_U^2} - \frac{\sigma_U^2}{\sigma^2+\sigma_U^2} \right)}, \tag{42}$$
$$\omega^U = \frac{\frac{N\sigma_E^2}{\bar{\theta}^2} - M\sigma^2}{\gamma W_1^a \left(\sigma^2\sigma_U^2 + \frac{\sigma_E^2}{\bar{\theta}^2}(\sigma^2 + \sigma_U^2) \right)}. \tag{43}$$

Q.E.D.

C Model sensitivity analysis

Figure A3: DAI prices, volatility sensitivity analysis across different values of ETH volatility

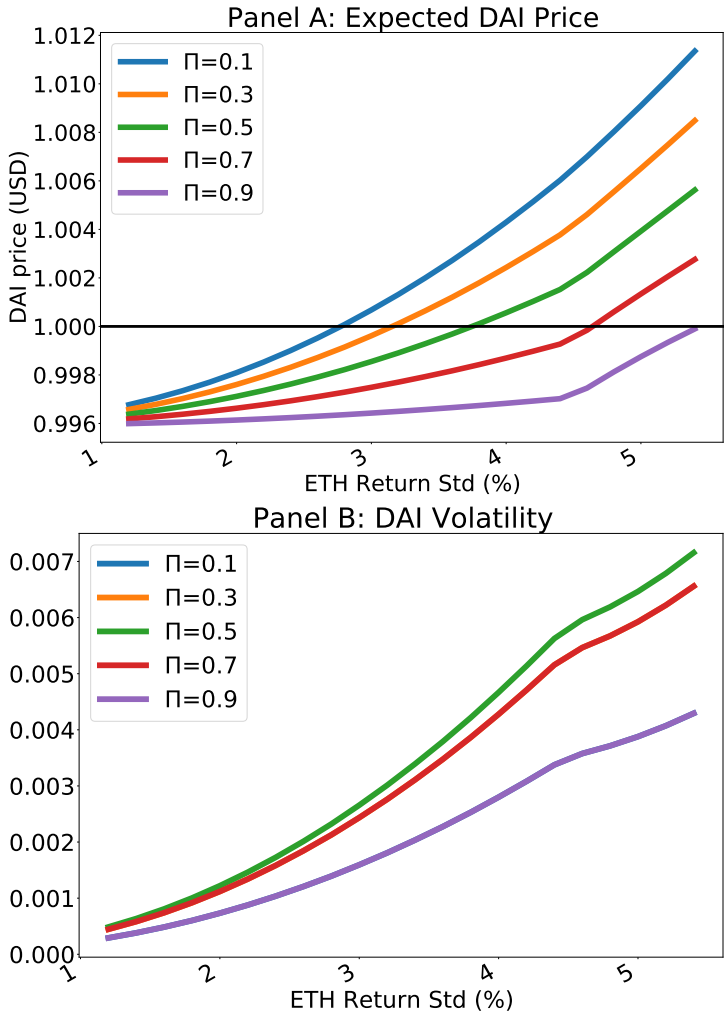

This figure plots the expected DAI prices and volatility as a function of ETH volatility, for different values of probability π of the good state of ETH returns. All other parameters are held constant. Panel A corresponds to the expected DAI price. Panel B corresponds to peg-price volatility, calculated as the standard deviation of peg-prices across the two states of collateral. The primitive parameters are as follows: $\gamma = 0.5$, $W_1^s = \$350$, $D(B) = \$50$, $D(G) = \$0$, $\bar{\theta} = 0.66$, $\sigma = 0.0188$, $i^B = 0.0324/252$, $i^L = 0.0139/252$, $r = 0.015/252$, $\mu_A = 1.0033$, $\mu_E(G) = 1.0668$, $\mu_E(B) = 1.0033$. The rest of the parameters in the model are computed numerically by optimizing the expected utilities (5).

Figure A4: Sensitivity analysis: DAI prices and volatility across different values of interest rate on DAI borrowing

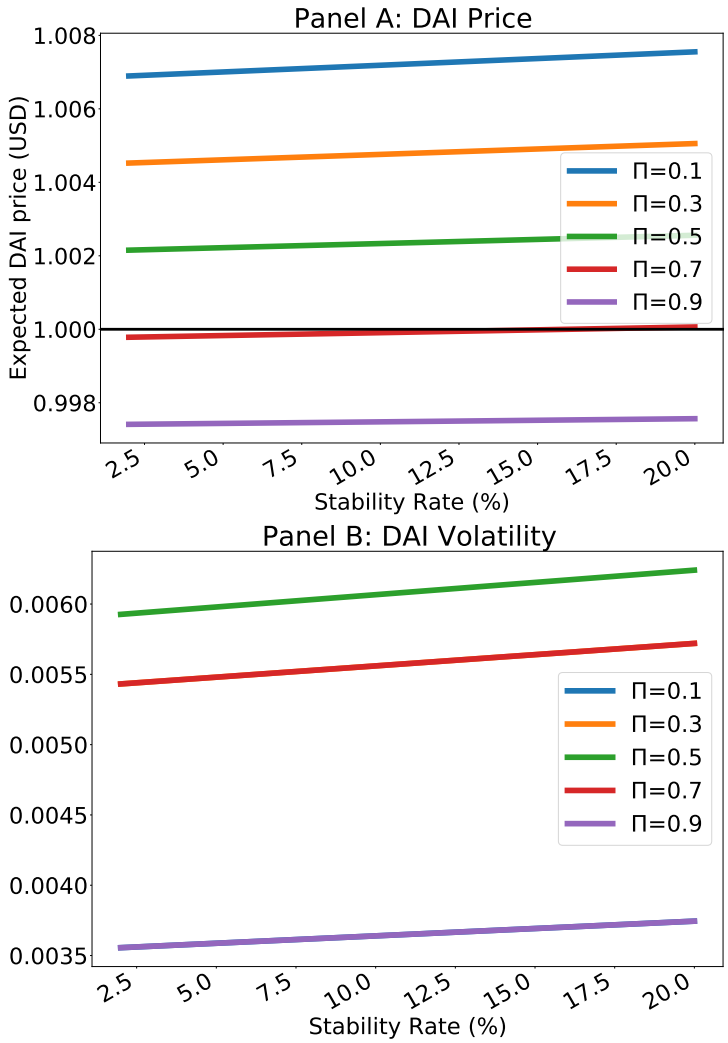

This figure plots the expected DAI prices and DAI volatility as a function of the DAI stability rate, for different values of probability π of the good state of ETH returns. All other parameters are held constant. Panel A corresponds to the expected DAI price. Panel B corresponds to peg-price volatility, calculated as the standard deviation of peg-prices across the two states of collateral. The primitive parameters are as follows: $\gamma = 0.5$, $W_1^s = \$350$, $D(B) = \$50$, $D(G) = \$0$, $\bar{\theta} = 0.66$, $\sigma = 0.0188$, $\sigma_E = 0.0459$, $i^L = 0.0139/252$, $r = 0.015/252$, $\mu_A = 1.0033$, $\mu_E(G) = 1.0668$, $\mu_E(B) = 1.0033$. The rest of the parameters in the model are computed numerically by optimizing the expected utilities (5).

Figure A5: Sensitivity analysis: DAI prices and volatility across different values of safe-haven demand

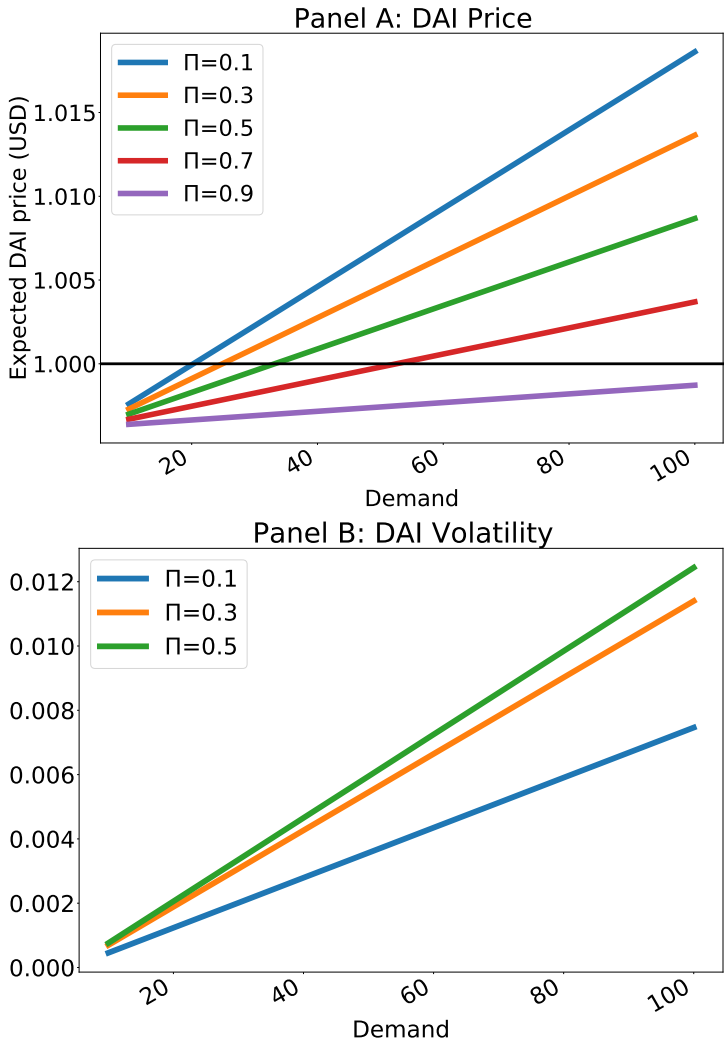

This figure plots the expected DAI prices and DAI volatility as a function of the DAI safe-haven demand in the bad state, for different values of probability π of the good state of ETH returns. All other parameters are held constant. Panel A corresponds to the expected DAI price. Panel B corresponds to peg-price volatility, calculated as the standard deviation of peg-prices across the two states of collateral. The primitive parameters are as follows: $\gamma = 0.5$, $W_1^s = \$350$, $D(G) = \$0$, $\bar{\theta} = 0.66$, $\sigma = 0.0188$, $\sigma_E = 0.0459$, $i^B = 0.0324/252$, $i^L = 0.0139/252$, $r = 0.015/252$, $\mu_A = 1.0033$, $\mu_E(G) = 1.0668$, $\mu_E(B) = 1.0033$. The rest of the parameters in the model are computed numerically by optimizing the expected utilities (5).

Figure A6: Sensitivity analysis: DAI prices and volatility across different values of wealth and risk aversion

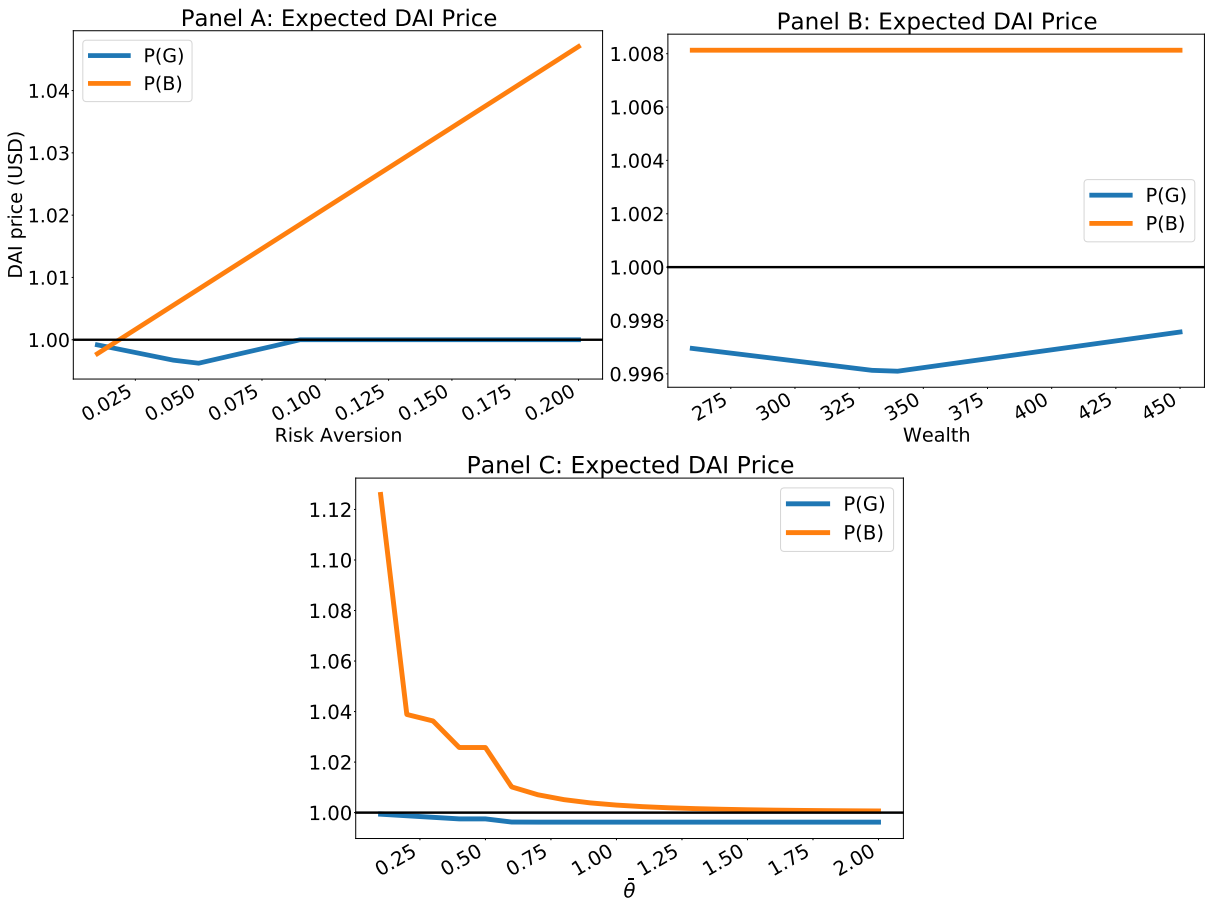

This figure plots the DAI prices during the good and bad states as a function of the risk average coefficient γ (Panel A), the wealth of speculators W_1^s (Panel B) and the DAI borrowing limit $\bar{\theta}$ (Panel C). All other parameters are held constant. The primitive parameters are as follows: $D(B) = \$50$, $D(G) = \$0$, $\bar{\theta} = 0.66$, $\sigma = 0.0188$, $\sigma_E = 0.0459$, $i^B = 0.0324/252$, $i^L = 0.0139/252$, $r = 0.015/252$, $\mu_A = 1.0033$, $\mu_E(G) = 1.0668$, $\mu_E(B) = 1.0033$. For panel A we assume $W_1^s = \$350$ and for Panel B we assume $\gamma = 0.5$. The rest of the parameters in the model are computed numerically by optimizing the expected utilities (5).

D Dynamic effects of ETH returns, liquidations, trading volume and stability rate

In this section, we use local projections (Jordà 2005) to test for the dynamic effects of ETH returns, liquidations, demand, and the stability rate on DAI prices and leverage. We consider the DAI/USD price, aggregate liquidations, ETH returns, and the leverage ratio as outcome variables. We project the change in the outcome variable, $Y_{t+h} - Y_{t-1}$, on the explanatory variable X_t using Equation (44). The specification allows for feedback effects using lagged values of the explanatory variable and outcome variable, and additional controls C_t. The baseline specification uses 1 lag. The impulse response of a shock to the explanatory variable on the outcome variables is traced through β_h.

$$Y_{t+h} = \alpha + \beta_h X_t + \sum_{k=1}^{L} \delta_k X_{t-k} + \sum_{k=1}^{L} \gamma_k Y_{t-k-1} + C_t + u_t, \qquad h = 0, 1, 2, ... \tag{44}$$

The results are shown in Figure A7. Panel A considers the effect of a *negative* 100 basis point shock to ETH returns, which leads to DAI premiums and an initial positive increase in liquidations, but a decrease in DAI borrowings. This is consistent with the empirical results using individual CDP data, where negative ETH returns increase the probability of liquidation and decrease DAI borrowings.

Panel B tests the effect of a 1 million USD shock in liquidations, which led to a fire-sale of ETH collateral to pay off the DAI debt. We observe contemporaneous DAI premiums and a negative ETH return, but that dissipates within one day. The lack of persistent effects of liquidations on ETH returns is due to DAI in circulation being a small fraction of the market cap of ETH.

Panel C tests the effect of a 1% increase in aggregate secondary market trading volume of DAI, which shows weakly positive DAI premiums and an increase in DAI borrowings, with insignificant effects on ETH returns.

Panel D traces the impulse response of the stability rate on the DAI price and the leverage ratio. We use the change in the stability rate as the explanatory variable, and find a positive effect on DAI prices over a long horizon. A 100 basis point hike in the stability rate increases DAI prices by approximately 5 basis points over the long-term and reduces DAI borrowings by 8 million USD over a horizon of 30 days. Differences between the panel regression specification and the local projections are rationalized due to cross-section versus aggregate system leverage and the time horizon of the effect.

Figure A7: Effect of ETH returns, liquidations, DAI trading volume and stability rate on DAI

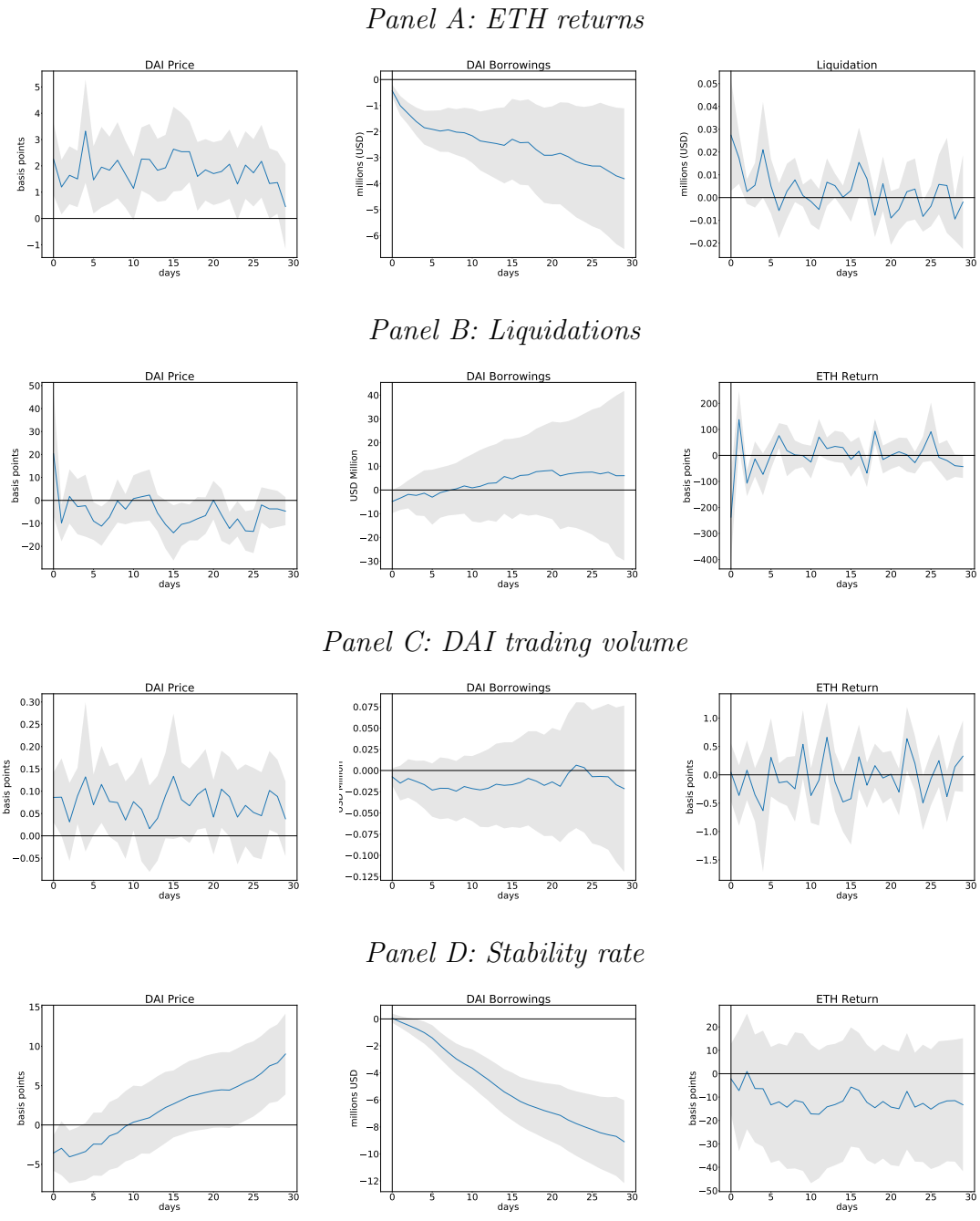

This figure illustrates the response of DAI price and leverage to: Panel A: A negative 100 basis point shock to ETH returns, Panel B: 1 million USD Liquidations, Panel C: 1% change in DAI trading volume, Panel D: 1% change in stability rate fee, using the method of local projections. Leverage ratio is based on aggregate measures of DAI borrowings and ETH collateral. Sample period is from 18 November 2019 to 31 March 2021, corresponding to the period of Multi Collateral DAI. 1 lag is included in the baseline specification. Gray area denotes 90% confidence interval using White heteroscedasticity-robust standard errors.

E PSM: Robustness tests

E.1 Robustness test #1: sensitivity of Treatment date

In this section, we aim to examine whether the difference-in-difference analysis in Section 5.3.1 is affected by the choice of the USDC collateral date. The complete effects of USDC collateral are likely to be realized several months after March 2020 since users gradually started using it as a collateral type. In order to perform a sensitivity analysis of the USDC introduction date, we plotted the difference-in-difference coefficients for various alternative collateral introduction dates in Figure A8. Despite considering different dates, we found that the treatment effect persists, implying that it is robust to alternative dates. The highest treatment effect of -104 basis points was observed on November 17th 2020, which is about one month prior to the implementation of PSM. This finding aligns with the impact of introducing USDC collateral before the implementation of PSM.

Figure A8: Sensitivity Analysis of Difference-in-Difference Coefficients to a Change in the Structural Date.

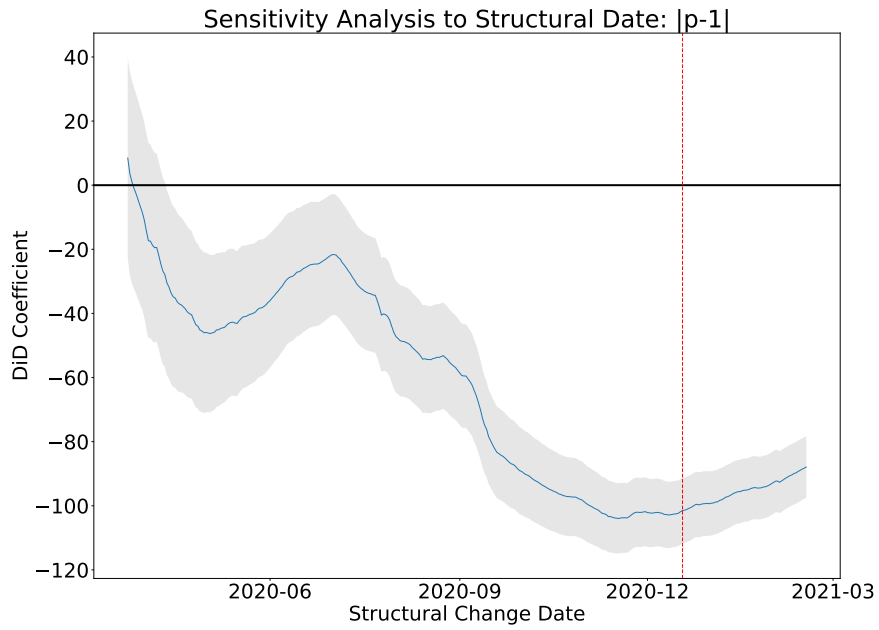

Note: This figure shows the difference-in-difference coefficient δ of the following design: $|p_t - 1| = \beta_t Post_t + \delta_t Post_t \times T_t$ by changing the structural change date $Post_t$. The outcome variable measures the absolute level of peg deviations on the left panel, and intra-day volatility of peg price deviations on the right panel. The treatment currency is DAI, and control group currency is USDC. The red dotted line indicates the structural change date of December 18th 2020 used in the baseline specification. White heteroscedasticity-robust standard error bands are reported at a 5% significance level.

E.2 Robustness test #2: Dynamic time trend to the pre-post migration

We expand the specification in equation (45) to incorporate a dynamic trend in the post-period. The difference-in-difference coefficient δ tracks the overall impact of the introduction of USDC collateral from 2020Q1 to 2021Q1, across each quarter. By tracing the net impact across quarters, we examine the hypothesis that the introduction of USDC collateral is gradual and occurs before the PSM date of December 18th, 2020.

$$|p_t - 1| = \alpha_0 + \beta T_i + \gamma post_t + \sum_{q=1}^{Q} \delta_q Q_{t+q} \times T_i + u_t \tag{45}$$

The difference-in-difference coefficients from specification (45) are displayed in Figure A9. The coefficients of interest for each quarter interacted with the treatment dummy represent peg price-deviations relative to USDC. The coefficients demonstrate a trend of increased DAI efficiency, with the most significant increase in the efficiency of the peg occurring in Q4 2020. Only in Q1 2021, immediately after the implementation of PSM, do we observe only a 10 basis point difference between USDC and DAI prices on average.

Figure A9: Difference-in-difference coefficients for dynamic panel specification

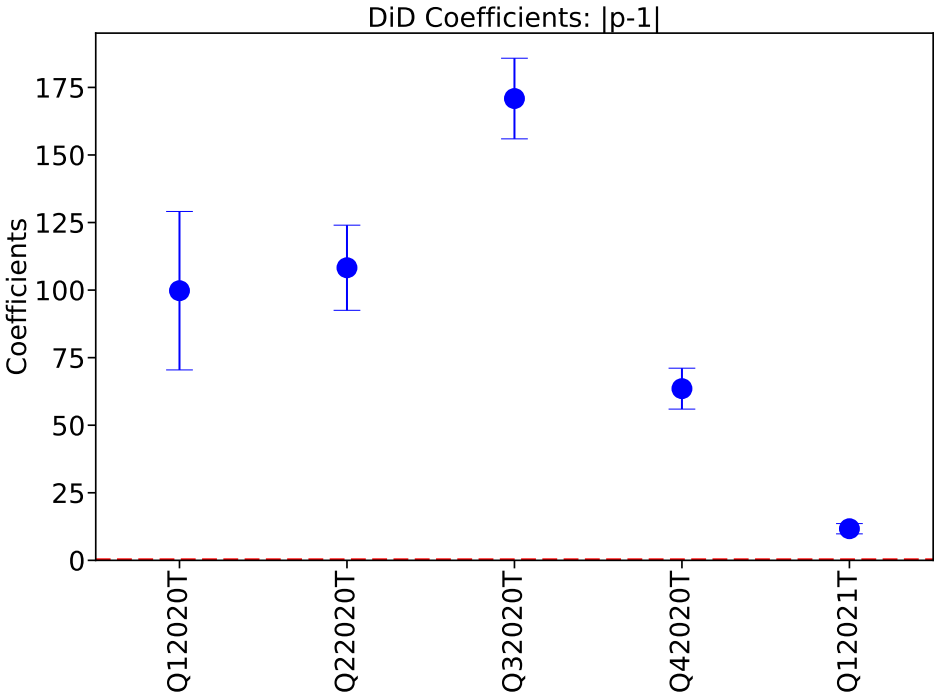

Note: Figure presents coefficients for a dynamic difference-in-difference specification with the absolute level of peg-price deviations. Coefficients measure the effect of the treatment interacted with each quarter. The sample is based on the balanced panel from 8 January 2020 to 31 March 2021. White heteroscedasticity-robust standard-error bars are plotted to construct a 95 percent confidence interval around coefficient estimates.

F MakerDAO auctions and governance

The Maker Governance protocol is responsible for various tasks, including the addition of new collateral types, regulation of smart contracts enforcing collateralized debt positions, and adjustment of risk parameters such as the liquidation ratio, debt ceilings, and stability and savings rate. Figure A10 shows several panels. Panel A displays the MKR price, while Panel B shows the MakerDAO token's launch with a supply of 1 million MKR. Panel C illustrates the net redemptions of MKR tokens. Panel D shows the system surplus, which is the amount of DAI generated from system fees, including Stability Fees and Liquidation Fees set by Maker governance. In Panel E, the ratio of the MKR price to the system surplus per unit of the MKR token is plotted. Note that the valuation of the MKR token is similar to a dividend paid to MKR stakeholders for supporting the governance protocol in maintaining the DAI peg. The valuation of a MKR token per unit of system surplus fluctuates between 100 to 500. Panel F depicts the strong correlation between the intra-day volatility of ETH and volatility in MKR.

The MKR governance token is used for voting on the management of the protocol and setting various parameters of the DAI stablecoin peg. Users can stake their MKR tokens to place their vote on their preferred stability rate, with each MKR token equaling one vote when locked in a voting contract. The outcome of a proposal is determined by the number of MKR tokens it receives.

In a related note Kozhan and Viswanath-Natraj 2022, we examine the dynamics of MKR token prices and present three empirical findings. First, an increase in the system surplus leads to a net burning of MKR tokens, resulting in an increase in the MKR token valuation. Second, the minting of MKR tokens devalues the MKR token. Finally, we propose that an increase in ETH volatility leads to an increase in MKR volatility and a decrease in the MKR token price. Empirical evidence supports all three hypotheses.

Figure A10: MKR price, MKR Supply, Burned/Minted Tokens and System Surplus

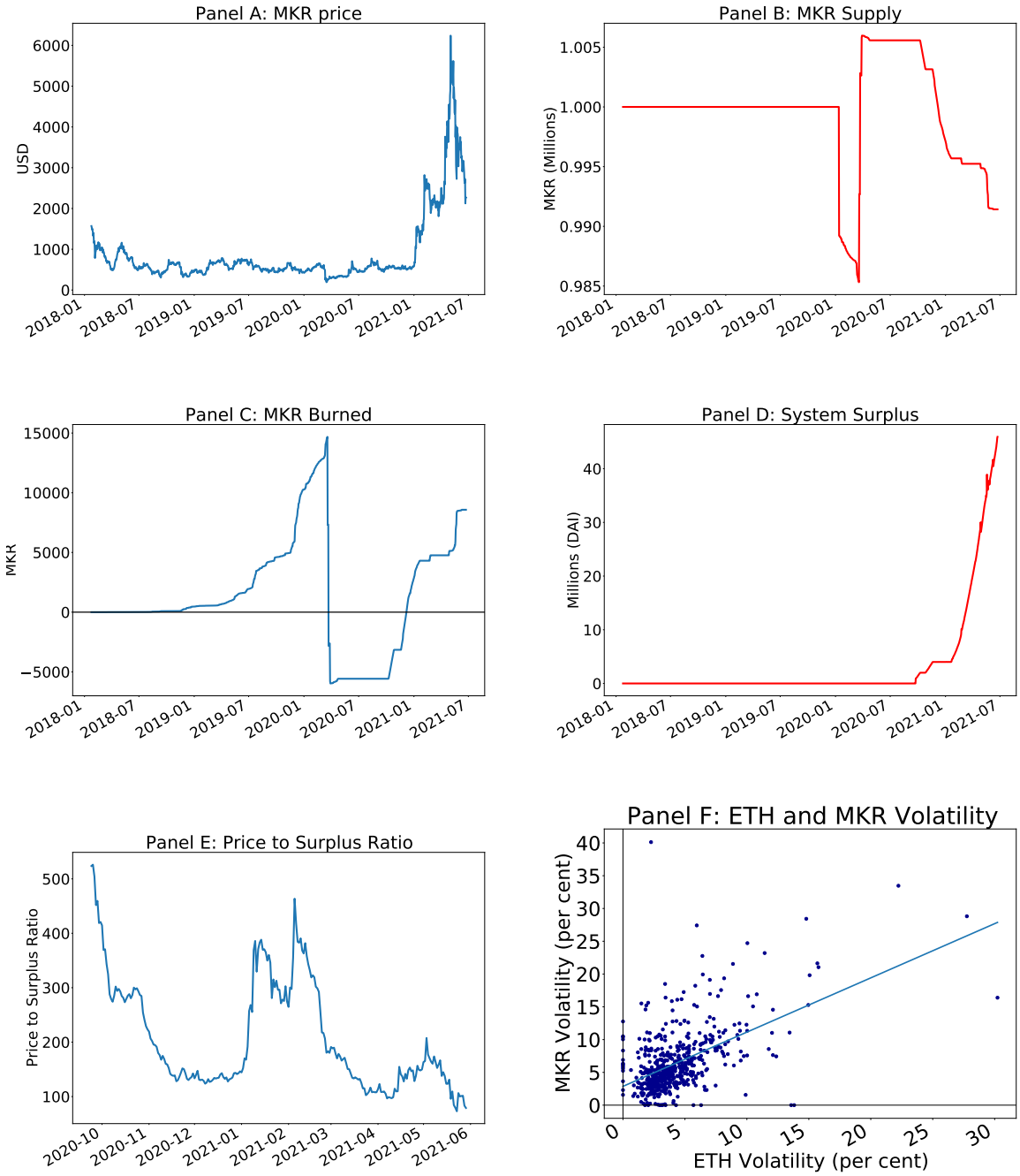

Note: This figure plots Panel A: MKR price, Panel B: MKR Supply Panel C: MKR Burned, Panel D: System Surplus, Panel E: Ratio of MKR Price to Unit Surplus, Panel F: ETH and MKR Volatility.